DRUG TOXICITY TESTING ON CHIPS

DEEPAK CHOUDHURY

B.Tech Biotechnology, VIT

A THESIS SUBMITTED FOR THE DEGREE OF DOCTOR OF PHILOOSPHY

NUS Graduate School for

Integrative Sciences and Engineering

NATIONAL UNIVERSITY OF SINGAPORE

2012

ACKNOWLEDGEMENTS

First and foremost, I would like to thank my wife Tan Le Kung for all the support and encouragement during my PhD studies. My sincere gratitude to my parents for always supporting the career path I have chosen. I would like to thank my supervisor Prof. Hanry Yu for his guidance throughout my thesis project. I would like to express my gratitude to my mentors Dr. Danny van Noort, who helped me in the design of the "Fish and Chips" and Dr. Ciprian Iliescu for teaching me all the details of microfabrication processes. They helped me sail through the rough times I had during my experiments. My sincere thanks also to my thesis advisory committee members, Dr. Kang Lifeng, Dr. Wang Zhengfeng and Prof. Edmund Lee for all their valuable comments and suggestions. I am also thankful to my lab colleagues both at NUS and at IBN, especially George, Dr. Baixue, Xuejun, Alvin, Bramasta, Abhisek, Narmada, Erica, Wen Hao, Loo Ling, Dr. Zhang Chi and Dr. Yi-Chin during day-to-day help, valuable feedback and friendship. I would take this opportunity to thank my collaborator A/P Vladimir Korzh and his lab colleague Dr. Kar Lai for providing me the transgenic fish embryos for my studies. I would also thank my roommates and friends Dr. Prashant, Dr. Nikhil, Dr. Ravi, Hemant, Dr. Ajay, Dr. Ashish, Dr. Axel, Dr. Ming Ni for their enjoyable company and inputs during my graduate studies. Last, but not least, I would thank my department NGS for my research scholarship and IBN A* Star for providing the funding and research space for my work.

LIST OF PUBLICATIONS

1. **D. Choudhury**, D.v Noort, C. Iliescu, B. Zheng, K.L. Poon, S. Korzh, V. Korzh and H. Yu. Fish and Chips: a microfluidic perfusion platform for monitoring zebrafish development, Lab on a Chip, 2011, DOI: 10.1039/c1lc20351g
    - Cover Page of the Journal
    - Media Release by IBN A * Star
    - Top 10 articles accessed online in Dec 2011 for the journal Lab on a Chip

2. **D. Choudhury**, X. Mo, C. Iliescu, L. L. Tan, W. H. Tong, and H. Yu. Exploitation of Physical and Chemical Constraints for Three-Dimensional Microtissue Construction in Microfluidics, Biomicrofluidics, 2011 DOI: 10.1063/1.3593407

3. B. Nugraha, X. Hong, X. Mo, L. Tan, W. Zhang, P.-M. Chan, C. H. Kang, Y. Wang, L. T. Beng, W. Sun, **D. Choudhury**, J. M. Robens, M. McMillian, J. Silva, S. Dallas, C.-H. Tan, Z. Yue, H. Yu. Galactosylated Cellulosic Sponge for Multi-Well Drug Safety Testing, Biomaterials, 2011, DOI:10.1016/j.biomaterials.2011.05.087

4. X. Mo, Q. Li, L.W.Y. Lui, B. Zheng, C.H. Kang, B. Nugraha, Z. Yue, R.R. Jia, H.X. Fu, **D. Choudhury**, T. Arooz, J. Yan, C.T. Lim, S. Shen, C.H. Tan, and H. Yu. Rapid Construction of Mechanically-confined Multi-cellular Structures using Dendrimeric Intercellular Linker, Biomaterials, 31[29] 2010 7455-7467

5. M. Ni, W.H. Tong, **D. Choudhury**, C. Iliescu and H. Yu. Cell Culture on MEMS Platforms: A Review, International Journal of Molecular Sciences, 10 ,2009 5411-5441

6. "Gratings on a dish" (Manuscript under preparation)

LIST OF PATENTS

- Technological disclosure submitted: "Gratings on a dish": Processing of large-area, low-cost diffraction gratings (holographic gratings and optical discs CD-R/DVD-R) for cell culture/cell alignment.

TABLE OF CONTENTS

ACKNOWLEDGEMENTS ……. 1

LIST OF PUBLICATIONS …… 2

TABLE OF CONTENTS…… 3

SUMMARY……. 7

LIST OF TABLES…… 8

LIST OF FIGURES……. 9

LIST OF SUPPLEMENATRY VIDEOS…… 12

LIST OF SYMBOLS AND ABBREVIATIONS…….. 13

CHAPTER 1 Introduction …….. 15

CHAPTER 2 Background and Significance…….. 19

2.1 The current issues facing the pharmaceutical industry…….. 20

2.1.1 Declining drug discovery success rates……. 20
2.1.2 Need to accelerate drug development pipelines……. 21

2.2 Miniaturization and drug discovery ……. 22

2.2.1 The benefits of miniaturization……. 22
2.2.2 Novel micro-scale platforms for pre-clinical studies……. 23

2.3 Zebrafish as a vertebrate model for pre-clinical drug screening…. 26

2.3.1 Zebrafish- a unique model for biological studies…… 26
2.3.2 Toxicity assessment in zebrafish…….. 27
2.3.3 Zebrafish for high throughput screens and disease models 30
2.3.4 Zebrafish and microtechnology…… 32
2.3.5 Limitations of current platforms and rationale for "Fish and Chips"……. 35

2.4 Diffraction gratings as a substrate for cell culture and drug testing.. 38

2.4.1 Cell adhesion and orientation along micro/nanogrooves…. 38

2.4.2 Usage of diffraction gratings for patterning surfaces …… 42

2.4.3 Limitations in producing current grooved surfaces and advantages of using diffraction gratings for cell culture…….. 48

CHAPTER 3 Objectives and Specific Aims……. 51

3.1 Specific Aim 1: To fabricate a microfluidic perfusion system for growing zebrafish embryos and perform drug testing…….. 51

3.2 Specific Aim 2: Processing of large-area, low-cost diffraction gratings (holographic gratings and optical discs CD-R/DVD-R) for cell alignment and potential drug testing…… 52

CHAPTER 4 Fabrication, characterization and optimization of Fish and Chips

4.1 Introduction…….. 53

4.2 Materials and Methods……. 56

4.2.1 CFD Simulations for fish tanks…….. 56
4.2.2 1st prototype: PDMS chip design…….. 56
4.2.3 PDMS chip fabrication and connection…….. 56
4.2.4 2nd prototype: Silicon-glass chip design…… 57
4.2.5 Silicon-glass chip fabrication……. 58
4.2.6 The perfusion flow set-up…….. 62
4.2.7 Flow characterization of the Fish and Chips by fluorescent dye studies……. 62

4.3 Results and Discussion…….. 63

4.3.1 Design of the Fish and Chips…….. 63
4.3.2 The fabricated Fish and Chips……. 68
4.3.3 Perfusion set-up…… 71
4.3.4 Optimization of the permeable membrane to cover the fish tanks
4.3.5 CFD simulations confirm that the design of fish tank ensures uniform exposure of media and drugs……. 73
4.3.5 Sigmoidal concentration profile of the dye……. 75
4.3.6 PDMS vs. Silicon-glass design…….. 77

4.4 Conclusions…… 78

CHAPTER 5 Zebrafish embryo culture on Fish and Chips……. 79

5.1 Introduction…… 79

5.2 Materials and Methods……. 81

5.2.1 Fish maintenance and crossing of fishes for embryos……. 81
5.2.2 Housing embryos on Fish and Chips…… 81
5.2.3 Live imaging of embryos on chip……. 82
5.2.4 Long-term embryo development and survival on chip……. 82
5.2.5 Heartbeat recording on chip…….. 82
5.2.6 Single-cell imaging of fish embryos on chip……. 83
5.2.7 Live imaging of embryos in 96-well plates…… 83

5.3 Results and Discussion…… 84

5.3.1 Collection and maintenance of embryos……. 84
5.3.2 High-resolution live imaging on chip……. 84
5.3.3 Fluorescence imaging on chip……. 86
5.3.4 Tissue and organ development on chip…….. 89
5.3.5 Comparison of embryo development on chip vs. 96-well titer plate

5.4 Conclusions…… 94

CHAPTER 6 Drug-toxicity on Fish and Chips………. 95

6.1 Introduction…… 95

6.2 Materials and Methods …… 97

6.2.1 Valproic acid and its formulation…… 97
6.2.2 Pilot study of valproic acid in microtiter plates…….. 97
6.2.3 Valproic acid study in Fish and Chips…… 97
6.2.4 Quantification of eyes and tail of developing embryos on chip

6.3 Results and Discussion……. 99

6.3.1 VPA effect on embryos on chip……. 99
6.3.2 VPA effect on tail length of the embryos in Fish and Chips 101
6.3.3 VPA effect on eyes of the embryos in Fish and Chips…… 103

6.4 Conclusions…….. 106

CHAPTER 7 Cell culture on diffraction gratings (Holographic gratings and optical discs CD-R/DVD-R) for potential drug testing……. 107

7.1 Introduction…… 107

7.2 Materials and Methods…….. 109

7.2.1 Processing of the diffraction gratings for cell culture……. 109
7.2.2 AFM/SEM characterization of the surfaces of the diffraction gratings…… 109
7.2.3 Zeta potential measurement of the surface……. 112
7.2.4 Water contact angle measurement of the surface…….. 112
7.2.5 Coating the surface with extracellular matrix proteins….. 112
7.2.6 Mammalian cell culture in Gratings on a dish…….. 112
7.2.7 F-actin staining of cells on the optical discs…….. 112
7.2.8 Measurement of cell alignment……. 113
7.2.9 Alamar blue assay for cell proliferation on the gratings….. 113

7.3 Result and Discussion……. 114

7.3.1 Micro/nanogrooves on the gratings surface…… 114
7.3.2 Characterization of the diffraction gratings surface…….. 117
7.3.3 Cell attachment and alignment on the surface of the gratings120
7.3.4 Cells showed similar proliferation on the grooves as the control surface……. 123

7.4 Conclusions …….. 125

CHAPTER 8 Conclusions……. 125

CHAPTER 9 Recommendations for future research……. 128

9.1 Scaling up the Fish and Chips…… 128
9.2 More organ-specific toxicity using Fish and Chips…… 129
9.3 Drug-testing on Gratings on a dish……. 129
9.4 Other biomedical applications on Gratings on a dish …… 130

CHAPTER 10 References…… 131

APENDIX I Cell culture protocols and explanation of the concentration gradient .....…. 140

SUMMARY

There is a need to come up with innovative methods to fasten the drug development pipeline. The current *in vitro* and *in vivo* methods for pre-clinical drug testing involve either costly human cells or expensive animal models. The need of the hour is to have more efficient and cost-effective platforms for doing drug screening of new molecular entities. Miniaturization can expand the capability of existing drug testing studies.

The thesis proposes two novel platforms for drug screening. First platform, “Fish and Chips” is based on the fact that zebrafish embryos are a valuable emerging vertebrate pre-clinical drug-testing model. Fish embryos were cultured dynamically in the microfluidics chips for longer duration demonstrating development of tissues and organs. High-resolution fluorescent images were obtained using transgenic embryos. Using a model drug valproic acid, the drug testing was done and quantification of organ effects was shown. The second platform is “Gratings on a dish”, which utilizes commercially available diffraction gratings as a cell culture substrate. The gratings surface was treated with organic solvents and was made amenable for cell culture by coating ECM proteins. When multiple cell types were cultured on the gratings, they aligned and cell growth was found to be similar as that of the control. Relevant cell types like cardiomyocytes and neuronal cells can be cultured and aligned on the gratings for better physiology and consequently for drug testing.

LIST OF TABLES

Table.1 Details of the holographic gratings and CD-Rs/DVD-Rs used for the studies.

Table.2 Concentrations obtained at various nodes along the microfluidic network

LIST OF FIGURES

Figure 1 FDA drug approvals.

Figure 2 Microfluidics in drug discovery.

Figure 3 High-throughput technologies available for zebrafish.

Figure 4 Schematic of vertebrate automated screening technology (zebrafish manipulation and imaging platform).

Figure 5 Nanogrooves on PS surface and cell alignment.

Figure 6 Examples of diffraction gratings.

Figure 7 Diffraction gratings of different groove shapes made by various methods.

Figure 8 Cells aligned on grooved collagen membranes.

Figure 9 Fabrication steps for silicon-glass, Fish and Chips.

Figure 10 Design of the PDMS device in AutoCAD.

Figure 11 Design of the silicon-glass device in L-edit.

Figure 12 Blown-out images of the Fish and Chips and arrangement of chips on a wafer

Figure 13 3D rendering of the design of Fish and Chips.

Figure 14 Side-view of the PDMS Fish and Chips.

Figure 15 Side-view of the silicon-glass Fish and Chips.

Figure 16 Actual Fish and Chips devices.

Figure 17 Perfusion set-up for Fish and Chips.

Figure 18 CFD simulations of the flow in fish tanks.

Figure 19 Characterization of the concentration gradient profile in the Fish and Chips.

Figure 20 Obtaining zebrafish embryos from the fish facility.

Figure 21 Bright-field image of embryos placed on Fish and Chips.

Figure 22 Fluorescent imaging on Fish and Chips.

Figure 23 Embryo development on Fish and Chips.

Figure 24 High-resolution images of various tissues and organs of the embryos on Fish and Chips.

Figure 25 Blood flow in the tail of the embryos.

Figure 26 Comparison between development of zebrafish embryos in the Fish and Chips and the microtiter plates.

Figure 27 VPA effects on embryos with 1 mM of drug perfusion.

Figure 28 Effects of VPA on tail development in embryos.

Figure 29 Effects of VPA on eye development in embryos.

Figure 30 Plot of the area of the eyes of control embryos as a function of time (hpf).

Figure 31 Plot of intensity of eyes of control embryos as a function of time (hpf).

Figure 32 Processing the substrate surface of CD-R and Gratings on a dish device.

Figure 33 Schematic of Gratings on a dish.

Figure 34 Topography of the diffraction gratings (CD-R/DVD-R/holographic gratings).

Figure 35 Zeta potential of the top surface of the processed optical discs to demonstrate the charge.

Figure 36 Water contact angles of CD-R/DVD-R/gratings surfaces.

Figure 37 SEM of the CD-R with gelatin coating showing the presence of gelatin nanospheres on the ridges and inside the grooves

Figure 38 Brightfield images showing 3T3 Cells cultured for 24 hrs on CD-R-Gratings on a dish.

Figure 39 Quantification of alignment of HL-1 cells growing on CD-R-Gratings on a dish.

Figure 40 F-actin staining for H9C2 cells after being cultured on holographic gratings (Gratings on a dish) of pitch 1 μm for 2 days.

Figure 41 Alamar blue assays for 3T3 fibroblasts proliferation on Gratings on a dish compared to that on the ungrooved opposite side (control).

Figure 42 New design for Fish and Chips.

Figure 43 Operation of the gradient generator

LIST OF SUPPLEMENTARY VIDEOS (On attached CD)

Video S1 Video showing the beating heart of a Tg(*cmlc2*:dsRed) embryo at 48 hpf.

Video S2 Z-stack image of the neuromast clusters in a 2-day SqEt4 embryo on chip.

Video S3 Video showing blood flow in the tail of the embryos at 80 hpf.

Video S4 Time-lapse movie of a developing embryo in Fish and Chips till 67 hpf.

Video S5 Time-lapse movie of a developing embryo in a 96-well plate.

LIST OF SYMBOLS AND ABBREVIATIONS

3D	three dimensional
3T3	cell lines from primary mouse embryonic fibroblast cells
AB	wild-type strain of zebrafish embryo
ADME	absorption, distribution, metabolism, and excretion
AFM	atomic force microscope
ALT	alanine transaminase
ATCC	American type culture collection
BD	blue-ray disc
Bio-MEMS	biomicroelectromechanical system
BLAs	biologic license applications
BOE	buffered oxide etch
CD	compact disc
CDER	Center for Drug Evaluation and Research
CD-R	compact-disc recordable
CFD	computational fluid dynamics
CYP	cytochrome 450
DI	deionized
DMEM	Dulbecco's Modified Eagle Medium
DMSO	dimethyl sulphoxide
DPF	days post fertilization
DRIE	deep reactive-ion etching
DVD	digital versatile disc
DVD-R	digital versatile disc recordable
ECM	extracellular matrix
EGFP	enhanced green fluorescent protein
ENU	ethylnitrosourea
FDA	Food and Drug Administration
GFAP	glial fibrillary acidic protein
H9C2	cell line from embryonic rat ventricle
HL-1	mouse atrial cardiomyocyte cell line
HPF	hours post fertilization
IACUC	Institutional Animal Care and Use Committee
IMCB	Institute of Molecular and Cell Biology
LA	lens anlage
LEDs	light-emitting diodes
MNNG	N-methyl-N′-nitro-N-nitrosoguanidine
NMEs	new molecular entities
NMP	N-Methyl-2-pyrrolidone
NOA63	Norland Optical Adhesive 63
PBS	phosphate buffer saline
PC	polycarbonate
PDMS	polydimethylsiloxane
PECVD	plasma-enhanced chemical vapor deposition

PET	polyester
PK	pharmacokinetics
PS	polystyrene
PTU	1-phenyl- 2-thiourea
RA	retina anlage
RIE	reactive-ion etching
SDS	sodium dodecyl sulfate
SEM	scanning electron microscope
SqET4	the reporter EGFP (enhanced green fluorescent protein) expressed in the mechanoreceptor cells
TEOS	tetraethyl orthosilicate
Tg(*cmlc2*:dsRed)	transgenic cardiac myosin light chain-2
UCSC	University of California, Santa Cruz
AV	atrial and ventricular
VAST	vertebrate screening platform
VPA	valproic acid
WCA	water contact angle

CHAPTER 1 Introduction

Currently the pharmaceutical companies are facing a serious challenge in producing new drugs. A host of characters including decrease in drug discovery, increasing clinical development costs,[1] patent cliff,[2] delays in drug approvals[3] and economic downturn has added to the woes of the pharma industry. Miniaturization has been explored as a tool in the drug discovery phase.[4] Starting from target identification, compound generation, lead identification and lead optimization all these processes can be modulated by microfluidics methods.[5] Lead optimization is the step that involves usage of relevant cell or animal models for evaluating the efficacy, pharmacology, pharmacokinetics and toxicity of a new molecular entity (NME). The *in vitro* models direct synthesis of new chemicals and are important for comprehending drug action and disposition; *in vivo* models give unique read-out from complex biological systems, which regulate concentrations at site of action and the pharmacologic response. If we can successfully integrate the *in vitro* and *in vivo* experimental data, then we can effectively predict the dose levels assumed safe and therapeutically beneficial. [6]

The popular animal models of drug testing have been rats, mice, guinea pigs, monkeys, dogs, rabbits etc.[7-9] Studies involving the current *in vivo* models are cumbersome, expensive, time and labor intensive, low-throughput and quite unpopular because of ethical concerns.[10, 11] Lately, zebrafish has emerged as a valuable vertebrate model for the pre-clinical drug-screening phase.[10, 12-17] There are many reports confirming the similarity in the toxicity profiles between zebrafish and mammals.[15, 18] The easy maintenance of zebrafish embryos, their smaller size, breeding in larger

numbers, transparency during development and faster development time are some of the unique features that has made it an attractive animal model. However, the current method of maintaining fish embryos in microtiter plates suffers from certain disadvantages.[19] The static culture does not allow replacement of drugs or media, leading to bolus drug doses. Replacement of media by aspiration is an invasive procedure causing stress to the embryos. Moreover, imaging of embryos gets tricky due to depth and meniscus of the media filling the wells. Embryos are not fixed to a plane of view and their movement hampers continuous imaging. Only a recent attempt to culture embryos in a flow-through system has been reported.[20] Hence, there is a great need to develop a perfusion system with appropriate well size for housing the fish embryos for long-term development and imaging. In addition, since drug studies always involve dosage-dependent effects, it would be important to include this aspect in the perfusion system. We have developed such a system, called "Fish and Chips" which answers the concerns with the microtiter plates.

In the case of the *in vitro* cell culture model, numerous microsystems have been explored for drug screening applications like microfluidics-based chips,[21] cellulosic scaffolds,[22] and 3D monolayers[23] etc. The idea is to make the cells physiologically more relevant by having more cell-cell and cell-matrix interactions.[24] In this context, certain cells like cardiomyocytes and neurons need to be aligned for their remodeling and maturation, more so if they have been freshly isolated.[25, 26] There are many chemical and physical methods for creating grooved substrates on which cells can be easily aligned. Chemical modifications of the surface include creating stripes of oxygen-plasma[27] or

phospholipid bilayers[28] etc. Physical methods have been used in plenty and include; laser irradiation[29], silicon-micromachining [30], electron beam lithography,[31] UV embossing,[32] nanoimprint lithography,[33] proton beam micromachining,[34] etc. However, while the chemical methods are non-specific, complicated and need rigorous conditions; the physical methods are time-consuming and need high-skilled labor.[35] Moreover, the creation of large-area grooved substrates is technologically challenging, requires costly equipments, and hence not easily accessible to most of the research labs.[35, 36] Hence, there is a need for cheaper and easier access to grooved surface for aligning cells. We have developed a system "Gratings on a dish" which comprises of commercially available diffraction gratings inside cell culture wells or dishes and can be readily used to culture cells. The aligned cells being physiologically relevant can be used for drug-screening or other biological applications.

In this thesis, two chips (Fish and Chips & Gratings on a dish) have been proposed for drug testing applications. To provide a background for these studies, a detailed literature review is provided in the next chapter. The advantages of microsystems have been commented upon for drug development purposes. The importance of zebrafish as a toxicity model has been assessed and its importance as a high throughput model being highlighted. A detailed background about cell alignment is given and usage of gratings for pattering has been elucidated. The sub-sections 2.3.5 and 2.4.3 provide rationale for Fish and Chips and Gratings on a dish respectively, which leads to the objectives and two specific aims in Chapter 3. In Chapter 4 the designing, fabrication and characterization of Fish and Chips is explained. Chapter 5 demonstrates zebrafish embryo

culture and imaging on the chip while Chapter 6 shows the actual drug testing on fish embryos using valproic acid as a model drug. In Chapter 7, characterization of the diffraction gratings has been done and cell alignment shown. Chapter 8 concludes the major findings of the studies and in Chapter 9 future possible work using the chips have been suggested. The thesis ends with Chapter 10 with a list of references.

Chapter 2 Background and Significance

This chapter presents the background information that defines the rationale for the thesis research. Section 2.1 highlights the current challenges facing the pharmaceutical industry and the need to hasten the drug development pipeline. Section 2.2 elucidates the advantages of miniaturization and its usefulness in the drug discovery applications. Section 2.3 clearly brings out the advantages of the zebrafish as a unique animal model system and how it has been exploited for various toxicity screens and disease models. The same section also reviews the previous work done in integrating the zebrafish model system with the microfluidics platforms, provides limitations of culturing fish embryos in current systems, and concludes with the need for a better perfusion system. Section 2.4 describes the cell orientation on grooved surfaces and various applications of this phenomenon. It highlights the past usage of diffraction gratings for patterning purposes and explains how the gratings can be exploited as a cheaper alternative of current grooved surfaces for cell culture (orientation/alignment).

2.1 The current issues facing the pharmaceutical industry

2.1.1 Declining drug discovery success rates

The global pharmaceutical industry is currently plagued by a crisis in productivity, and desperately needs new sophisticated tools to steer the development of new drugs.[37] The crisis is caused by the declining drug discovery success rates and the high clinical development costs (which is critical to help predict the behavior of potential new drugs in humans from performance in animals and cells). According to the 2006 review by Adams and Brantner,[38] the cost of developing a new drug molecule has gone up over the years and could range from 500 million dollars to excess of 2000 million dollars depending on the therapy or the company developing it. To add to it is the much dreaded "patent cliff" when during the forecast period, 9 of the 14 companies will lose patent exclusivity on their highest-revenue drug of 2008, with the bulk of losses occurring in the 2011–2012 time frame.[2] The estimated loss of $140 billion in revenues by 2016 will take a large bite out of a global business that is expected to rise in sales of $750 billion this year.[39]

An ageing global population is certain to drive pharmaceutical drugs for newer indications such as macular degeneration and Alzheimer's disease. Drugs that can address rising complex disorders such as cancer as well as lifestyle disorders like obesity are also likely to experience stronger demand. As the patient groups become more fragmented and there is improvement in the diagnostic methods, the demand for evidence-based personalized medicine is likely to increase.[40] The sector is also facing unprecedented challenges caused by the economic downturn and the heightening regulatory pressures. The US Food and Drug Administration (FDA) approvals in 2008 totalled 21 new

molecular entities (NMEs) and 3 biologic license applications (BLAs) that were evaluated by the Center for Drug Evaluation and Research (CDER). This number is a slight increase over previous years of 18 in 2007, 22 in 2006 and 20 in 2005. (Fig. 1) Delays in regulatory decisions were also a significant approvals-related trend in 2008. [3]

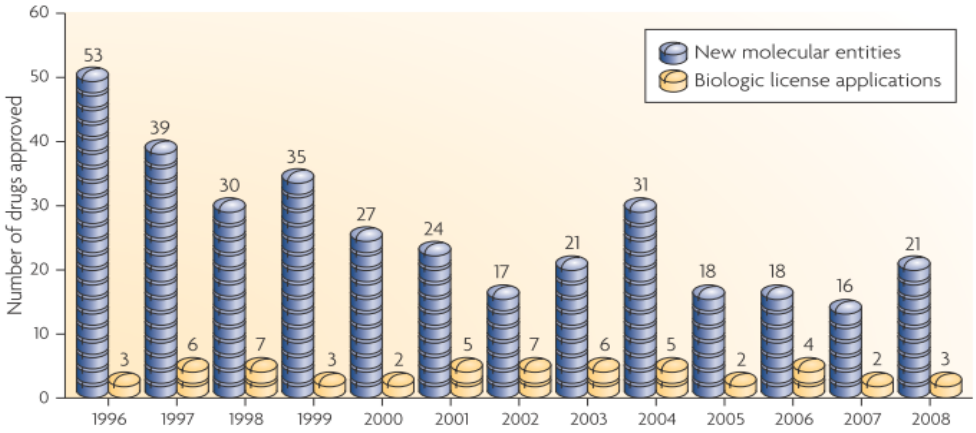

Figure 1: FDA drug approvals.[3] New molecular entities and biologic license applications approved by the US FDA's Center for Drug Evaluation and Research by year. Although there were more approvals in 2008 compared to 2007, it is still short of the higher approval rate of the 1990's.

2.1.2 Need to accelerate drug development pipelines

The enormity of the challenges demands large pharmaceuticals companies to enhance their drug development pipelines. The search for drugs includes robust and fast methods to find, refine and test a probable drug candidate. The discovery of the candidate molecule with unique qualities out of a nearly unlimited number of possibilities is laborious, time consuming and heavily depends on technological resources that are available for handling small liquid volumes, automation, and high-throughput processing and analysis. [5]

2.2 Miniaturization and Drug discovery

2.2.1 The benefits of miniaturization

Miniaturization can enhance the proficiency of existing bioassays, technologies for separation and chemical synthesis techniques. Various components, like pumps, valves, heaters and mixers can be included within fluidic systems to enable the easy manipulation of fluids. The reduction to micrometer scale does not change the nature of molecular reactions but molecular diffusion, the laws of scale for surface/volume and transport of heat leads to spike in throughput. In general, the process of generating new drugs includes two stages: drug discovery and drug development. The discovery stage is divided into target selection, lead identification and pre-clinical studies, while the development stage encompasses clinical trials, manufacturing and product lifecycle management.[4] (Fig. 2) The pre-clinical studies involve both relevant cell culture models and animal models for identifying the efficacy, toxicity, pharmacokinetics (PK) and pharmacodynamics (PD) of a new chemical entity.

Here microfabricated devices/platforms may provide solutions in development of *in vitro* toxicity models: [41]

- The microchannels/chambers replicate the physiological flow conditions better
- They are compact and can be easily multiplexed
- Less use of costly cells and tissues which may reflect precise metabolism
- Less use of a subject chemical; useful when expensive compound
- Cheaper than a macro scale device and can be built in less time
- Many copies of the device can be used at the same time to reproduce the results and save labor

- Integration of different functional units for reaction like valves, mixer and heater
- Fast and controlled heat supply as well as cooling is facilitated due to high surface to volume ratio

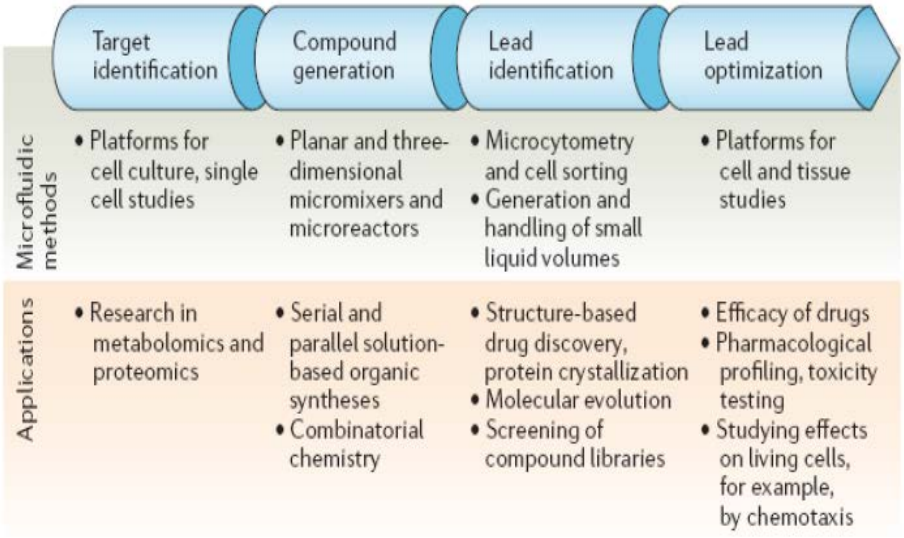

Figure 2: Microfluidics in drug discovery. The figure depicts drug discovery pipeline and the steps that can benefit with the help of microfluidic methods. [5]

2.2.2 Novel micro-scale platforms for pre-clinical studies

The holy grail of the pharmaceutical industry is to be able to predict toxicity from a cell culture.[11] The search for the appropriate *in vitro* platforms in the pre-clinical phases has confounded the researchers for long. Unpredicted drug metabolisms along with drug-induced liver toxicity are the major causes of post-market drug withdrawal.[42] In some studies, cardiovascular related toxicity also ranks similar to hepatotoxicity.[43] If we are able to accurately predict the efficacy, toxicity and PK of drugs in the earlier pre-clinical stages, it would greatly improve the productivity of the drug development

process.[44] The pre-clinical phase involves the evaluation of a NME so that the false lead candidates can be eliminated.

Doing drug research at cellular level helps to bridge the gap between relatively simpler biochemical assays and animal testing. [21] The cells cultured should be faithful to the *in vivo* behavior and hence highly functional. The answer to maintain functional cells *in vitro* is to capture the *in vivo* cellular microenvironment, which includes greater cell-cell, cell-matrix and cell-soluble factor interactions.[45, 46] Microfluidics cell culture chips are popular category of micro-scale platforms, which have been explored for maintaining cell phenotypes.[21] Functional tissues of important metabolizing organs like liver [24] and kidney [47] have already been established in chips. There have been attempts to fabricate 'Human on chip' designs, which houses more than one tissues connected in series via circulation so that it can mimic the circulatory system (which interacts multiple organs in living organisms). [46, 48, 49] Apart from maintaining three dimensional (3D) cell culture system, microfluidics perfusion bioreactors keep the culture system sterile during entire culture periods and simultaneously provide nutrient supply and waste removal (keeping the culture conditions stable). [21, 24, 50]

Another micro-scale platform for cell culture has been polymeric scaffolds. [22, 51] The cells in scaffolds occur in 3D multi-cellular aggregates with very strong cell-cell contact. Hepatocyte spheroids have been shown to maintain many *in vivo* characteristics like polarity, expression of transporters, metabolic functions and improved cytochrome 450 (CYP450) enzyme activities.[22] Spheroid culture has also been demonstrated using microfabricated silicon nitride membranes.[52] This membrane was used for sandwich

culture of primary hepatocytes. The spheroids showed apical polarity, biliary excretion, enhanced drug sensitivity.

Although researchers have been able to predict the drug responses using *in vitro* models, animal testing is still considered the gold standard for pre-clinical studies. The conventional animal studies using popular animal models are costly, complicated, time and labor intensive, with low-throughput and ethical issues. Zebrafish being small, cheap and a whole-animal model offer a unique advantage for exploration in micro-scale platforms and complement popular animal models.

2.3 Zebrafish as a vertebrate model for pre-clinical drug screening

2.3.1 Zebrafish - a unique model for biological studies

The zebrafish, *Danio rerio,* is a powerful vertebrate model for studying a range of biological phenomena.[53] They are small tropical freshwater fishes which originated in northern India and the adjacent countries. The zebrafish comes from a family of freshwater fishes called Cyprinidae.[54] The zebrafish embryo, due to its unique characteristics, is well suited for studies in genetics, embryology, development, and cell biology.

The zebrafish embryos are now becoming an important vertebrate model for pre-clinical drug discovery applications.[10] Many studies have confirmed that mammalian and zebrafish toxicity profiles are extremely similar.[15, 18] Zebrafish has many inherent advantages for drug screening: they are small, inexpensive to maintain and easily bred in large numbers, where a single spawning can produce ~100-200 eggs. [15] This ensures that even a small-scale facility can produce enough eggs for having statistical significant sample sizes for various studies. The morphological and molecular basis of tissue and organ development of this animal model is very similar to other vertebrates, which also includes humans. Zebrafish embryos are completely transparent, facilitating easy observation and analysis. All the precursor tissues of the brain, heart, eyes and muscles can be directly observed using light microscopy. *In vivo* observation of live or whole mount fixed specimens including the visualization of vital dyes, antibodies, fluorescent tracers and riboprobes is also possible.[15]

In contrast to other vertebrate models, zebrafish completes embryogenesis in the first 72 hours. By 5 days post fertilization (dpf), zebrafish develop discrete organs and

tissues, which includes heart, brain, liver, kidney, intestines, pancreas, muscles, bone, nerve systems and sensory organs. Since single embryos can be maintained in fluid volumes as small as 100 µl for the first five to six days of development, they can be kept in individual microtiter wells supported by nutrients stored in the yolk sac.[15] Reagents can then be added directly to the solution in which the embryos develop, simplifying drug dispensing and facilitating analysis. Zebrafish larvae, which are permeable to small molecules through their skin and gills, provide easy access for drug administration and vital dye staining.[18] Small molecules, including peptides, dyes and drugs can be simply dissolved in fish water and freely diffuse into the zebrafish in the presence of a carrier [e.g. 0.1% Dimethyl sulphoxide (DMSO)]. Highly hydrophobic compounds, large molecules and proteins that cannot easily diffuse through skin can be directly injected into the yolk sac, the sinus venosus or the circulation.

Recently, morpholino antisense oligonucleotides are available for suppressing the expression of specific proteins inside a developing embryo (also called the "knock-down" approach).[55] This is helpful in analyzing the effect of a specific protein in development or drug response. Moreover, embryos can also be microinjected with plasmids or capped mRNA to express proteins of choice in the whole embryo or in a particular tissue. The whole genome of the zebrafish is already been sequenced and can be accessed at the University of California, Santa Cruz (UCSC) weblink. [56]

2.3.2 Toxicity assessment in zebrafish

Various drugs have been shown to affect the zebrafish organs:

Cardiotoxicity: In zebrafish, the heart is the first organ to develop and function and a beating heart forms by 22 hpf. Drug effects on cardiac functions, including rhythimicity, heart rate, contractility and circulation are visually assessed in zebrafish at 2 dpf using a simple dissecting microscope. The drugs mitoxantrone, terfenadine, clomipramine and thioridazine, shown to evoke cardiomyopathy, arrhythmia, negative inotropic effects or QT prolongation in humans, also caused bradycardia, [57] abnormal atrial and ventricular (AV) ratio, decreased contractility and slow circulation in zebrafish. In adult zebrafish QT (duration of the ventricular action potential) prolongation in the ECG is taken as an important drug effect.[58]

Hepatotoxicity: Drug-induced liver injury has been recognized by the pharmaceutical industry as a major toxicological problem. Reporter enzyme assays for example biotin and carboxylase present in zebrafish liver and gut have been employed to study the organ specific toxicity after the treatment with merbarone and carbamate.[13] The major CYP enzyme CYP3A4 has been shown to be upregulated in zebrafish treated with dexamethasone, similar to the CYP3A4 response in humans.[59] Visual assessment of liver necrosis is also an accepted method for studying hepatotoxicity in zebrafish. Untreated zebrafish exhibited clear liver tissue, whereas after brefeldin A treatment, zebrafish liver appeared amorphous and gray, indicating necrosis. [13]

Histopathology is also performed on zebrafish samples after drug treatment to check for fat deposits and fibrosis after gamma hexachlorocyclohexane.[60] The collagen in liver tissues can be quantified by the common Masson's trichrome staining method.[61] For

adult zebrafish, after drug treatment, liver histopathology can be performed to assess the levels of liver function enzymes, such as alanine transaminase (ALT) in serum.[62]

Neurotoxicity: Neurotoxic effects of drugs in zebrafish are commonly assessed by checking for the levels of glial fibrillary acidic protein (GFAP) – a universal marker for neurotoxicity.[63] Other assessments include dopaminergic neuron-specific toxicity, motor neurons, neuronal apoptosis and drug effects on motility.[15]

Developmental toxicity: As zebrafish embryos develop outside of the mother and are transparent they are ideal for analysis of drugs that are potential teratogens. In addition, the developmental biology of zebrafish has been well studied and >1000 mutations in developmental pathways have been described.[64] Ethanol[65] and Valproic acid (VPA),[66] which is a histone deacetylase inhibitor, are some of the most commonly studied teratogens in zebrafish. VPA is a well-known teratogen which causes birth defects in children born to women taking this drug during pregnancy.[66] After treatment with VPA, fish embryos show various abnormalities, such as a crooked and shortened tail, shortened axis, oedema and pigment perturbations. [67]

Genotoxicity: Genotoxic properties of compounds must be assessed during drug development because of the potential for mutagenic drugs to cause cancer. Both ENU (ethylnitrosourea) and MNNG (N-methyl-N′-nitro-N-nitrosoguanidine) have been shown to cause tumors in adult transgenic zebrafishes that were exposed to the toxins as embryos or larvae. [68]

Obviously, as a drug-screening model zebrafish has some limitations.[17] Whereas it has most of the organs similar to those in mammals, (liver, pancreas, thyroid, thymus, bile bladder, *etc*.) it lacks some of these (*e.g.* prostate and mammary gland) while some

others maintain some degree of similarity. The swim-bladder resembles the lung [69] and the organization of the skin is similar to that in mammals.[70] In evolutionary terms zebrafish are more distant than primates, which most closely resembles humans. Therefore, the usage of this model system needs to be approached carefully. Importantly, primates and other mammals are too expensive to be used in a large-scale drug screens. Hence, the zebrafish model could complement the classic mammalian models as a first step for *in vivo* drug screening.

2.3.3 Zebrafish for high throughput screens and disease models

In the context of drug discovery, the ease with which zebrafish embryos can be obtained, coupled with their optical clarity, have led to the realization that high-throughput drug screening can be done using embryos arrayed in a microtiter plate format. Love *et al*.[71] have described these platforms, which not only provide high-throughput capability but also significant biological value (Fig. 3). In spite of prominent usage of mouse in modeling human disease, several aspects of murine biology have restricted its regular use in large-scale genetic and therapeutic screening.[71] Many research groups who are interested in an embryologically and genetically flexible disease model have now started using zebrafish. Zebrafish biology grants easy access to all developmental stages, and the transparent clear embryos and larvae enable real-time imaging of developing pathologies. Sophisticated mutagenesis and screening methodologies on a large scale and in a cost-effective way is not possible in other vertebrate systems. Hence, researchers have generated zebrafish models for a wide range of human diseases.[55]

The coupling of pharmacology and disease modelling in zebrafish promises to be especially productive, and it is especially in the area of discovery of new drugs that zebrafish offers advantages over other animal models. Zebrafish is the principal whole-animal vertebrate model for the screening of chemical libraries when it comes to looking for lead compounds with a desired therapeutic bioactivity. Lately, the identification of zebrafish models of genetic and acquired disease has allowed the union of these models with large-scale small-molecule screens, and has resulted in the discovery of new lead therapeutic compounds.

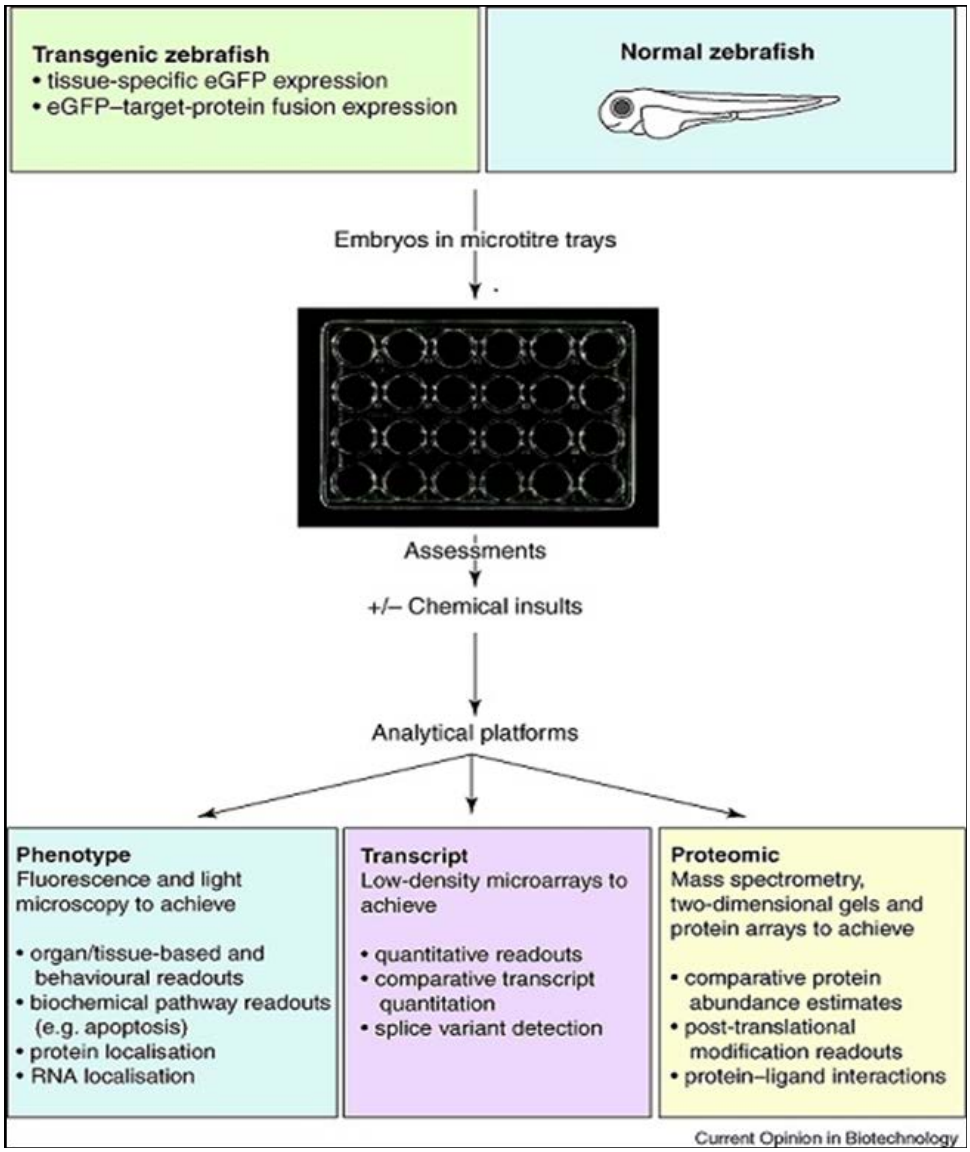

Figure 3: High-throughput technologies available for zebrafish.[71] Transgenic and normal zebrafish embryos can be treated with chemicals/drugs/foreign compounds and later the embryos can be analyzed at the phenotype, transcript and proteomic levels.

2.3.4 Zebrafish and microtechnology

Apart from the classical microtiter plates and Petri dishes, microfabricated platforms have also been explored for various applications in case of zebrafish embryos. In one of the earliest studies, Son *et al.*[72] utilized a droplet-based microfluidic method for

transferring zebrafish embryos. The authors demonstrated the digestion of the chorion of the fish embryo by mixing the droplet with zebrafish embryo with another droplet containing the digestive reagent. The embryo hatched normally into a fish after droplet-based transport as well as dechorionation. In another work, Funfak *et al.* [73] demonstrated normal development of embryos in static culture inside a Teflon tubing. The methods involved growing the embryos inside micro-fluidic segments and move those segments with an organic carrier liquid (perfluromethyldecalin, PP9). Here, the authors also showed developmental abnormalities under the influence of anionic surfactant sodium dodecyl sulfate (SDS).

Other studies involve exploiting the combination of electroporation and microfluidics for delivering foreign compounds into zebrafish embryos. Huang *et al.*[74] developed an electroporation microchip system that could deliver the dye trypan blue and quantum dots into the zebrafish embryos with efficiency of 62% and 36% respectively. Bansal and co-workers[75] devised another electroporation set-up with optimized voltage, pulse-length and number of pulses for transecting both the yolk as well as single cells in the embryos. They got a high survival rate of 91.3% and 89 % of embryos and transfection efficiency of 38% and 50% respectively for GFP-DNA and GFP-mRNA. For the first time they also showed simultaneous delivery of more than one compound at different places inside an embryo. In a very simple design, a team of students developed a microfluidic-bioreactor for housing the embryos, which utilized a gravity-driven pump.[76] The authors claimed that the embryos could survive for a few days in this single-well polydimethylsiloxane (PDMS) device; although the relevant biological data was found wanting.

A very recent study has shown zebrafish embryonic development in a microfluidic flow-through system.[20] In this three-layered bonded glass device, the authors have been able to monitor the development of the embryos for 5 days. Apart from minor phenotypic effects, the development was found to be normal for the embryos. Later the authors performed an acute ethanol toxicity test and scored for various morphological abnormalities. This particular biochip also highlighted the potential for performing high-throughput experiments on the embryos.

Pardo-Martin *et al.*[77] have devised a high-throughput vertebrate screening platform (VAST) in which they can manipulate and orient 2-day fish embryos for cellular resolution imaging (Fig. 4). This platform operates through a sequence of steps: loading of embryos, a photo-detection system of (Light-emitting diodes) LEDs to distinguish between embryos and air bubbles and debris, two stepper motors for rotating capillary tube and hence the embryos, focusing, upright and inverted imaging possible by a hybrid microscope, manipulation of embryo by a laser and final dispensing of the embryos. The authors found the survivability and post manipulation developmental delay of the embryos to be similar in the system as well as the control. They also showed neuronal regeneration after damage by laser microsurgery.

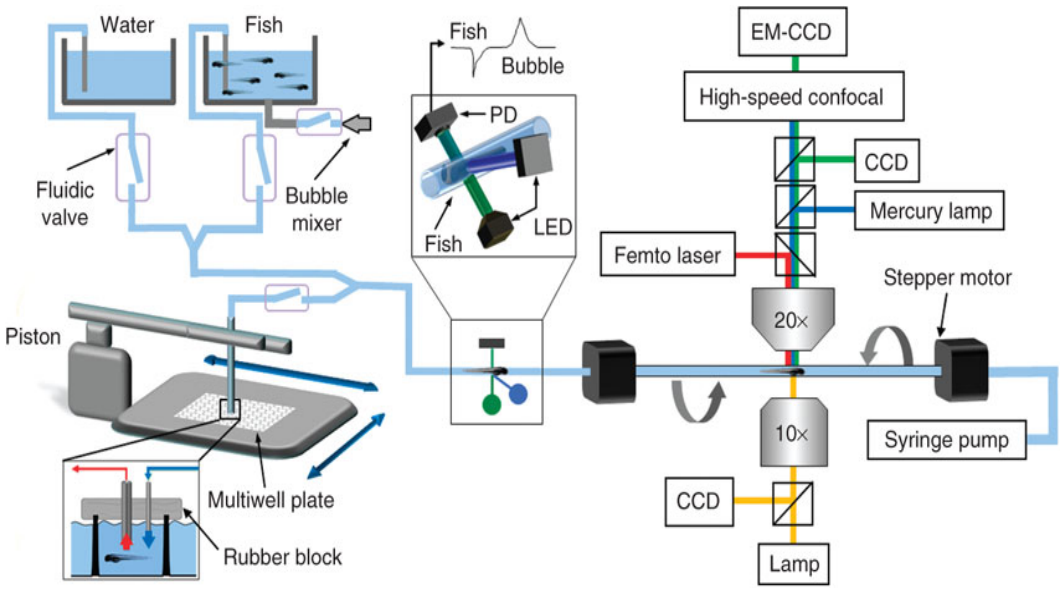

Figure 4: Schematic of vertebrate automated screening technology (zebrafish manipulation and imaging platform). Each cycle of the VAST consists of the following steps: loading, detection, positioning, rotation, focusing, imaging, laser manipulation and dispensing. [77]

2.3.5 Limitations of current platforms and rationale for "Fish and Chips"

The current methods for drugs screening in zebrafish embryos are not adequate. The classical method involves screening in 96 or 384 well microtiter plates.[78] Single embryos are maintained in volumes as small as 100 µl for the first five to six days of development.[18] The microtiter plates do not allow for a perfusion, which means there is no replenishment of media or drugs leading to bolus drug dosage. While replacing the media, the aspiration could cause stress to the embryos and hence would require extreme care. In addition, imaging of embryos in microtiter plates at times are distorted by both the depth of the media filling up the well and the meniscus of the media. Furthermore, live imaging is not possible since the embryos are not constrained to a fixed plane of view.

The most common way of visualizing organs and tissues in embryos [>10-15 hours post fertilization (hpf)] is by first mounting them in a viscous media, such as low-melting agarose or methyl cellulose, and then manually orienting the embryos using fine needles[79] which is a laborious process. Developed embryos need to be anesthetized with tricaine (ethyl m-aminoboenzoate) to restrict their motion and a drop of saline has to be continuously applied to keep the embryos from drying. Therefore, these methods are not suitable for dynamic long-term culturing and imaging of embryos.

The glass microfluidic biochip[20] described in an earlier section could overcome some of the above mentioned disadvantages, but it lacks a concentration gradient generator and hence different concentrations of individual drug or chemical always need to be fed at the inlets. The size of the wells is large and not meant to constrain the embryos and hence would hamper the high-resolution live imaging due to movement of the embryo. The VAST,[77] also explained in earlier section, although permits large-scale chemical screens, it is only applicable for embryos that have hatched out of their chorion. Embryos during gastrulation (1-10 hpf) are highly vulnerable to shear stress due to the high aspiration rates used in this method. This means that live imaging of developing organs in the embryo before 48 hpf in this system is not possible.

Therefore, there is a need of a system, which could satisfy the following characteristics for effective drug screening in zebrafish embryos in early hpf:

- A microfluidic-based dynamic culture platform for zebrafish embryos, which would not only simulate the actual flow conditions in which the embryos grow and develop but refreshment of media and drugs.

- A concentration gradient generator for providing a series of various drug concentrations enabling dose-dependent drug effects on the zebrafish embryos.
- The dimensions of the tank should ensure that the embryo could not move out of the plane of view, thus facilitating live imaging.
- The design should ensure constant and uniform perfusion of media and drug across the whole embryo.
- The material of the device should ensure low-absorption of drug and waste products.
- The device should be able to maintain a temperature of 28.5^{o} C, the optimal physiological temperature for zebrafish embryos.
- The device should be easily scaled-up for high-throughput studies.

2.4 Diffraction gratings as a substrate for cell culture and drug testing

2.4.1 Cell adhesion and orientation along micro/nanogrooves

Basement membranes are ubiquitous throughout the vertebrate body and act as the substrate for the cellular process lying over them.[80] The membranes are made up of extracellular matrix (ECM) components including glycosaminoglycans, fibrous proteins like fibronectin and collagen, nanofibers of growth factors and cytokines, hyaluronic acid, laminin etc. The membrane displays unique features of pores, fibers and ridges in the scale of nanometers.[54, 81] Hence, it is important to study the effect of synthetic micro-nano structured surfaces, which could mimic the topographical cues inside a living body.

Micro/nanogrooved substrates have been explored over the years for orienting/aligning cells in a particular direction for engineering tissues,[82] stem cell differentiation[83] and mechanobiology studies[84] etc. The phenomenon by which cells align along the micro/nanogrooves is called as "contact guidance" and was observed for the first time by Harrison in the year 1912.[85] Weiss [34] defined contact guidance as the process, which occurs, when a cell on a given oriented substratum assumes a corresponding orientation and moves along that line. In this scenario the cell shape and movement are aligned along the topographical features of the substrate and this suggests changes in cellular cytoskeleton.[86]

The earlier methods for guiding cells along a surface were by modifying the surface chemistry of the substrate. The polystyrene (PS) surface is most commonly used for cell culture[87] and has been modified by negative-silver-ion implantation[88], oxygen-plasma treated stripes[27] and phospholipid bilayers[28] to orient the cells. However, the chemical modification of the surface needs rigorous conditions, usually complicated

methods, or coating materials not easily available. If the modified surface layers are thick, then it can modulate the mechanical and functional properties of the material.[89] Many surface modification methods like chemical oxidation or corona results in a milieu of functional groups on the surface instead of just one intended (non-specific reaction). In fact, topography (physical cues) has shown to be a stronger stimulus than chemical ligands for eliciting contact guidance in neurons.[90]

The very first method for making grooves by a physical method was by D.M. Brunette,[30] who simply adapted the micromachining of silicon wafers (from semiconductor industry) and then transferred the grooves to an Epon substrate for cell culture. One of the popular methods to induce periodic grooves on the PS surface is via the ultraviolet-laser irradiation (ULI)[29] (Fig. 5A). *Lu et al.* showed that the water contact angle of the laser-irradiated surface decreased significantly and the human tongue squamous cells carcinomas (HTSCC) showed enhanced attachment and stretched morphology on grooves. In another study using laser-irradiation, Rebollar *et al.*[91] generated nanogrooves on PS foils, which had a periodicity of 200-430 nm and a depth of 30-100 nm. They demonstrated that these nanostructures can guide cell alignment along definite directions and mainly the alignment happens only when the periodicity of those structures is above a critical value and depends on cell-type (Fig. 5B). In UV embossing,[32] carrier films are coated with an UV-curable polyester resin, then printed with an embossing tool containing the micro/nanopattern and photopolymerzied thereafter. Nanoimprint lithography pioneered by Stephen Y. Chou in 1996,[33] involves the usage of compression molding to create a thickness contrast pattern in a thin resist

film coated on a substrate, followed by anisotropic etching to transfer the pattern through the entire thickness of the resist.

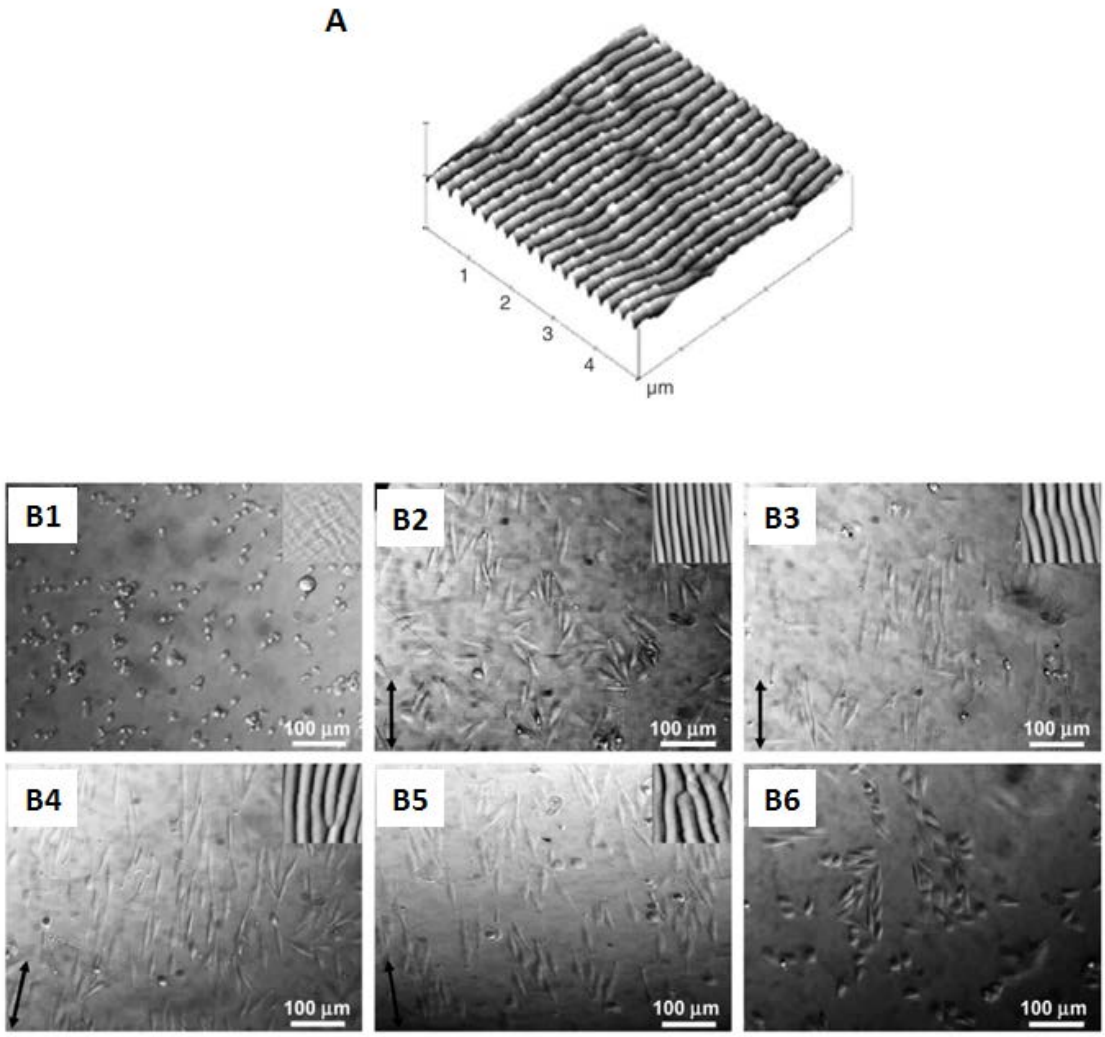

Figure 5: Nanogrooves on PS surface and cell alignment. (A) AFM image showing a three-dimensional view of the PS surface irradiated by laser. Nanogrooves are easily seen with amplitude and periodicity of 30.42 and 290.2 nm respectively.[29] Phase contrast microscopic images of CHO-K1 cells 6 h after seeding on (B1) unmodified PS surface, (B2) PS irradiated at normal incidence, (B3) PS irradiated at 15º (B4) PS irradiated at 30º , (B5) PS irradiated at 45º, and (B6) tissue-culture PS Petri dish, 27 h after seeding. Arrows indicate the direction of the nanogrooves. Magnified AFM images (2 µm x 2 µm) of the PS foils are shown in the insets of the panels. [91]

Electron-beam lithography was employed by Rajnicek *et al.* [31], where they fabricated the grooves on one 6.5 cm square electron beam mask plate and finally cut the plate into 8 individual microscope slides with a diamond saw. Other physical modification of the cell-culture surfaces for cell adhesion and orientation have been photolithography,[92] proton beam micromachining[93] etc. All these methods, involve costly clean-room equipments and protocols. Most of these physical methods to fabricate grooved surface also involve lengthy procedures and need highly skilled labor.[94]

Cells have been shown to align on the grooves, irrespective of the material of the substrate including, polystyrene,[29] polyester,[80] silicon,[30] quartz,[95] polycarbonate,[25] PMMA,[93] epoxy resin,[96] acrylic,[97] titanium,[98] NiTi alloy,[99] poly-lactic acid and its derivatives,[100-102] silicone rubber,[103] silk films[104] and collagen [105] etc.

The aligned cells have been explored for various tissue-engineering applications; growing sheets of vascular smooth muscle cells,[82] remodelling and maturation of isolated cardiomyocytes[106, 107] contact guidance and regeneration of neurons,[31] healing corneal epithelium,[108] orienting osteoblast-like cells,[109] myoblasts[110] and fibroblasts[111] etc. Human mesenchymal stem cells have been shown to differentiate into neuronal lineage[112] after being cultured on nanogratings with growth factors or into osteogenic/adipogenic/chondrogenic on aligned collagen.[113] In another study, human embryonic stem cells were directly differentiated to selective neurons on nanoscale groove patterns without the aid of growth factors.[83] This not only saves expensive reagents but also avoids the trouble to precisely control the exact concentration of those reagents for efficient differentiation. Functional cardiomyocytes growing on grooved surface aided by electric-field stimulation have also been explored for pharmacological

applications.[81] The heart *in vivo* is an anisotropic organ and the cardiomyocytes are aligned in the heart because of the arrangement of the collagen fibers. Hence replicating this anisotropic structure *in vitro* would produce aligned contraction, which is essential for heart function.[114]

The response (morphology and function) of various cell types to different aspect ratios of the grooves have also been studied in great depth.[111] For cells to be aligned, studies have shown that grooves and ridges ranging from 35 nm to 25 μm in width and 100 nm to 5 μm in depth can induce cell alignment. Thus, cell alignment is a robust process in response to topographical cues regardless of the materials of the grooved substrates and dimensions of the grooves within a certain range. However, the creation of large area grooved substrates (especially nanogrooves) presents a technological challenge, involves expensive instrumentation, is time-consuming and not easily available to most of the labs for cell-based screening or research applications.[94, 110]

2.4.2 Usage of diffraction gratings for patterning surfaces

A diffraction grating is an optical device with a periodic structure, which is able to split and diffract light (containing combined wavelengths) into several beams travelling in various directions[115] (Fig. 6). The directions of those beams will depend on the spacing of the grating and the wavelength of the light so that the grating acts as a dispersive element. Diffraction gratings find use in varieties of applications like:

- Spectrometers – tools used to measure different properties of a light source
- Monochromators – tools used to consolidate light wavelengths
- Holograms – three-dimensional images embedded in a flat surface

- Fiber-optic communications – by splitting the data transmitted into varying wavelengths, multiple data streams can be send over the same strand of wire
- Optical Storage Mediums – Digital Versatile Disc (DVD) , Compact Disc (CD) and Blu-Ray disc (BD)
- Lasers – commonly used in devices such as the DVD player or gaming console
- Light Polarization Devices

Figure 6: Examples of diffraction gratings. (A) Holographic diffraction grating film of size 6" X 12" sheet held against light (B) A CD-R with light shined upon.

The first step in making diffraction gratings is to make or rule a master grating. Then one can replicate this master into many numbers of exact copies/replicas for saving capital and ensure consistency of the product. The master gratings are usually manufactured by three main methods:[115]

- Holographic recording - Highly polished and precisely-figured blanks are coated with a layer of photosensitive material, and are then exposed to fringes created by the interference of two coherent laser beams. Later, chemical treatment of the

photosensitive layer selectively dissolves the exposed areas of the photoresist layer, leaving grooves in relief.

- Ion-etching of holographic master- It uses an ion etching system to mill the surface atoms through a holographic mask. The illumination, and successive chemical processing, of a laser-generated interferogram in photoresist form the holographic mask.
- Mechanical - Classically ruled master gratings are made by first evaporating a coating of gold or aluminum onto a highly polished substrate, and then mechanically burnishing triangular grooves using a definite diamond tool.

Gratings of various shapes are depicted in Fig. 7. CD-R and DVD-R are perhaps the simplest examples of diffraction gratings. A CD-R is usually made from polycarbonate and the patterns are drilled in the form of a single spiral track (pregroove).[116] The usual width and depth of each line on the spiral track of a CD-R are approximately 750 and 130 nm respectively, while the separation between the two lines is about 1.5 μm (Fig. 7B).[117] Since the diameter of a typical CD-R (~120 mm) is much larger compared to the distance between two lines and thus under an optical microscope, the lines appear parallel with almost infinite radii of curvatures. The aluminum coating on the polycarbonate surface also has the similar patterns that appear as parallel lines under a microscope. We could easily separate the polycarbonate disk and the aluminum foil from each other. Whereas in case of a DVD-R, there are two joined layers of polycarbonate surface which could be dislodged by applying force between them. The usual width and depth of each line the spiral track of a DVD-R are approximately 400 and 70 nm respectively, while the separation between the two lines is about 800 nm (Fig. 7C). [117]

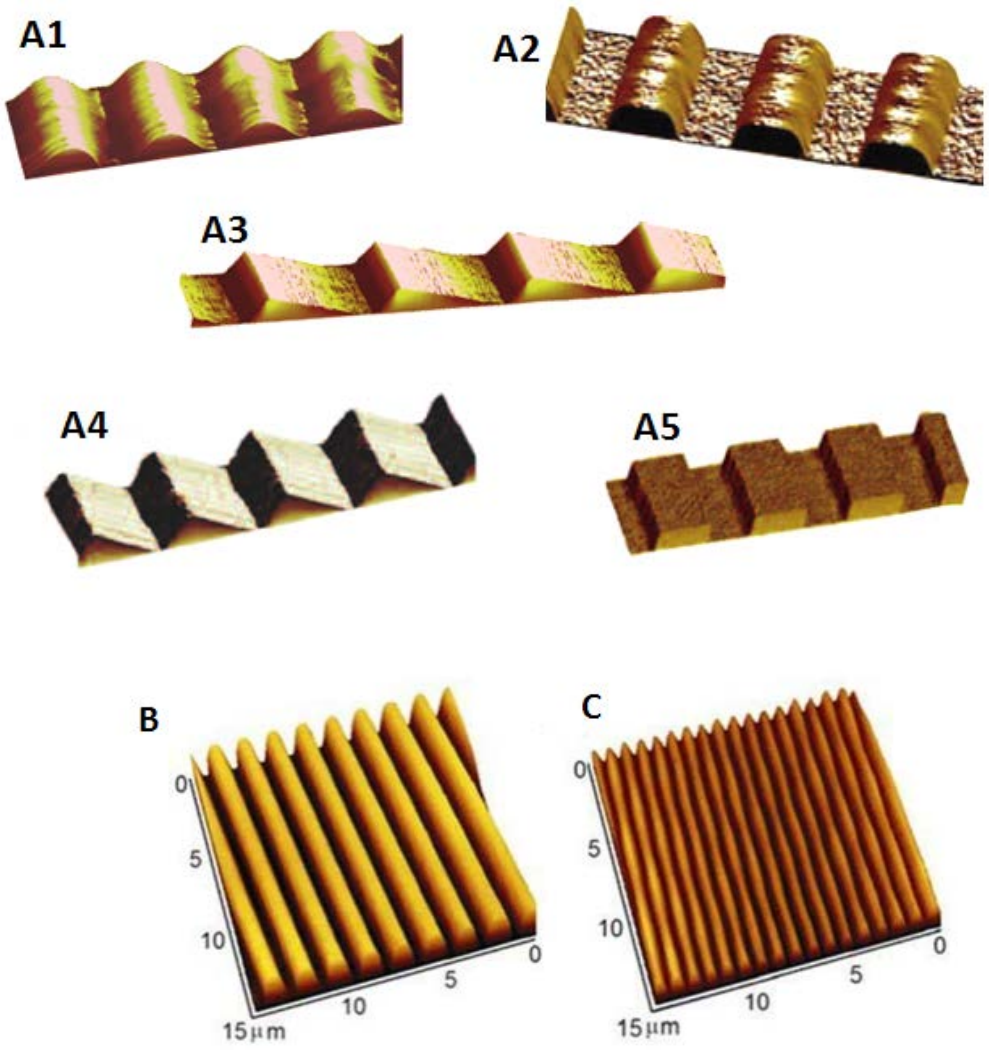

Figure 7: Diffraction gratings of different groove shapes made by various methods.[115] (A1) Sinusoidal made by holographic recording. (A2) Initial pseudo sinusoidal by holographic recording. (A3) Triangular holographically recorded and ion etched groove profile. (A4) Diamond ruled sawtooth profile by mechanically ruling. (A5) Laminar holographically recorded and ion etched groove profile. AFM scans of peeled patterned (aluminium) foils of (B) a CD-R with stripe periodicity, 1.5 μm; stripe width 750 nm; stripe height 130 nm and (C) a DVD-R with stripe periodicity 800 nm; stripe width ~400 nm; stripe height ~70 nm. [117]

An important point to note is, the CD-R and DVD-R mentioned here and later used in the experiments are different from the conventional CDs (compact discs) or DVDs (digital versatile discs). The conventional CDs/DVDs already come with stored data and the surface topography is completely different from the CD-Rs/DVD-Rs. The CDs/DVDs are molded from a master, which transfers the digital data in the form of pits and lands on the polycarbonate surface. While in case of CD-Rs/DVD-Rs, the spiral pregroove (named so because it's molded before any data are written on the disc) is molded from a metal stamper. The pregroove helps to guide the laser beam while writing and reading data. We have exploited this pregroove to our benefits for cell culture and cell alignment.

Chowdhury *et al.* [118] for the first time demonstrated that, the two dislodged layers of polycarbonate and aluminum from the CD-R could be used to generate similar 2D patterns. They generated submicron-scale color patterns on overhead projector (OHP) films and microscope glass slides. In another elaborate study, Mukherjee *et al.*[117] used the patterned foils of CD-Rs/DVD-Rs and the patterned flexible stamps of polyvinyl alcohol (PVA) [made from CD-Rs/DVD-Rs as mold] to imprint various kinds of polymers. They successfully patterned PDMS and polyacrylamide (PAA) based hydrogels, thermoplastics like polystyrene, polymethyl-methacrylate (PMMA) etc., both on planar as well as curved surfaces.

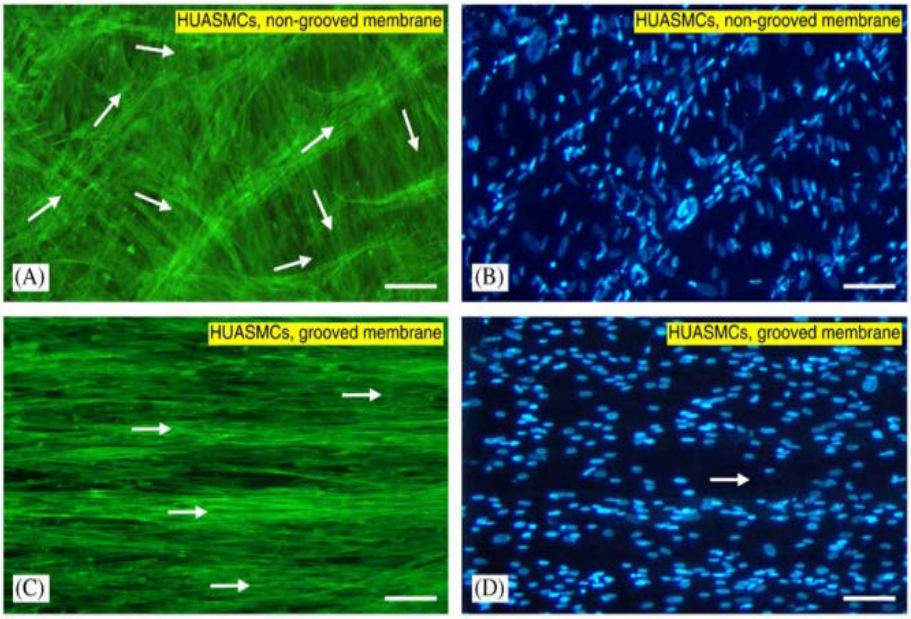

Figure 8: Cells aligned on grooved collagen membranes. Human umbilical artery smooth muscle cells (HUASMCs) were cultured for 6 days on collagen membranes either lacking grooves or with grooves made with phonograph records. The cells were doubly labeled with phalloidin (A and C) and DAPI (B and D). On the non-grooved surfaces, the cells organized into multi-direction streams as reflected with the F-actin staining (A), while on grooved surface cells aligned along the horizontal grooves (C). Orientations of the long axis of the nuclei correlated with the orientation of F-actin (B and D). [105]

Robert B. Vernon and co-workers[105] have exploited the commercially available diffraction gratings (plane-ruled diffraction gratings and holographic diffraction gratings) as well as phonographic records to act as templates for collagen membranes (Fig. 8). This was the first study showing a self-supporting microgrooved scaffold made wholly from a natural biological material, i.e., native, fibrillar type I collagen. Human fibroblasts and smooth muscle cells were cultured on these membranes showing strong adhesion, proliferation and spreading. In a similar study, Gil *et al.*[119] made use of reflective diffraction gratings as replica substrates. Patterned PDMS surfaces were prepared by casting on a series of gratings, later silk films were prepared by casting silk solution on the prepared PDMS substrates. Human corneal fibroblast cells were cultured on the thin

silk films and the effect of groove width and depth was measured with respect to cell proliferation, cell orientation and ECM alignment.

2.4.3 Limitations in producing current grooved surfaces and advantages of using diffraction gratings directly for cell culture and drug testing (Gratings on a dish)

The creation of large area grooved substrates presents a technological challenge and depends on costly and tedious clean-room equipments and protocols.[35] We propose that the surface of the commercially available diffraction gratings (optical discs like CD-Rs/DVD-Rs and holographic gratings) can be directly utilized to culture cells and align them for various applications when the materials are properly processed. These gratings come at very small fractions of a cost compared to the costly clean room methods used by labs for generating the patterns on substrates.

The diffraction gratings have been used as templates in a few studies for patterning other polymer surfaces like collagen and silk for cell culture applications (described in previous section). However, no one has shown direct cell culture on the surface of the diffraction gratings which upon simple processing is possible. Since the surface of the gratings contain other layers of materials (acrylic and dyes in the case of optical discs) and is non-sterile, it has not been obvious to consider culturing cells on the gratings directly. In this regard, our innovation includes the sequence of processing steps to make the gratings amenable for culturing cells. The processed gratings are subsequently cut into smaller pieces and incorporated into the cell culture wells/dishes (Gratings on a dish).

This novel way of utilizing easily available diffraction gratings as a cell culture platform (Gratings on a dish) would open up avenues for large-scale adoption of aligned

cells for biomedical research and development applications. For example, it is known that replicating the cardiomyocyte alignment *in vitro* can improve the velocity of propagation, force of contraction and gene expression of both contractile proteins and adult phenotype markers in the cardiomyocyte.[25, 120] It can also increase the calcium movement across the sarcoplasmic reticulum and the cytoplasm.[121] Moreover, replicating the cardiac anisotropy would help to study the arrhythmogenesis *in vitro*, as the velocity of the signal propagation is more along the longitudinal axis compared to the transverse. [122]

Diffraction gratings as direct cell-culture substrate offers important advantages over the currently made grooved surfaces:

- The micro-nano grooves on the gratings can simulate biomechanical cues of the extracellular matrix materials around the cell
- These could be utilized for cell culture on large surface areas (e.g. the holographic gratings we have used are in the form of 6" X 12" sheets or 6" X 200' roll) Compared to the gratings, the patterned size produced by other methods are:
    a. laser irradiation - for petri dish of up to 6 cm in diameter
    b. hot embossing - mold silicon of 4" in diameter
    c. electron beam lithography - 5mm x 5mm block of quartz
- The retail market price of
    a. CD-R/DVD-R is <S$1 a piece (e.g. ~60 cents for an Imation CD-R) [123]
    b. Holographic grating ~S$8 (Edmund optics, Holographic diffraction film) [124] for a 6"x12" sheet size (one holographic grating can be used for ~7, 24-well plates)

- The commercially available gratings are ready-to-use with faster, easier and fewer processing steps for cell culture
- User is free from costly clean-room equipments and lengthy protocols
- Involves transparent substrates and hence convenient to image
- Small labs, or start-up companies with less capital can utilize the gratings for elaborate biological studies
- The used CD-Rs/DVD-Rs, which are discarded as waste and pose environmental concern , can be re-used before they are recycled[125]

CHAPTER 3 Objectives and Specific Aims

This thesis aims to propose two novel microfabricated platforms for drug testing. As covered in section 2.3.5, the current zebrafish platforms for drug testing (microtiter plates) suffer from numerous disadvantages including static culture, distortion during imaging and bolus drug dosage etc. We aim to fabricate a microfluidics chip "Fish and Chips", which would enable us to overcome the limitations posed by the microtiter plates. The chip would also include a gradient generator to enable dosage-dependent drug effects on the developing zebrafish embryos. As highlighted in section 2.4.3, fabricating the current micro-nanogrooved surfaces for cell culture are extremely laborious and involves a large amount of capital and skilled workforce. To answer this problem, we aim to exploit the commercially available diffraction gratings for cell culture. Our device "Gratings on a dish" would be able to maintain the cells in their matured phenotypes for drug testing applications. All these efforts are elaborated in the following sections about the two specific aims of the thesis research, with a hypothesis and experimental design for each aim.

3.1 Specific Aim1: To fabricate a microfluidic perfusion system for growing zebrafish embryos and perform drug testing

Hypothesis

A multichannel microfluidic platform can be fabricated with an integrated gradient generator, which would restrict the embryo movements enabling high-resolution imaging and dosage-dependent drug testing.

Experimental design

- Design and fabrication of Fish and Chips in two schemes: PDMS and silicon-glass

- Characterization and optimization of flow in the chip
- Optimization for embryo culture and high-resolution imaging on chip
- Proof-of-concept drug testing on chip with a model drug

3.2 Specific Aim2: Processing of large-area, low-cost diffraction gratings (holographic gratings and optical discs CD-R/DVD-R) for cell alignment and potential drug testing

Hypothesis

The commercially available diffraction gratings can be processed and made suitable for cell culture and cell alignment.

Experimental design

- Processing of diffraction gratings with organic solvents and assembly of Gratings on a dish
- Characterization of the diffraction gratings
- Optimization of ECM coating, cell number, media for successful culture of cells on gratings
- Measurement of cell alignment, cell viability and proliferation on the gratings

CHAPTER 4 Fabrication, characterization and optimization of Fish and Chips

4.1 Introduction

The design of a microfluidic perfusion system depends on a host of characters: the choice of material for conducting the liquids, the choice of the substrate for chip attachment, the basic layout of the chip, mode of fabrication, sterilization and packaging of the device.[126] The materials for the microfluidic channels should be able to easily conduct liquids through it. Many a times the substrate material is same as the conducting material like PDMS microfluidics channels on PDMS substrate or different like PDMS microfluidic channels on glass substrate. The traditionally used materials for lab-on-a-chip devices have been silicon[127] and glass.[128] Polymers have also been explored to fabricate the chips.[129, 130] Some common polymers used include PDMS,[84] PMMA,[131, 132] polycarbonate,[133] polysulfone,[134] UV-curable like Norland-optical adhesive (NOA63) [108] etc.

However, PDMS remains the choice of most users for fabrication of microfluidic systems for biomedical applications.[135, 136] The various advantages of PMDS which makes it so popular are: cost-effectiveness, non-cytotoxic, transparent, low autofluorescence enabling easy imaging, autoclavable and gas permeable etc.[137] Moreover, PDMS being a flexible elastomer it supports the creation of valves and pumps integrated in the chip itself.[138] Soft-lithography a concept introduced by George Whiteside's group is the most common way to fabricate PDMS chips.[26, 139] We have followed this approach in fabricating our PDMS version of Fish and Chips.

Silicon which had laid the foundation of the semiconductor industry[140] is also being increasingly exploited for Bio-MEMS applications.[141] Kotzar *et al*.[142] have done a

thorough study of silicon-derived materials for biocompatibility. They showed that materials like single crystal silicon, polycrystalline silicon, silicon dioxide, silicon nitride, single-crystal silicon carbide, and the photo epoxy SU-8 substrates were not toxic to mouse fibroblasts in *in vitro* cultures. Silicon-based materials have been used for various applications like amorphous silicon membrane for hemodialysis,[143] scaffold for attachment and growth of mammalian cells,[144] porous silicon fabricated from single crystal silicon has been exploited for drug delivery.[145] An important advantage of using silicon for microfabrication is the capacity to fabricate features with large aspect ratio of almosts, 1:20, i.e. for a given width, almost 20 times more depth for the same feature. Hybrid silicon-glass devices offer some unique advantages[146] including packaging and world-to-chip connections and hence we fabricated our second prototype Fish and Chips in silicon and glass.

For microfluidic chips designed for drug testing it is important that we are able to check the effect of various dose levels simultaneously. There have been few studies involving the usage of gradient generators to automatically generate multiple concentrations of compounds [147] or drugs [148] in microfluidic devices. Precise designing of the microfluidic network which allows for controlled diffusive mixing of substances can generate various shapes of gradients[149] like linear, periodic, parabolic etc. Most of these works utilize a fluorescent dye assay to determine the experimental values of the concentrations. The gradients generated with microfluidic channels are spatially and temporally stable compared to other alternative methods like Boyden chamber[150] or through regular pipetting for diffusion.[151] We have incorporated a sigmoidal gradient generator in our design and tested the fidelity of it using Rhodamine G dye study.

Computational fluid dynamics (CFD)[152] is an useful tool that has only recently been employed for biological studies in microscale environment. CFD enables to better comprehend the hydrodynamic environment and the factors that can affect it. Previously CFD has been popular in chemical and mechanical engineering fields, but now it is enabling us to grasp the impact of fluid flow and transport on cell phenotype and function and hence providing advantage on the design and optimizations aspects of a cell culture chip.[153] We also employed CFD to simulate two different flow schemes in our Fish and Chips.

4.2 Materials and Methods

4.2.1 CFD simulations for fish tanks

For the design of the chip, two different flow schemes were envisioned. In the first one, in which the flow would travel diagonally across the fish tanks from inlets to the outlets, while in the second one the flow would just pass along the bottom of the tank. CFD simulations of the flow pattern across the tanks were performed using CoventorWare (Coventor, USA) to determine which flow would be more advantageous for the study.

4.2.2 1st prototype: PDMS chip design

The design consists of drawing two mask layers in AutoCAD (Autodesk Inc, USA). The dimensions of the inlet and outlet channels were 50 μm and 100 μm, respectively. The diameter of the inlet and outlet holes was 700 μm. Different dimensions of the fish tanks were tried from 1.2 to1.5 mm.

4.2.3 PDMS chip fabrication and connection

The two layers of the chip were made from the two respective silicon templates by replica molding PDMS (Dow Corning, USA). For both layers, a mixture of 1:10 (curer: base) was degassed in a vacuum oven (VWR International, USA) and spin-coated (Laurell Tech.,USA) on a master at 50 rpm, resulting in a 250 μm thick layer. This was cured for 2 hrs at 80^{o}C (Memmert, Germany). Holes where punched for the 2 inputs to the gradient generator and the 8 outputs with the help of a punch machine (Technical Innovations Inc., US). The the fish tanks were punched using 1.2-1.5 mm diameter punchers. The PDMS structure was then plasma-oxidized with a Corona Surface Treater (Electro-Technic Products, USA) before irreversibly bonded to a microscope slide, which

also had the plasma treatment. Tygon tubing (Fisher Scientific International, USA) of inner diameter 0.05 cm was connected to small stainless steel tubes (New England Small Tubing Company, USA) of inner diameter 0.035 cm, which in turn were inserted into the punched holes, for a firm fit for both inlets and the outlets. The tygon tubing connected to the inlets was later connected to a syringe pump (Harvard Scientific, USA) via syringes for perfusion.

4.2.4 2nd prototype: Silicon-glass chip design

The silicon-glass chip was designed using L-Edit Pro software (Tanner, USA). For the ease of fabrication, 4 different masking layers were designed in the software. Each of the masking layers drawn in different colour schemes in the software define a certain component of the chip as follows:

1. The inlet channel, microfluidic gradient generator, fish tanks and via channel
2. The fish tanks, outlet channels, inlets and outlets
3. Etch through holes such as inlet/outlet holes, via connection and fish tank from the inlets surface
4. Etch through holes; such as inlet/outlet holes, via connection and fish tank from the outlets surface

The width of the inlet channels was 50 µm whereas the outlet channels were kept 100 µm. The diameter of the inlet and outlet holes was 700 µm. The fish tanks had circumferential wall with diameter of dimensions 1.4 mm.

All the four layers were written into four different masks with a laser writer (Heidelberg Instruments, Germany). The chrome mask was developed by using a mixture of the developer AZ 400 and water (1:4 ratio). The masks were cleaned in an ultrasonic

NMP (N-Methyl-2-pyrrolidone) for 15 mins. Later the masks were dried in an oven (70 ºC) and used for photolithography.

4.2.5 Silicon-glass chip fabrication

The Fish and Chips was obtained by a sequence of photolithographic, etching and bonding steps. The main steps of the fabrication process are shown in Fig. 9. The fabrication process consists of two DRIE (deep reactive-ion etching) steps on both sides of the silicon wafer. In order to achieve this, two masking layers (photoresist and PECVD SiO_2) are used on each side of the wafer. A photoresist mask was used to pattern the etch-through holes while the SiO_2 mask was used for the definition of the microfluidic circuits. The fabrication process was performed on 4" double-side polished, 1 mm thick single crystal silicon wafers, with <100> crystallographic orientation and resistivity of 1-100 Ωcm. The wafers were cleaned in a piranha solution (H_2SO_4 /H_2O_2 in ratio 2:1) at 120 ^oC for 20 minutes, which removes organic contaminants from substrates, followed by rinsing in deionized (DI) water and spun dry (Fig. 9(b)). A 1µm-thick SiO_2 layer was deposited in a PECVD furnace (SPTS, USA) – at low frequency (380 MHz), with a RF power of 700 W, from pure SiH_4 and N_2O with flow rates of 50 sccm and 400 sccm, respectively, at a pressure of 450 Pa, and a deposition temperature of 300 ºC. The deposition of the oxide layer was performed on the both sides of the wafer (Fig. 9(c)). In the next step (Fig. 9(d)), a photolithographic process was performed in order to define the mask for the microfluidic gradient generator.

The photolithographic process was followed by the etching of the oxide layer in an RIE (reactive-ion etching) system (STS, USA) using CHF_3 and O_2 at flow rates of 40 sccm and 4 sccm respectively, pressure of 100 mbar and an applied power of 150 W. The

SiO_2 mask for the channels on the opposite side of the wafer was carried out in a similar way (Fig. 9(e)). A third masking layer (that defines only etch through holes such as inlet/outlet holes, via connection and fish tank) was applied on the back of the wafer (Fig. 9(f)) followed by a classical deep RIE (Bosch process) 400 µm deep on an ICP DRIE system (Alcatel, USA) - (Fig. 9(g)). After removing, the photoresist layer in an NMP (N-Methyl-2-pyrrolidone) solution the dry etching process of (100-µm depth) is further performed through the SiO_2 mask to etch the microfluidic gradient generator (Fig. 9(h)). A 300 nm thick TEOS (Tetraethyl Orthosilicate) layer was deposited with a PECVD reactor on the generated surface as etch-stop layer (preventing notching effect) (Fig. 9(i)) for the next dry etching processes. In a similar manner, the outlet channels were fabricated (Fig. 9 (j-l)). For these steps, the processed silicon wafer was temporarily bonded with wax on a dummy silicon wafer (Fig. 9(k-l)). To de-bond the dummy wafer, it was kept on a hotplate at 110 ºC and later cleaned in an ultrasonic NMP tank. The SiO_2 layer –used in the previous steps as mask – was removed in a classical BOE (buffered oxide etch) solution (Fig. 9(m)).

In order to generate a hydrophilic top surface for the microfluidic structure a 150 nm thick thermal SiO_2 layer was grown using a classical dry oxidation process in a oxide furnace (Tystar, USA) at 1000 ºC for 30 min (Fig. 9(m)). In the next step (Fig. 9(n)), the silicon wafer was anodically bonded to a glass wafer (4” CORNING 7740, 500 µm thick). This bondable glass wafer had a coefficient of thermal expansion similar to the silicon wafer. The bonding was performed at 350 ºC, with an applied voltage of 1000 V and applied force of 500 N. After bonding, the glass was thinned to 150 µm for a better

visualization under the microscope. Thinning was performed using an optimized wet etching process in HF(49%)/HCl (37%) in ratio of 10/1[154], assuring a final roughness of the glass surface of around 10 nm.[155] The process was performed with a mechanical protection to the other side of the wafer (wax bonding on a dummy silicon wafer - process previously described). The glass material was selected due to its chemical composition, being suitable for bonding to silicon and also for wet etching.[156] The wafer was finally diced into individual chips using dicing saw equipment (Disco, Japan).

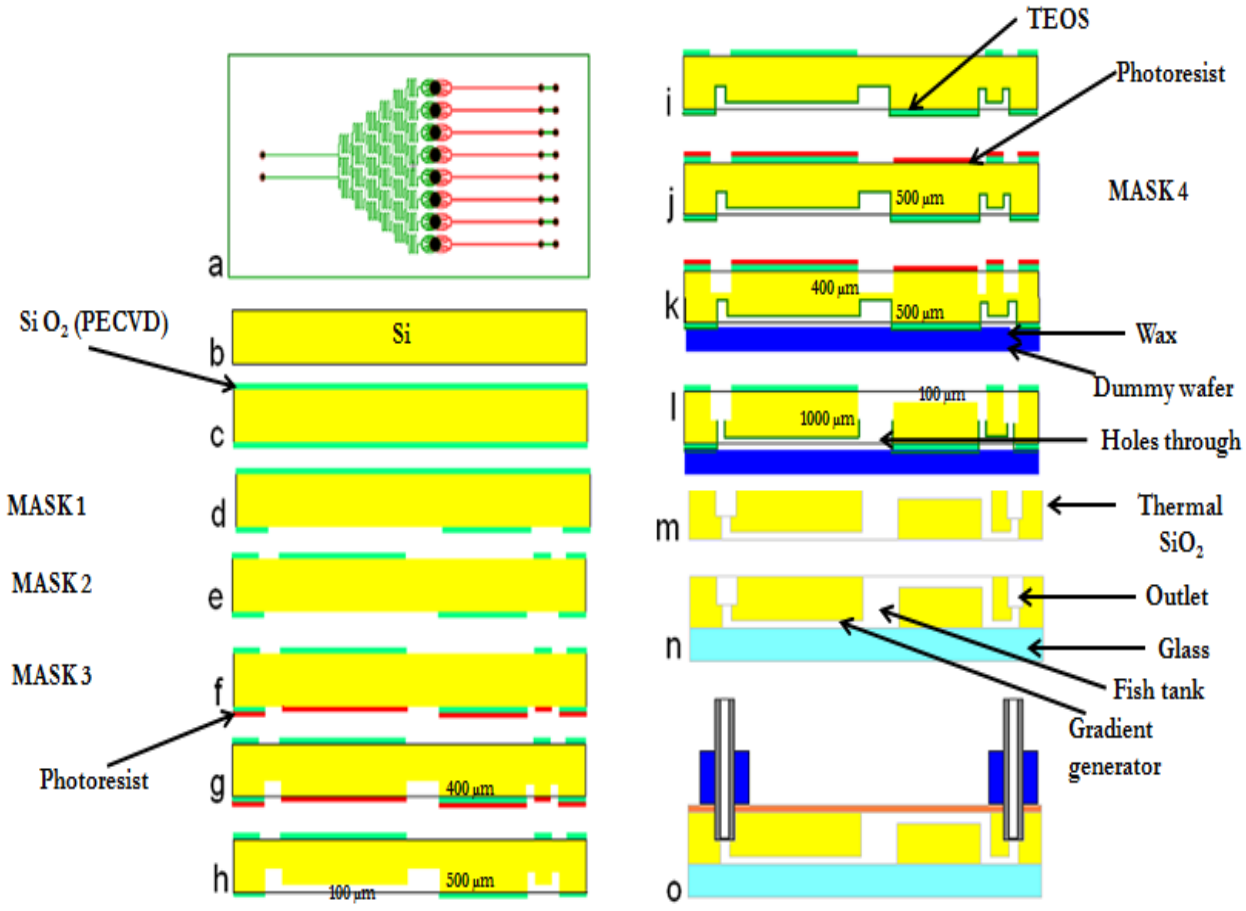

Figure 9: Fabrication steps for silicon-glass, Fish and Chips: It shows a sequence of photolithography, etching and bonding steps. (a) layout of the chip (explained in detail in Fig. 11); (b) 1 mm-thick silicon wafer; (c) Deposition of 1 µm-thick PECVD SiO_2 on the both sides of the wafer; (d) Patterning of the SiO_2 layer (mask 1 with the inlet channels and flow gradient); (e) Patterning of the SiO_2 layer- opposite side- (mask 2 with the outlet channels); (f) Deposition of the photoresist mask 3 for etch-through holes; (g) DRIE etching of Si– 400 µm deep (etch through holes); (h) Removal of the photoresist mask and etching of microfluidic flow gradient– 100 µm deep; (i) Deposition of 300 nm PECVD TEOS (protection layer); (j) Deposition of the photoresist mask for etch-through holes (mask 4 on the opposite side of the wafer); (k) DRIE etching of Si – 400µm deep (etch through holes) while the Si wafer was temporary bonded on a support wafer; (l) Removal of the photoresist mask and etching of microfluidic channel– 100 µm deep. Now all the holes are through (1000 µm etched in total); (m) Removal of the SiO_2 and TEOS layers and growing of 120 nm thick thermal SiO_2 (dry); (n) Anodic bonding of the silicon wafer on a Pyrex glass wafer; (o) Dicing and packaging (explained in detail in Fig. 15) of microfluidic chip.

4.2.6 The perfusion flow set-up

The chips were operated by the syringe pumps with tubings, valves and syringes acting as the interface.

4.2.7 Flow characterization of the Fish and Chips by fluorescent dye studies

The fully assembled PDMS chip was bonded with a thin strip of PDMS on top to cover the fish tanks. A stock solution of 800 µM of the dye Rhodamine G was prepared in 1X PBS (phosphate buffer saline). A working concentration of 100 µM was used for the dye study. The PBS-based dye solution was filtered and degassed before perfusing through the chip. The chip was then primed by introducing 1X PBS at both the inlets with 1 ml syringes (Becton, Dickinson and company, USA) and by applying pressure manually. The priming syringes were withdrawn carefully. Then 100 µM Rhodamine G solution and 1X PBS were introduced into each of the 2 inlets of the device at a combined flow rate of 200 µl/hr with the help of a syringe pump (Harvard Scientific, USA).

After 4 hours of perfusion, fluorescence images of each of the fish tanks were captured with a Fluoview 500 confocal microscope (Olympus, Japan) at 433 nm laser excitation. The fluorescence intensity of 100 random points in each image was determined using Matlab (MathWorks, USA). The average fluorescence intensity in each tank was calculated and normalized against the highest dye concentration.

For the silicon-glass device, the flow characterization was done in similar way as the PDMS device. But instead of thin strip of PDMS, an oxygen permeable membrane (USA Scientific, USA) was used to cover the top of the fish tanks.

4.3 Results and Discussion

4.3.1 Design of the Fish and Chips

The PDMS device (Fig. 10) was designed with AutoCAD and the silicon-glass device (Fig. 11) by L-edit software. The four layers of the design of the silicon-glass device are depicted here. For the silicon-glass device, the close-ups of the inlet layer, outlet layer and gradient generator are shown with dimensions (Fig. 12A-B). The design was such that four Fish and Chips could be accommodated on a 4" silicon wafer (Fig. 12C).

The diameters of the inlet and outlet holes were made 700 µm so that the steel tubing would have a tight-fit with the chip. The width of the channels from the inlets (including the gradient generator) was kept 50 µm to allow a build-up of resistance and hence optimum mixing of the streams to easily generate a gradient. Just before the gradient opens up into the fish tanks, the channels were widened to 100 µm for enhanced flow. The outlet channels from the fish tanks were kept widened at 200 µm for easy and faster disposition of spent media from the fish tanks. The lengths of the inlet and outlet channels were kept long for convenience in imaging from the top of the chip. While imaging from the top, using an up-right microscope the objective lens needs to be close to the top surface of the chip and shorter channels would mean the lens would face resistance from the tubings connections nearby.

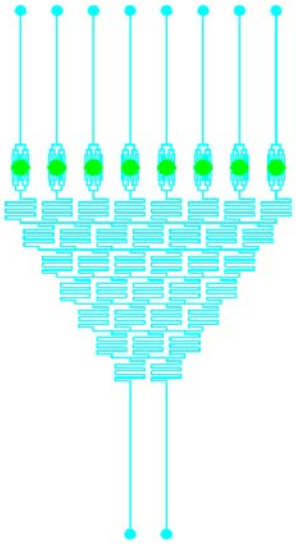

Figure 10: Design of the PDMS device in AutoCAD. The two inlets directly draw into a gradient generator, which flows into the 8 fish tanks. The outlets are drawn out from the fish tanks. The diameters of the inlets and outlets are same (700 µm). The width of the inlet channels and the gradient generator is 50 µm whereas the outlets are 100 µm wide.

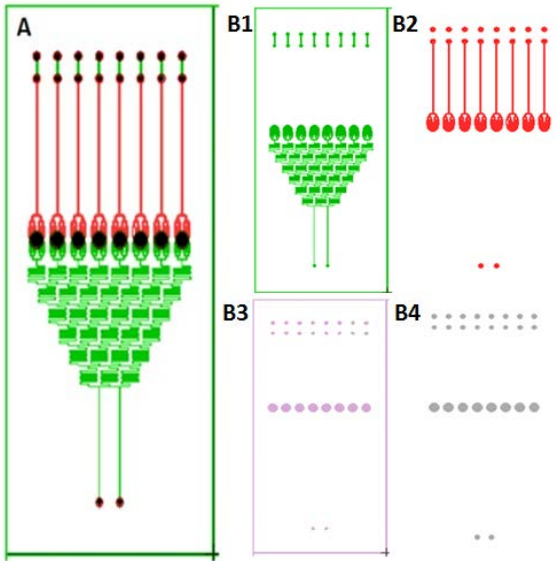

Figure 11: Design of the silicon-glass device in L-edit. **(**A) Image showing all the four design layers superimposed in the software. Design of four individual design layers (masks) of silicon-glass device are extracted on the right. (B1) Layer to define the inlet channel with the microfluidic gradient generator; (B2) Layer to define the outlet channels; (B3) Layer to define only etch through holes such as inlet/outlet holes, via connection and fish tank from the inlets surface; (B4) Layer to define only etch through holes such as inlet/outlet holes, via connection and fish tank from the outlets surface.

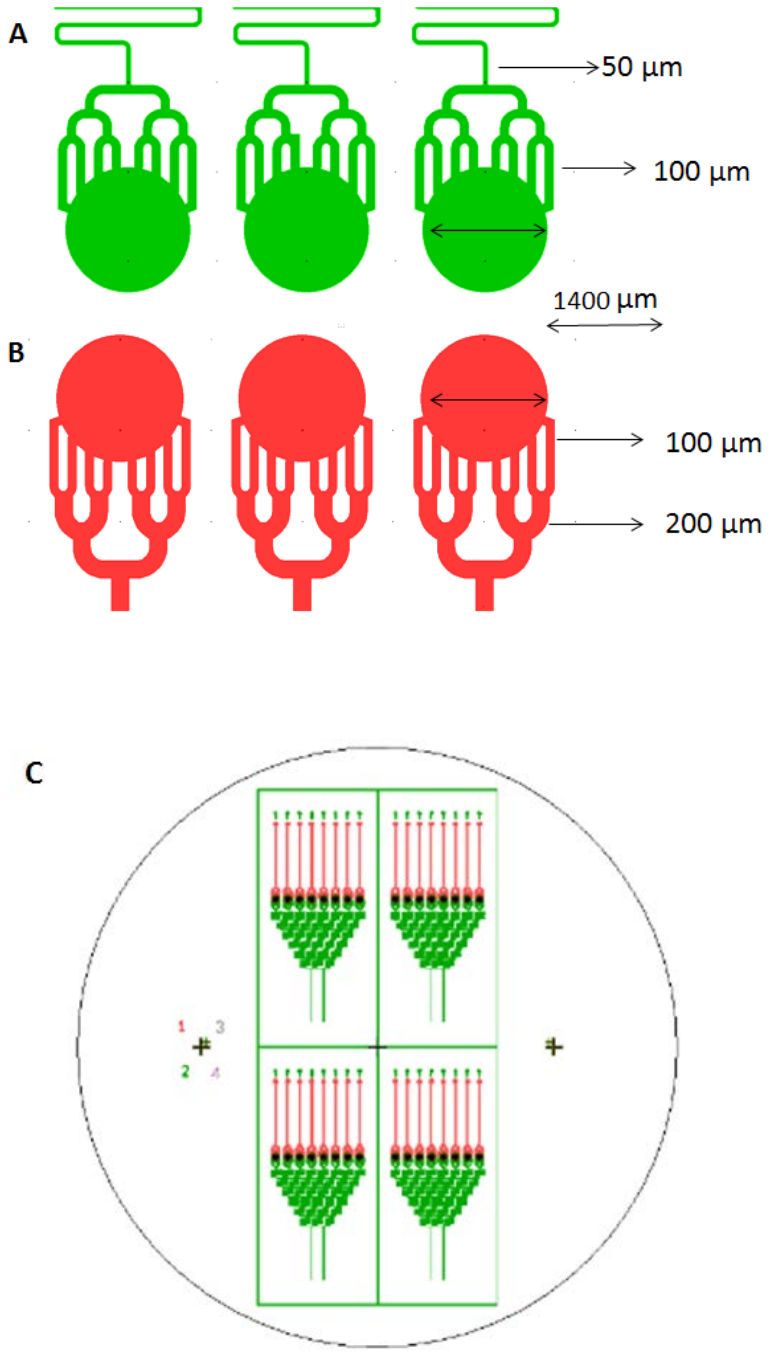

Figure 12: Blown-out images of the Fish and Chips and arrangement of chips on a silicon wafer. (A) Gradient generator leading to Fish tanks (B) From fish tanks to outlet channels. As seen, the inlet and outlet layers act through a network of narrow channels near the fish tanks to get uniform and gradual fluid passage through the tanks. (C) The design showing positioning of four chips on 4" wafer space. The wafer was finally diced into individual chips using dicing saw equipment.

In both the designs (PDMS and silicon-glass), the device consisted of mainly three parts (as clearly depicted in the 3D rendering done in Fig. 13):

(a) Two inlets feeding into a sigmoidal gradient generator made at the bottom of the chip

(b) Eight fish tanks named C1-C8 (C1 for highest drug concentration and C8 lowest) and

(c) Waste collection channels from each of the fish tanks ending in eight outlets.

To address the distribution of the drug solution in the horizontal plane, the input to the tanks branch out to cover the plane of the entire well.

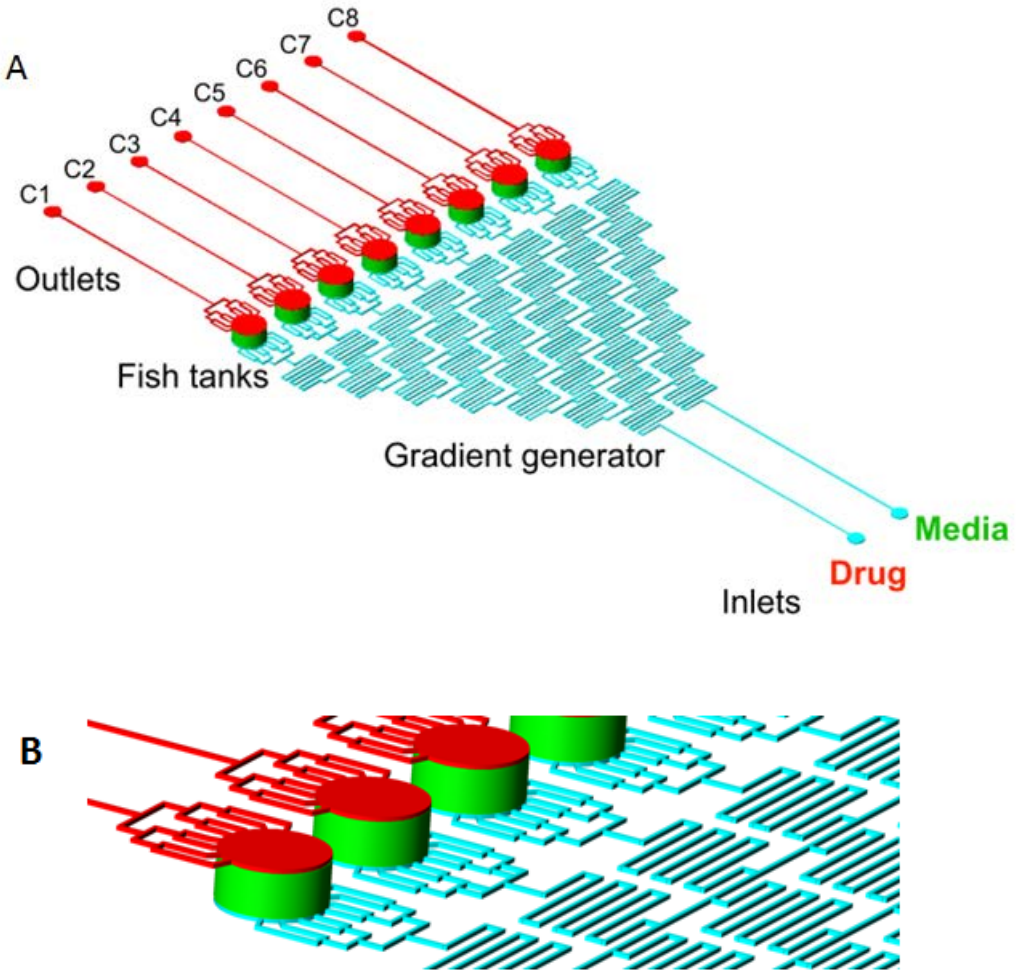

Figure 13: 3D rendering of the design of Fish and Chips. (A) Chip layout. It consists of three parts: inlet layer drawing into the gradient generator, fish tanks and waste channels ending in outlets. (B) Blown-out image showing the fish tanks.

4.3.2 The fabricated Fish and Chips

Structurally the components of the PDMS chip are (Fig. 14):

a) Two different layers, inlets and outlets were replica molded in PDMS and were bonded by oxygen plasma. The inlet and outlet holes were punched with manual punching machine (Schmidt Technology, Germany) the fish tanks were punched with hand-held punch.

b) A 100 µm coverslip bonded to the two-layered PDMS chip by oxygen plasma

c) A 100 µm thick PDMS membrane is spin casted and is used to cover the fish tanks

Similarly, the components of the silicon-glass chip are (Fig. 15):

a) A 1 mm thick silicon wafer was etched on both sides. The eight fish tanks each of diameter 1.4 mm, as well as the two inlets (for media and drug), the eight outlets and via connections (that bring the fluid from the top circuit to the bottom of the chip for fluidic connection with the outlet tube) were etched-through the silicon. The steps in the etch-through inlet/outlet holes were performed for potential packaging options.

b) A 150 µm-thick glass wafer bonded on the bottom of the silicon wafer

c) A 100 µm-thick permeable (removable) membrane (USA Scientific, USA) was used to cover the fish tanks. The pre-sterilized polyurethane membrane is permeable to O_2, CO_2 and water vapours and uses a non-cytotoxic acrylic adhesive, approved by FDA.

The actual PDMS and silicon-glass chips are shown in Fig. 16A and Fig. 16B respectively.

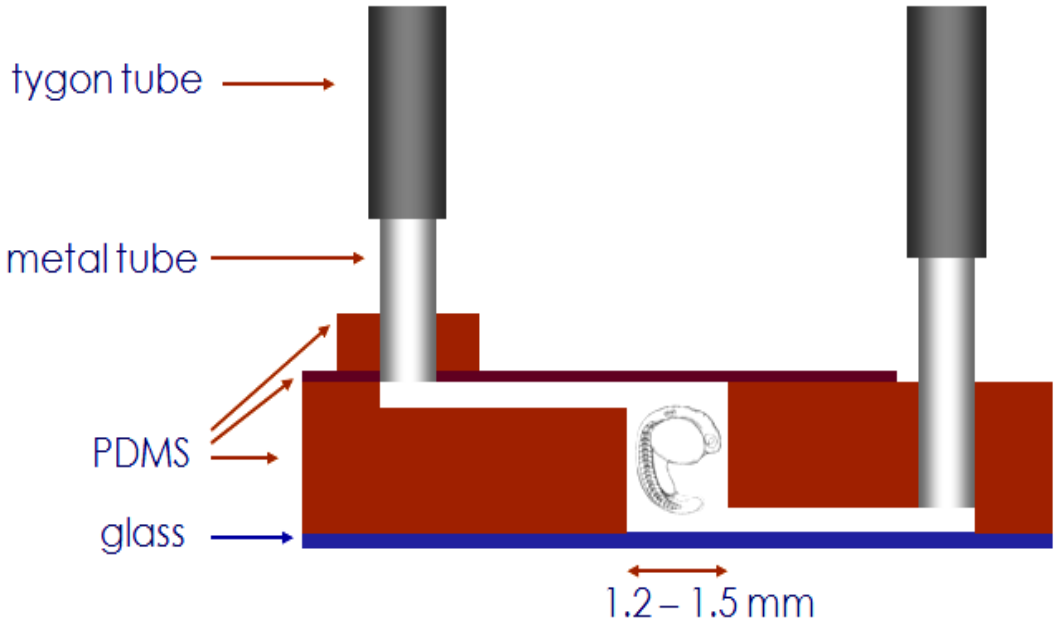

Figure 14: Cross-sectional view of the PDMS Fish and Chips: The two-layered PDMS device is plasma-bonded to the glass bottom. Another thin PDMS layer just covers the fish tank and keeps the embryo in place. The dimensions of the fish tank was varied between 1.2-1.5 mm. Tygon tubing was connected to small stainless steel tubes, which in turn were inserted into the punched holes, for a firm fit.

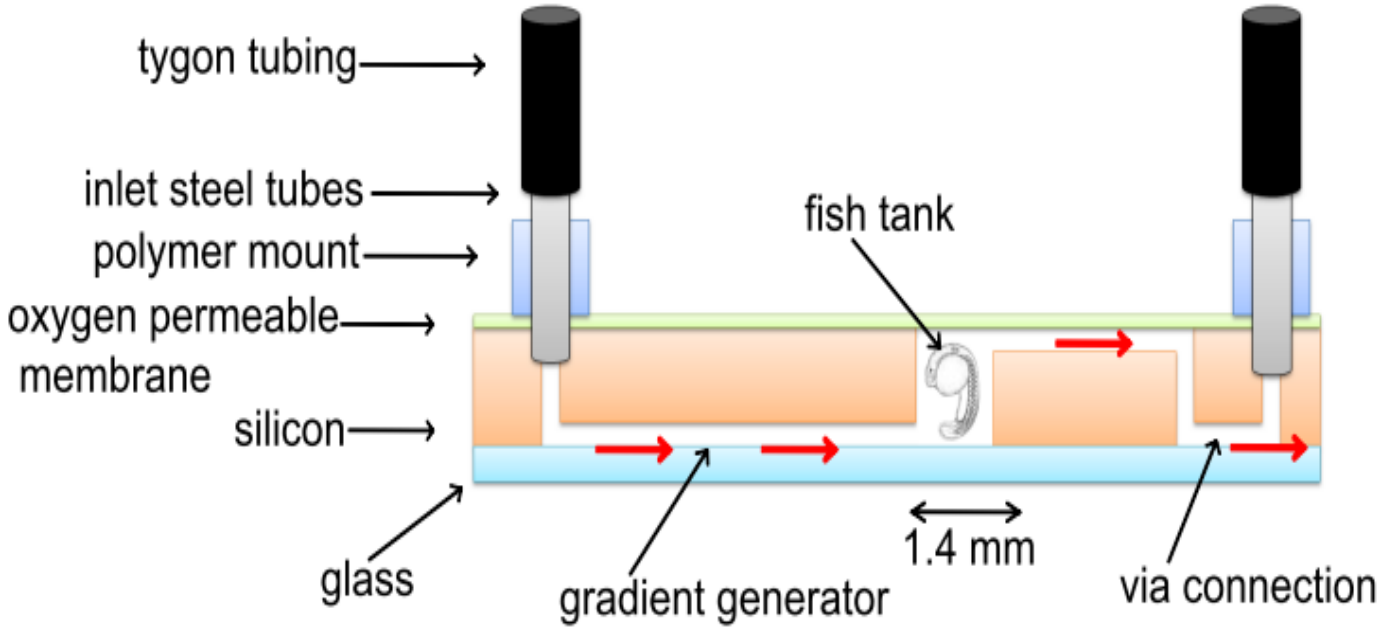

Figure 15: Cross-sectional view of the silicon-glass Fish and Chips: The etched silicon wafer is anodically bonded to the glass bottom. The oxygen permeable membrane would keep the embryo in place. The flow indicated by the arrows, travels diagonally across the well, as to ensure the drug solution envelopes the embryo. The inlet/outlet connectors were fabricated using a polymer-printing machine and were mounted on the silicon surface using UV curable glue. Stainless steel tubes were mounted in the polymeric connectors. Tygon tubing was connected to the small stainless steel tubes for interfacing with the syringe pump. The via connection was designed to ensure that, there is certain depth for the outlet steel tubes to go through for a robust fit.

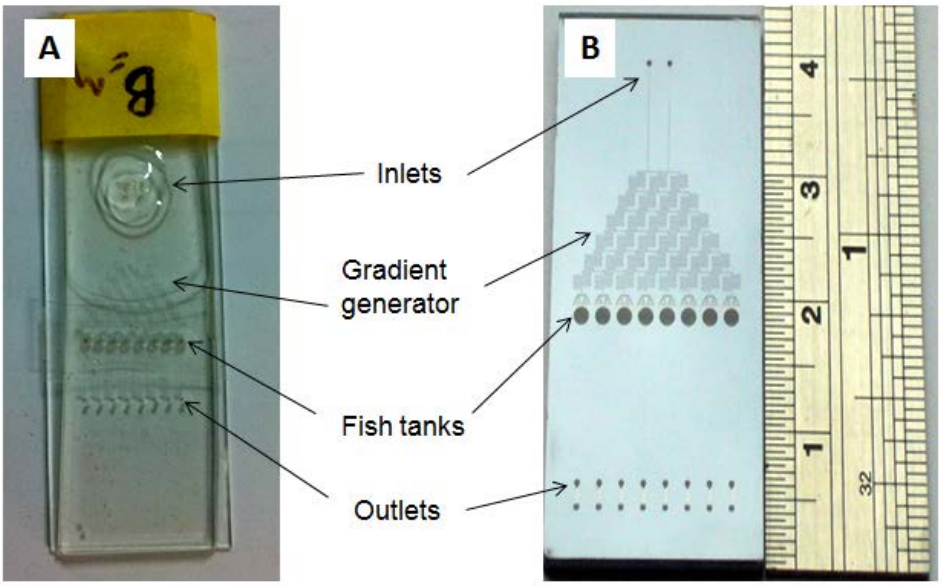

Figure. 16: Actual Fish and Chips devices. (A) PDMS device. The dimensions of the device was same as a glass slide, 22 mm X 60 mm (B) Silicon-Glass device. The dimensions of the devie was 20 mm x 42 mm.

4.3.3 Perfusion set-up

After the Fish and Chips was ready, it was important to optimize the perfusion set-up. The flow set-up includes the chip with its connectors at both inlets and outlets. Both inlet and outlet connectors were fabricated using a polymer printing machine (Eden 350, 3d solutions, France) and were mounted on the silicon surface using UV curable glue (NOA 63, Norland, USA). Stainless steel tubes (New England Small Tubing Company, USA) were mounted in the polymeric connectors. The inlet/outlet holes etched on silicon chip easily allows in positioning these connectors (Fig. 17). For the inlets, Tygon tubing (Fisher Scientific International Inc, USA) was connected to the small stainless steel tubes, at one end, and to syringes at the other end via 4-way valves with a luer connection (Cole–Palmer, USA). For outlets, Tygon tubing was connected to steel tubes at one end, and rest of the tubing were put inside the waste bottle.

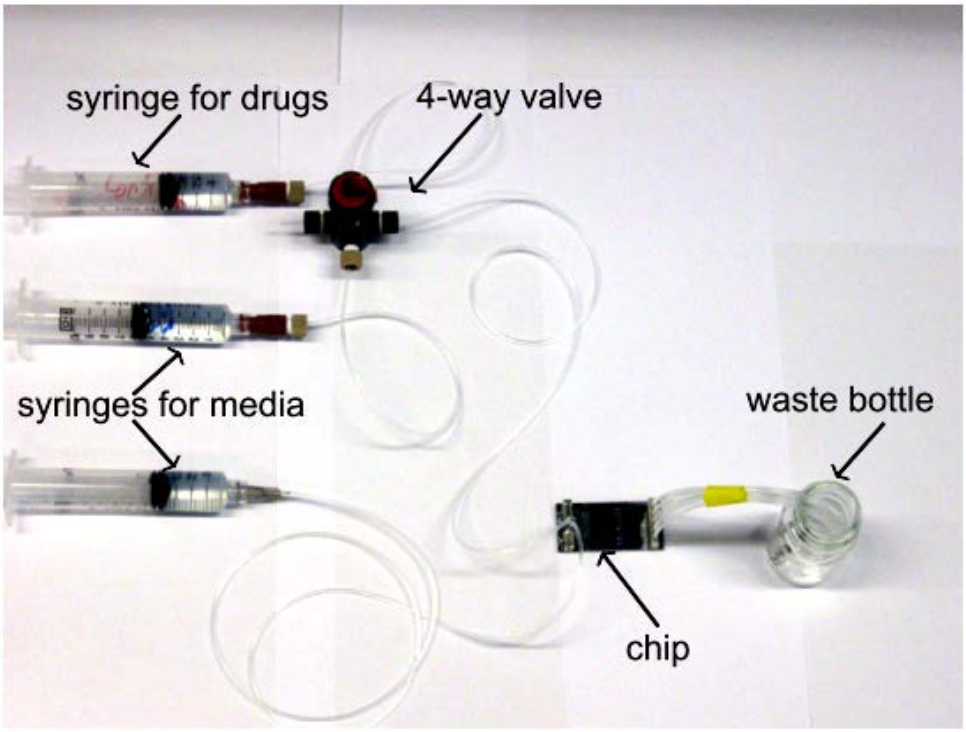

Figure 17: Perfusion set-up for Fish and Chips. The chip was first perfused with media from two of the inlets using syringes. After the embryos were placed on chip and covered with the oxygen permeable membrane, the 4-way valve was opened towards syringe containing drugs. For non-drug perfusion, only egg water was pushed through the syringes using a syringe pump (pump not shown).

4.3.4 Optimization of the membrane to cover the fish tanks

Various materials were tried in order to cover the top of the fish tanks, so that to ensure the media or the embryos do not come out during perfusion. A thin layer of PDMS could be attached on the surface after the embryos are seeded in the tanks. However, just a simple attachment did not ensure leak-proof settings and so the PDMS layer needed to be bonded on the top surface. However bonding the PDMS membrane affected the viability of the fish embryos placed in the fish tanks. We also explored thin glass coverslips to be bonded on the top of the PDMS and silicon-glass devices. Finally, a

commercially available oxygen permeable membrane made from polyurethane was successfully used to cover the fish tanks. This 100 µm membrane film was removable.

4.3.5 CFD simulations confirm that the design of fish tank ensures uniform exposure of media and drugs

The branched inlets and outlets design at the tanks (Fig. 12A-B) ensured equal distribution of the flow over the surface of the tank. The fish tank volume was ~2 µl. CFD simulations confirm that when the flow travels diagonally across the fish tank, the medium envelope the embryos without relying on diffusion (Fig. 18B). In contrast, if the flow passes at the bottom of the tank, only diffusion would allow for nutrients and waste exchange (Fig. 18A). For this design, only the part of the embryo near the bottom of the well would receive the flow while the rest of the embryo would experience little flow and hence has to depend on diffusion.

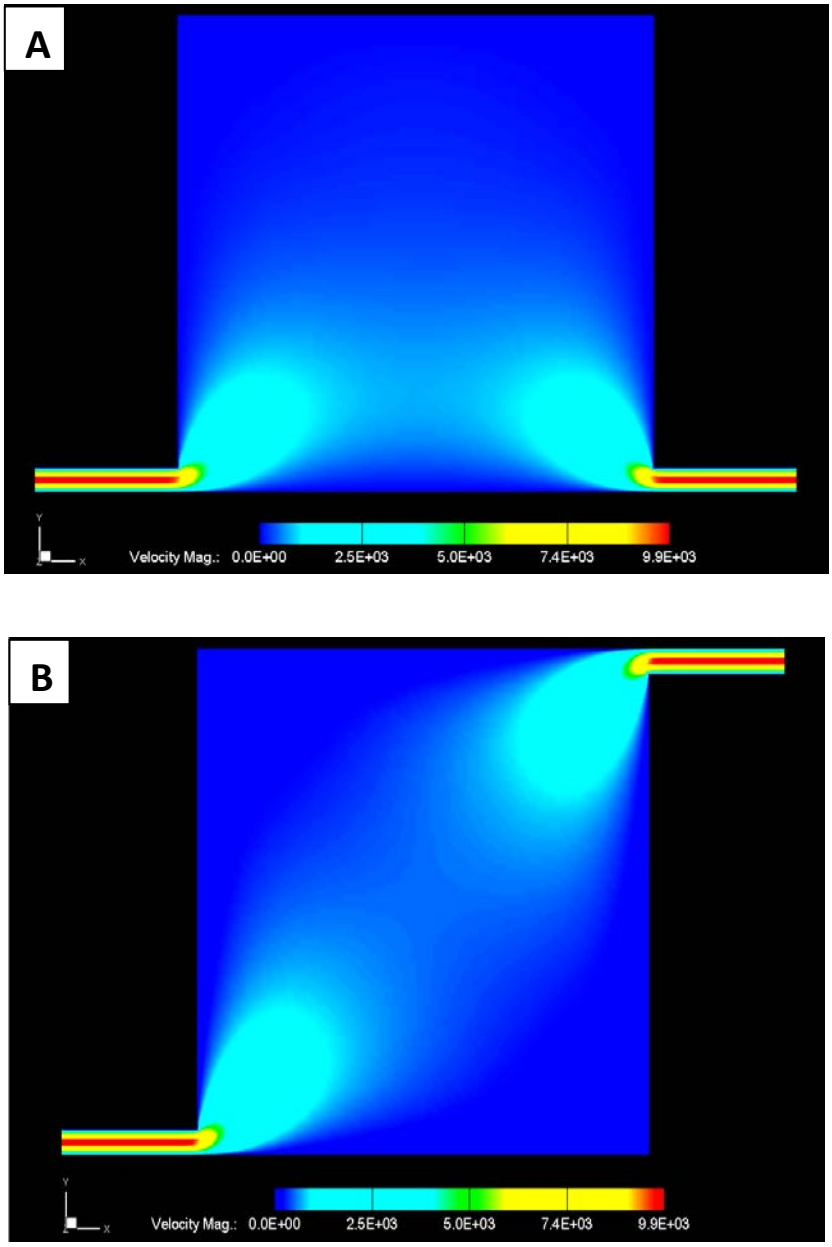

Figure 18: CFD simulations of the flow in fish tanks (cross-sectional view). (A) Simulation of the flow pattern in the case of the channel passing under the well. (B) Simulation of the flow when the flow has to travel diagonally across the well. The latter ensures the drug solutions will envelope the embryo, not relying on diffusion. Red indicates the highest, while blue indicates zero flow rates.

4.3.6 Sigmoidal concentration profile of the dye

The gradient generator incorporated in this design has a sigmoidal distribution pattern. The sigmoidal generator is made up of a branching microfluidic network that creates a concentration gradient by utilising laminar flow and diffusive mixing.[147, 149] As streams of various solutions flow down the microfluidic network, they split at the nodes, combine with neighbouring streams and are mixed 1:1 by diffusion as they pass through the channels. Theoretical values of the concentrations were calculated based on the design of the sigmoidal concentration gradient generator.

Fig. 19 shows the confocal micrograph of the tracer dye in all the 8 fish tanks of the silicon-glass chip. As we go from C1 towards C8, there is decrease in the fluorescent intensity of the images and hence it implies decrease in the dye concentration. The sigmoidal concentration profile of the tracer dye, Rhodamine G concurred with the theoretical values (calculated before). Only the experimental concentration from the tank C7 appeared to deviate from the theoretical value. This could be due to imperfections in fabricating the channel.

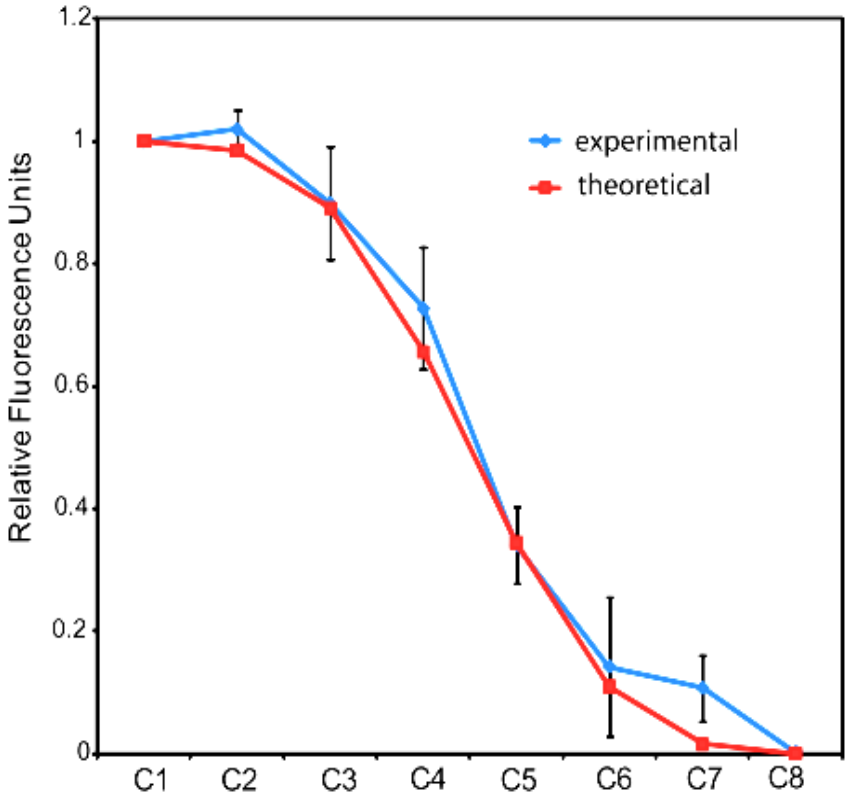

Figure 19: Characterization of the concentration gradient profile in the Fish and Chips. The top panel shows the confocal micrographs that correspond to gradients of Rhodamine G solution in various tanks in Fish and Chips. The bottom panel depicts the average fluorescent intensity on each of the fish tanks normalized against the highest intensity of the tanks. The blue line indicates the experimentally determined values while the red line indicates theoretically calculated values. The experimental values concurred with the theoretical values for dye concentration. Data are represented as average ± standard deviation of 3 independent experiments.

4.3.7 PDMS vs. Silicon-glass design

While PDMS offers some flexibility in fabrication and operation of microfluidics chips, we encountered several challenges regarding reproducing the device and hence decided to use silicon-glass device for all further studies. The issues with the PDMS device were:

- Since it was a 2-layered PDMS device, it was essential to keep the thickness of the top (outlet) and bottom (inlet) layers always uniform during replica molding
- The fish tanks (1.2 mm-1.4 mm) punched in the PDMS chip were not uniform
- Aligning the input and output layers of the chip during the oxygen plasma bonding was always problematic
- The PDMS chip could not be washed or reused for drug studies
- The hydrophobic nature of PDMS could interfere while doing hydrophobic drug studies

In contrast, the silicon-glass device could be fabricated more precisely and was easily reproducible. The silicon-glass device could also be reused after a wash with piranha. Moreover, for packaging and commercialization purposes the silicon-glass device seemed more practical.

4.4 Conclusions

We were successful in fabricating the multi-channel Fish and Chips in two different schemes; PDMS and Silicon-Glass. The microfluidic platform consisted of three parts: a microfluidic gradient generator, a row of eight fish tanks, in which the fish embryos are individually placed, and eight output channels. A unique perfusion system ensured a uniform and constant flow of media to the center of the fish tank. We also demonstrated that the gradient generator incorporated in the design was functional and was sigmoidal in nature. The perfusion system and the oxygen permeable membrane were also optimized for the usage of zebrafish embryos. We also highlighted the advantages of silicon-glass device over PDMS and decided to use it for next studies (culturing fish embryos and drug testing).

CHAPTER 5 Zebrafish embryo culture on Fish and Chips

5.1 Introduction

Zebrafish are available in many research facilities/labs and also across many pet stores. "*The zebrafish book* " by Westerfield[79] has remained as an important source for laboratory culture of zebrafish and for various biological studies involving them. Adult fishes can be easily maintained in aquarium/tanks with temperature set at 28.5 ºC (maximum at 31 ºC and minimum at 25 ºC). For keeping the media favorable to the fishes, commercial sea salts are added to dechlorinated tap water. Embryos and larvae need strict control of media and are raised usually in egg water. When embryos are out of their choions, they are in need of more calcium and hence should be kept in embryo medium. The adults should be fed 1-2 times during the day from a variety of food items like ground dry or moist trout pellets, live adult brine shrimp, daphnia, drosophila and drosophila larvae. The debris produced in the fish tanks can easily be siphoned off from the bottom of the tank or a filter can be used. For our studies, we obtained zebrafish embryos from the fish facility at Institute of Molecular and Cell Biology, Singapore (IMCB).

Microscopic investigations are usually preceded with mounting the zebrafish in low-melting 1.2% agar (rigid mounting medium) or in 3% methylcellulose (less rigid medium). These mounts are also regularly used for holding embryos during microinjection procedures. However, mounting is not feasible for long-term culturing and dynamic imaging because it is laborious process, needs anesthetizing agent and constant application of media drops to keep the embryos alive. Microtiter plates although allow

long-term culture of embryos with high-throughput[71] but imaging becomes troublesome due to the embryo movement and also with height and meniscus of the egg buffer.[20] Microtiter plates are also static culture systems and fish embryos/adult fishes experience slow-moving water as they develop naturally in streams or rivers etc. [157] The microfluidic system employed previously for fish embryos had bigger well sizes and also lacked a gradient generator.[20] Another flow-through system VAST was only feasible for embryos beyond 48 hpf and detrimental for younger embryos.[77]

Many zebrafish germ-line transgenics (mutants) have been developed either through pseudotyped retroviral-vector infection or through DNA-injection approaches.[158] The *in vivo* fluorescent reporters like green fluorescent protein (GFP), blue fluorescent protein (BFP), red fluorescent protein (DsRed) and enhanced green fluorescent protein (EGFP) have been expressed in those mutants.[159-161] These reporters (protein markers) under specific promoters can highlight stage-specific, tissue-specific and cell type-specific expression of selected genes in developing and adult zebrafish.

In this study, we have used our silicon-glass Fish and Chips for culturing wild and transgenic fish embryos and perform high-resolution imaging. The flow conditions and temperature were optimized. High-resolution live imaging was done in both bright-field and fluorescent mode using wild-type fish and two transgenic lines. Various tissues and organs successfully developed over a period of few days on chip.

5.2 Materials and Methods

5.2.1 Fish maintenance and crossing of fishes for embryos

Zebrafish were maintained according to established protocols[79] in agreement with the IACUC regulations (Biological Resource Center of Biopolis, IACUC application no. 100527) and rules of the IMCB zebrafish facility. Three different lines of fish were used: wild type strain AB; a transgenic line, Tg(*cmlc2*:dsRed) or transgenic cardiac myosin light chain-2, with the specific dsRed expression in the myocardium[74]; a transgenic line, SqET4 [162], in which the reporter EGFP (enhanced green fluorescent protein) expressed in the mechanoreceptor cells. The transgenic Tg(*cmlc2*:dsRed) and SqET4 lines were used for fluorescent imaging.

5.2.2 Housing embryos on Fish and Chips

To prime the chip, a syringe pump (Harvard Scientific, USA) was used at both the inlets and perfused with egg water at 1000 µl/hr. The flow rate was then reduced to 200 µl/hr. Eight healthy fish embryos were selected and placed inside the fish tanks using a sterile micropipette under a stereomicroscope (Motic, USA). The tanks were then covered with an oxygen permeable film using tweezers. Under the microscope, the chip was placed on a heating stage at 28.5 ºC. Drugs were injected via a 4-way valve.

After the experiment the Fish and Chip was cleaned in piranha solution (H_2SO_4 /H_2O_2 in ratio 2:1 at 120 ^oC for 20 minutes) and reused again upto four times. The transgenic Tg(*cmlc2:*dsRed) and SqET4 embryos were placed on the chip at 48 hpf. In case of a dead or defective embryo within 2 hours of experiment (*e.g.* injured suffered to embryos while placing them in the tank), we replaced the embryos by carefully removing the membrane and placing a new embryo from the same batch of embryos in the tank.

After more than 2 hours of experiment, dead or defective embryos were not replaced anymore. To filter out the diseased/unfertilized/contaminated embryos we waited until 8 hpf before using them for studies.

5.2.3 Live imaging of embryos on chip

The fish embryos were imaged using inverted microscopes Olympus IX 51 (Olympus, Japan) and Zeiss Axiovert 200M; a stereomicroscope SteREO Lumar.12 and a line-scanning confocal microscope LSM 5 Live (Carl Zeiss, Germany). Images were at high magnification to view the detailed morphology of the zebrafish embryos. Two different cameras were used for capturing the images and videos; Retiga-2000R Fast 1394 (QImaging, Canada) and AxioCam MRc (Carl Zeiss, Germany). Best-focused images were selected from a set of *z*-stack scans.

5.2.4 Long-term embryo development and survival on chip

To check whether the Fish and Chip can be used as a platform for long-term culture, healthy wild type AB embryos were obtained and placed in the tanks at 8 hpf. The chip was perfused with egg water through both the inlets. The embryos were imaged at certain time intervals (10-30 mins) for nearly 4 days and the development of various organs were observed. No 1-phenyl- 2-thiourea (PTU) was added to the egg water for this study.

5.2.5 Heartbeat recording on chip

A transgenic fish line Tg(*cmlc2*:dsRed) or transgenic cardiac myosin light chain-2, with the specific dsRed expression in the myocardium[74] was used to record the heart-beats. Tg(*cmlc2*:dsRed) embryos at 48 hpf were seeded on the Fish and Chips and normal

media perfusion was carried out. A stereomicroscope SteREO Lumar.12 fitted with a camera AxioCam MRc (Carl Zeiss, Germany) was used for the study.

5.2.6 Single-cell imaging of fish embryos on chip

A transgenic line, SqET4, in which the reporter EGFP (enhanced green fluorescent protein) expressed in the mechanoreceptor cells[162] was used for this study. SqET4 embryos at 48 hpf were placed on the Fish and Chips and normal media perfusion was carried out. After 1 hr, media flow was stopped and imaging was carried out using confocal microscope LSM 5 Live (Carl Zeiss, Germany).

5.2.7 Live imaging of embryos in 96-well plates

Fish embryos aged 8 hpf were placed in 96-well plates with an embryo per well. Each well was pipetted 100 µl of fish water. A Zeiss Axiovert 200M microscope was used for automated imaging of the embryos for 48 hours. Images were taken every 15 minutes.

5.3 Results and Discussion

5.3.1 Collection and maintenance of embryos

The fishes in the zebrafish facility (IMCB) were kept under a light: dark cycle of 14:10 hrs (Fig. 20A-B). The embryos were obtained by random mating of wild-type fish or by crossing one transgenic and one wild-type fish as described.[79] Overnight adult fishes, a random pair of male and female, were kept in a fish tank separated by a divider and upon its removal in the morning fishes mated and fertilized eggs were obtained (Fig. 20C-D). The fish embryos were maintained in an incubator (New Brunswick Scientific) at 28.5 °C and their development was measured in hours post fertilization.[163] After 8 hpf the dead and unhealthy looking embryos were discarded. Pigmentation was inhibited by adding 0.2 mM 1-phenyl- 2-thiourea (PTU) in the egg water to improve observation conditions of the Tg(*cmlc2:*dsRed) and SqET4 embryos.[164] The stock salts [40 g Sea Salts (Instant Ocean, USA) added to 1 L distilled water] was prepared in the fish facility. Clean egg water (1.5 ml stock salts added to 1 L distilled water = 60 µg/ml final concentration) was collected in a bottle from the fish facility and 2-3 drops of methylene blue was added per litre of egg water as an antifungal reagent.

5.3.2 High-resolution live imaging on chip

AB wild type embryos housed at 48 hpf in the tanks were imaged with a stereo microscope. The bright-field images show that the chorion with an embryo inside fit nicely in the fish tank leaving little room for any movement, except rotational (Fig. 21A). High magnification image (Fig. 21B) can distinguish the eyes, brain, yolk sac, trunk and chorion of the embryo. Higher resolution images of organs open up avenues for studying organ-specific disease models and drug toxicity effects

Figure 20: Obtaining zebrafish embryos from the fish facility. (A) IMCB state-of-the art fish facility (B) Adult fishes maintained in bigger tanks with continuous flow of salt water. (C) The fish tank used for obtaining embryos. Overnight, a random pair of male and female was kept in a fish tank separated by a divider. (D) Mating of adult fishing giving rise to embryos in the morning. Fish embryos are placed in a petri dish with egg water/media before putting in an incubator. Inset showing embryos clearly at 1 hpf.

.

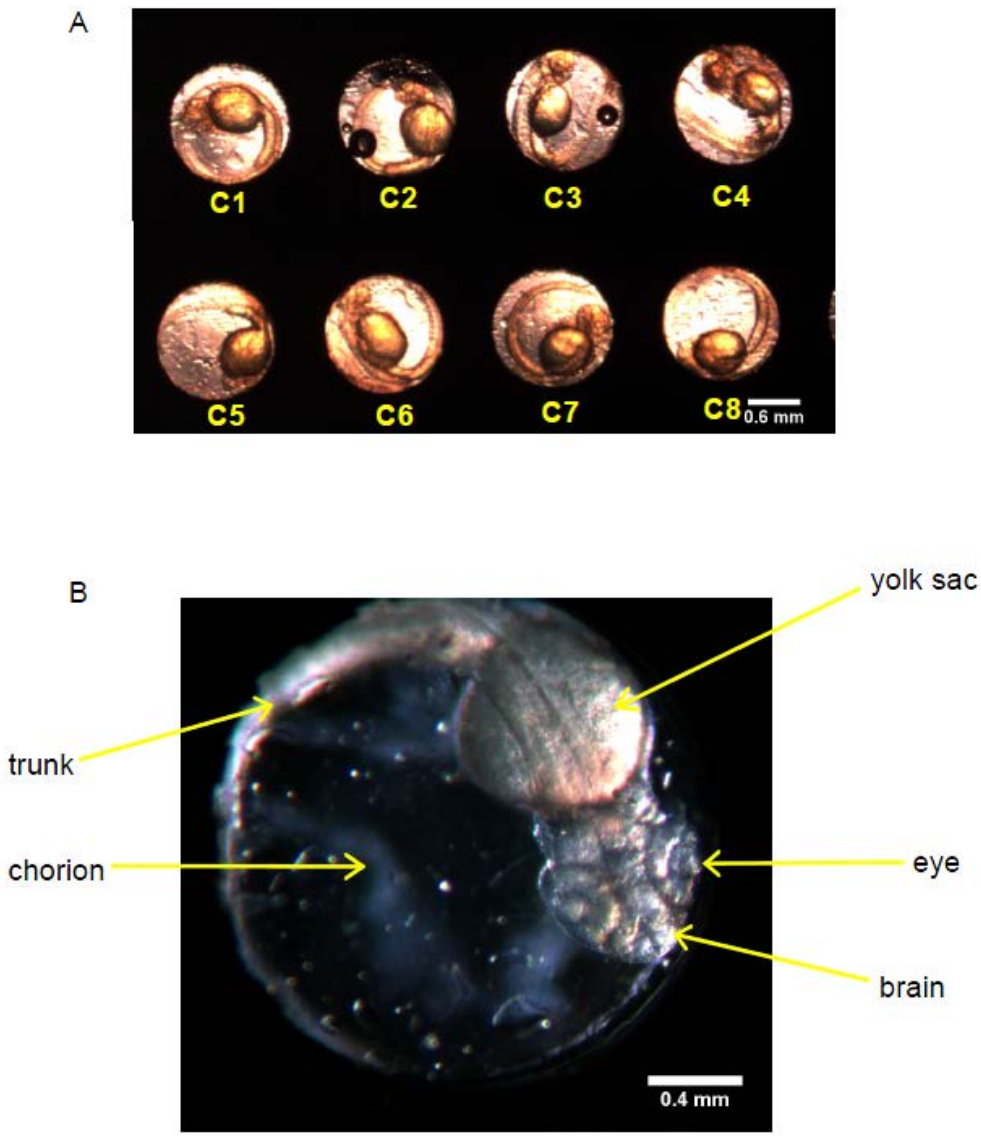

Figure 21: Bright-field image of embryos placed on Fish and Chips. (A) Image of fish embryos placed in 8 tanks. The embryos are constrained and do not have any motion except rotational. (B) Higher magnification image of a single embryo in a tank. The various organs like eyes, trunk, chorion, brain are easily visible.

5.3.3 Fluorescence imaging on chip

For fluorescence imaging, we placed the transgenic Tg(*cmlc2*:dsRed) embryos inside the tanks and a video of the heartbeat (150 beats/min) was captured at 5 frames/sec

(Fig. 22A and Supplementary video S1). The two chambers of the heart (ventricle and atrium) are distinctly identifiable. The sequence shows the alternating contraction and expansion of the two chambers of the heart. One can envision that the effects of cardiotoxic drugs on fish embryos could be studied by either quantifying the rate of heartbeat, contractility or by observing the change in shape and size of the heart with a high-speed camera.[165]

Together, the mechanosensory neuromasts in the skin of the fish's head and trunk represent an important sensory organ called the lateral line.[166, 167] The mechanoreceptors (also known as hair cells) of the lateral line convert the water current stimuli to electrical signals. This sensory system is responsible for many important behaviors like swimming against current, prey detection and/or predator avoidance, social behaviors such as schooling, and sexual courtship. The hair cells of the lateral line and mammalian inner ear have striking morphological and functional similarity and therefore zebrafish is fast gaining popularity as a model to study the molecular mechanism of hearing and its diseases.

We imaged the sensory cells of the neuromasts in the head of the 2-day old SqET4 embryos. A Z-stack of the neuromast clusters was acquired by confocal microscopy (Fig. 22B and Supplementary video S2). The oxygen permeable membrane on the top of the fish tank did not hamper imaging. Three clusters of neuromasts were imaged on different focal planes. Therefore, our Fish and Chips could serve as a platform to study mutations affecting differentiation of mechanoreceptors in the lateral line as disease models and screening for drugs protecting against ototoxic agents.[168, 169]

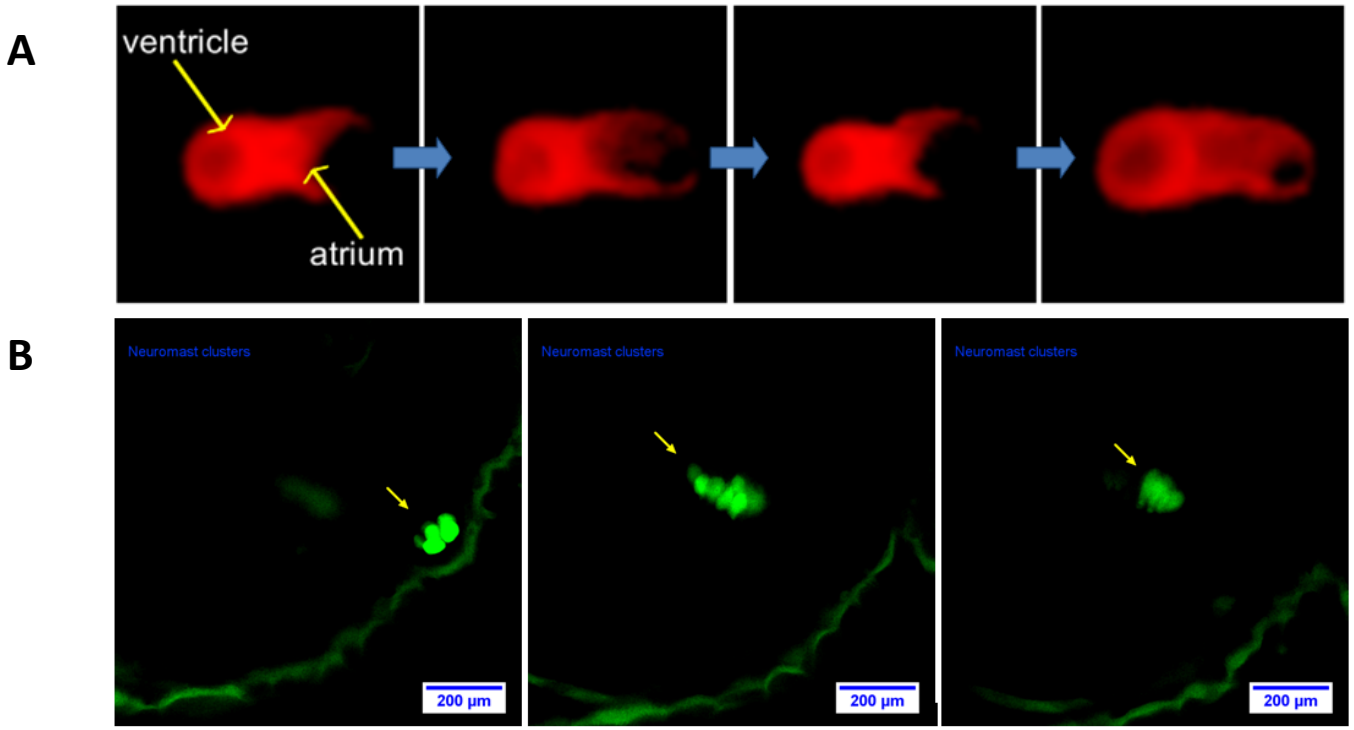

Figure 22: Fluorescent imaging on Fish and Chips (A) Four continuous frames from the video (Supplementary video S1) of the embryo heartbeat showing the alternative contractions and relaxations of the heart chambers. The outline of the heart is very clear with two distinct chambers atrium and ventricle easily visible. The transgenic Tg(*cmlc2*:dsRed) embryos were placed in the fish tanks at about 48 hpf. (B) Three clusters of neuromasts in the head of the 2-day old SqET4 embryos placed in Fish and Chips. The images are from three different focal planes (Supplementary video S2). Each cluster appears to have a group of 4-5 supporting cells. Neuromasts are comprised of a ring of supporting cells, which surround a central cluster of sensory hair cells.

5.3.4 Tissue and organ development on chip

The Fish and Chips was also evaluated as a platform to monitor the long-term development of the embryos. Healthy AB embryos were placed in the tanks at 8 hpf and imaged intermittently for 4 consecutive days to track their tissue and organ development (Fig. 23). The embryos developed normally across the 8 fish tanks in the absence of the drug. The images shown are from two different embryos. Important sensory organs like eyes, ears (each of which contains 2 otoliths for balance and hearing) and olfactory bulbs were easily visible. Other tissues and organs like the hindbrain, pectoral fin, epidermis, vertebrae, neural tube, fat (lipid) droplets, melanophores, yolk extension and developing cloaca were also imaged (Fig. 24).

The development of eyes in zebrafish is an important and complex process and their retina and lens show similar morphology to other vertebrates including humans.[170] Therefore, zebrafish is now appreciated as an animal model to study human eye diseases.[171] There is similarity in lipid metabolism pathways between mammals and fish.[172] Visualization of fat (lipid) droplets helps to explore the fish embryos as a model for adipocyte development and morphology. In fact methods have also been developed to visualize zebrafish adipocytes *in vivo* by labelling neutral lipid droplets with Nile Red.[173] Currently the global obesity epidemic merits a serious understanding of the developmental and environmental factors regulating fat storage. Zebrafish is also a prime genetic model to undergo rapid physiological colour change which many a times is guided by melanophores distribution related to background adaptation.[174] The absence or reduction of pigmentation (melanophores) due to drug studies has also been accounted

for.[66] The growth and development of the tissues and fish organs on chip is demonstrated, suggesting opportunity to evaluate embryotoxicity *in vivo* and monitor the changes in development due to different drug concentrations. A video of the blood flow in the tail of the fish was also captured showing individual red blood cells (Supplementary Video S3 and Fig. 25). Development of vasculature can be estimated from the blood flow-rate.

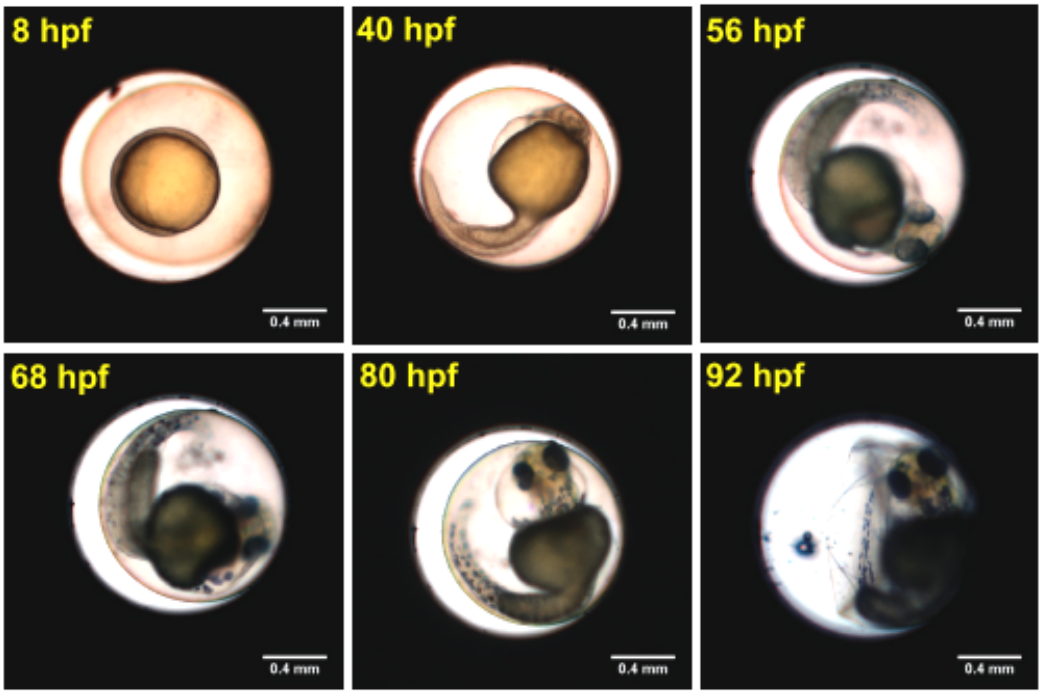

Figure 23: Embryo development on Fish and Chips. Images of a single embryo taken at various time points of development (hpf). The maturation of pigments over time leads to a darker colour embryo.

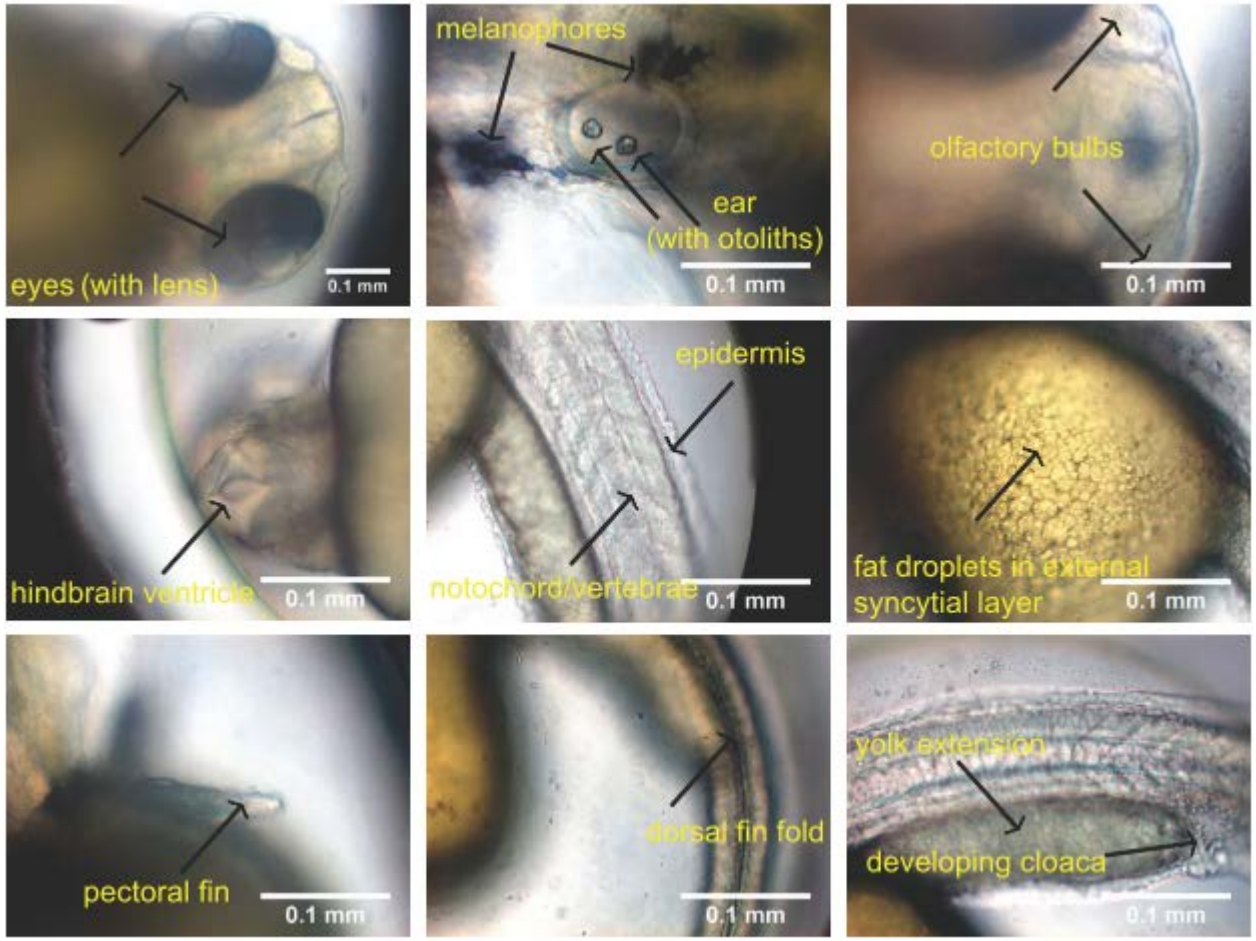

Figure 24: High-resolution images of various tissues and organs of the embryos on Fish and Chips. Eyes, ear (with otoliths inside), olfactory bulbs, melanophores, hindbrain ventricle, notochord, epidermis, fat droplets, pectoral fin, yolk extension and developing cloaca were observed in two developing embryos.

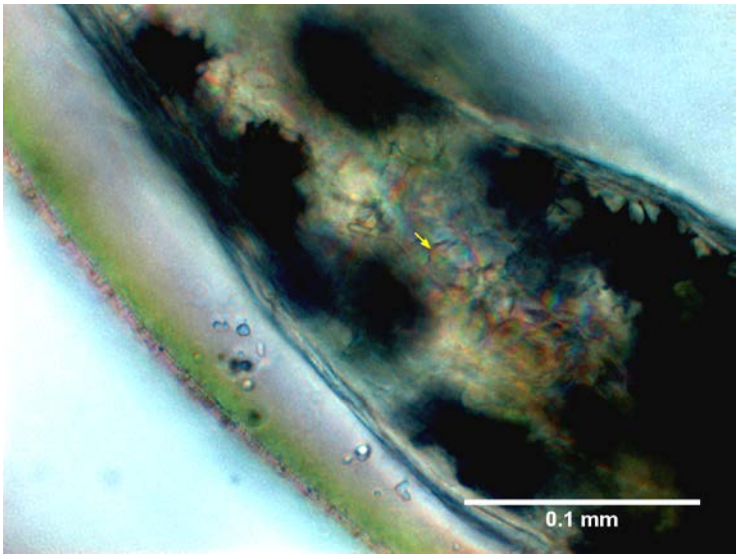

Figure 25: One frame from the video showing blood flow in the tail of the embryos at 80 hpf.

5.3.5 Comparison of embryo development on chip vs. 96-well microtiter plate

Time-lapse movies show the embryonic development on the chip compared to similar development in microtiter plates. The Supplementary Video S4, illustrates the development of the fish embryo at different stages in Fish and Chips. The Supplementary Video S5 meanwhile, shows the embryo development in a 96-well microtiter plate. In terms of organ development, both the chip and the microtiter plate showed similar results (Fig. 26A-B). However, in 96-well plate the embryo is not constrained and hence drifts out of the field of view (Fig. 26B-C and Supplementary Video S5). In our Fish and Chips, the physical confinement of the embryos prevents any drifting and thus enables continuous imaging.

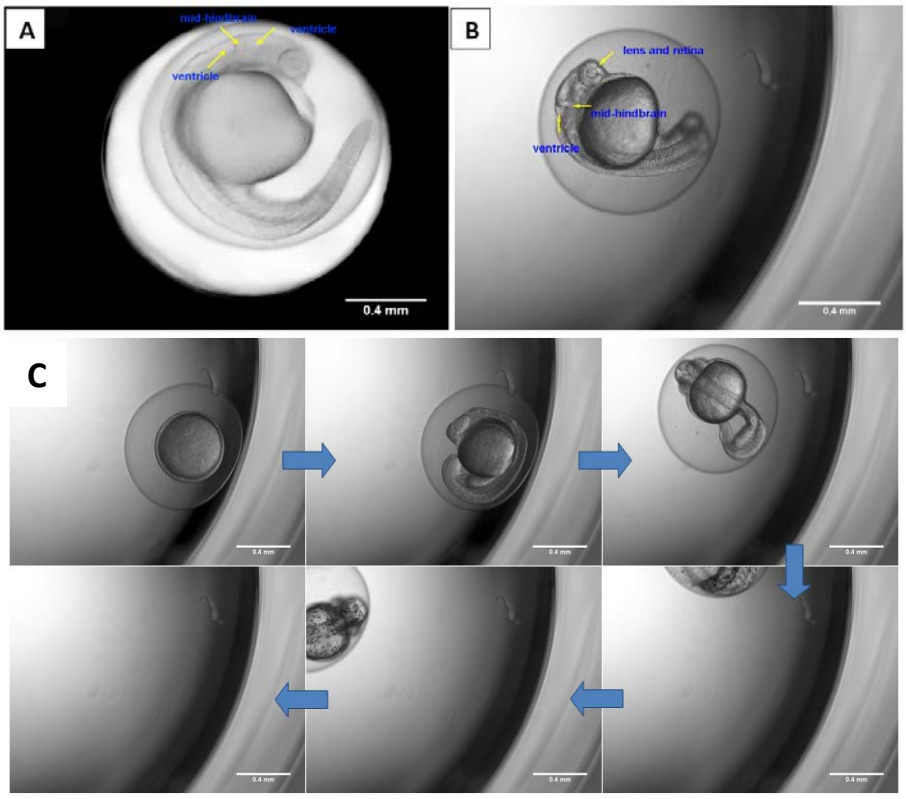

Figure 26: Development of zebrafish embryos in the (A) Fish and Chips and the (B) microtiter plates. Both the chip and the microtiter plates showed similar development in terms of appearance of organs at various hpf. While the embryos remain constrained in the Fish and Chips, the embryos in the microtiter drifted freely, going out of the field of view. (C) Various frames from the Supplementary video S5 of embryo development in microtiter plates. The embryo starts to drift due to the involuntary motions (which start to appear at about 15 hpf). The embryo gets out of the frame of the view and hence continuous imaging is virtually impossible.

5.4 Conclusions

We showed that the zebrafish embryos can fit tightly inside the fish tanks and can be imaged at high-resolution. Fluorescent imaging was done at single-cell resolution for neuromast cells. Dynamic recording of heartbeat provides important physiological information of the growing embryos in chips. The growth and development of the tissues and organs on chip was demonstrated, which offers a unique opportunity to evaluate embryotoxicity *in vivo* and monitor the changes in development due to different drug concentrations. This platform may also be used for studying organ-specific disease models.

CHAPTER 6 Drug-toxicity on Fish and Chips

6. 1 Introduction

Zebrafish as a model organism is increasingly used for assessing drug toxicity and safety[15] and many studies have already confirmed the similar toxicity profiles between mammals and zebrafish.[14, 18] Toxicity effects of drugs on various organ-systems have already been demonstrated in fishes; teratogenesis, cardiotoxicity, neurotoxicity, hepatotoxicity, genotoxicity etc.[14, 78] Different assays are in use to check for the toxicity effects. For a well-known teratogen like ethanol, the effects could be summed up under a phenomenon called fetal-alcohol syndrome[175] and the readouts may be cyclopia,[65] craniofacial abnormalities,[176] deficits in learning and memory and defects in visual function.[177] Cardiotoxic agents like tetrachlorodibenzo-para-dioxin (TCDD) can reduce the heart rate; decrease the overall size of the heart, cause pericardial edema and defect in position of two heart chambers.[78, 178] For adult fishes, electrocardiogram (ECG) can be used to record the heartbeats and detect for QT prolongation due to drug effects.[179] 1-methyl-4-phenyl-1,2,3,6-tetrahydropyridine (MPTP) damage to dopaminergic can be studied using whole mount *in situ* hybridisation and quantification of neuronal loss is done by finding the total area occupied by the dopaminergic neurons[180] or simply counting their number.[181] Behavioural defects due to drugs like domic acid may involve aberrant response to touch, reduction in swimming and rapid movement of pectoral fins in the fish larvae.[182] Neuromasts are the zebrafish counterpart of inner hair cells and have been shown to be affected by drugs like cisplatin, gentimicin and quinine.[169]

Although drug studies on fish embryos have been carried out regularly in microtiter plates,[71] we have already highlighted the issues of using such plates in section

5.1. For proof of concept drug testing on our Fish and Chips, we chose valproic acid (VPA). VPA is a well-known teratogen which causes birth defects in children born to women taking this drug during pregnancy.[66] After treatment with VPA, fish embryos show various abnormalities, such as a crooked and shortened tail, shortened axis, oedema and pigment perturbations.[67] We investigated the effect of this drug on embryo eye and tail development.

6.2 Materials and Methods

6.2.1 Valproic acid and its formulation

All chemicals and reagents were purchased from Sigma-Aldrich (Singapore) unless otherwise stated. Stock solutions of the drug valproic acid (VPA) were prepared in dimethyl sulfoxide (DMSO). The stock concentrations of the drugs used were 100 mM.

6.2.2 Pilot study of valproic acid in microtiter plates

A pilot study was carried out in 96-well plate to identify the lethal concentration of VPA for the zebrafish embryos.

6.2.3 Valproic acid study in Fish and Chips

AB wild type embryos were collected from the zebrafish facility as described in section 5.3.1. No PTU was added for this study as the drug VPA is known to cause pigment perturbations in the fish embryos. The chip was primed; eight healthy embryos were placed into fish tanks at 8 hpf and the tanks were covered with an oxygen permeable membrane. At this point the embryos were imaged. The 4-way valve at the drug-side inlet was opened to the syringe containing the drug solution of 1 mM of VPA. The embryos were observed after 24 hours of drug perfusion.

Later, to quantify the effect of VPA on the development of tail and eye, representative concentrations 0.01 mM and 0.05 mM of the drug was simultaneously perfused through both inlets as a way to increase the statistical significance. The embryos were imaged continuously every 10 minutes for 60-72 hours.

6.2.4 Quantification of eyes and tail of developing embryos on chip

Quantitative studies were done for the developing eyes and the tail of the embryo. Only those frames were chosen, in which the organs (eyes and tail) were clearly visible. NIS-Elements AR 3.2 (Nikon, Japan) software was used to calculate the length of the tail, the size of the eye (area) and the intensity of the eye pigmentation.

The tissue post the anus (cloaca) represents the growing tail bud of an embryo.[163] A polyline function (length measurement) was used to mark and measure the tail. The maximum periphery of retina at an available focus was chosen as the region of interest for calculating the size of the eye. A 5-point ellipse function (area measurement) was used to select the region for the eye. The same region of the eye was used for calculating the pigmentation intensity, which illustrates formation of the pigmented epithelium of the retina and correlates with maturation of the retina. The values for length and area were converted from pixels to microns.

6.3 Results and Discussion

6.3.1 VPA effects on embryos on chip

Firstly, a pilot study was carried out in 96-well plate to identify the lethal concentration of VPA for the zebrafish embryos. We chose 1 mM as the maximum drug dosage for 24 hr perfusion in our chip. This 1 mM get diluted due to the gradient generator, resulting in eight different concentrations, *viz*. 1 mM, 0.98, 0.89, 0.65, 0.34, 0.1, 0.01 and 0 mM, from lethal to non-lethal. Embryos treated with the highest 4 concentrations died after 24 hours of drug perfusion. Those embryos treated with moderate 0.34, 0.1 and 0.01 mM concentration caused a shortening of the tail and hence partially developed (Fig. 27). Whereas, the control concentration of 0 mM did not affect development of embryos and embryos appeared normal after 1 day of perfusion.

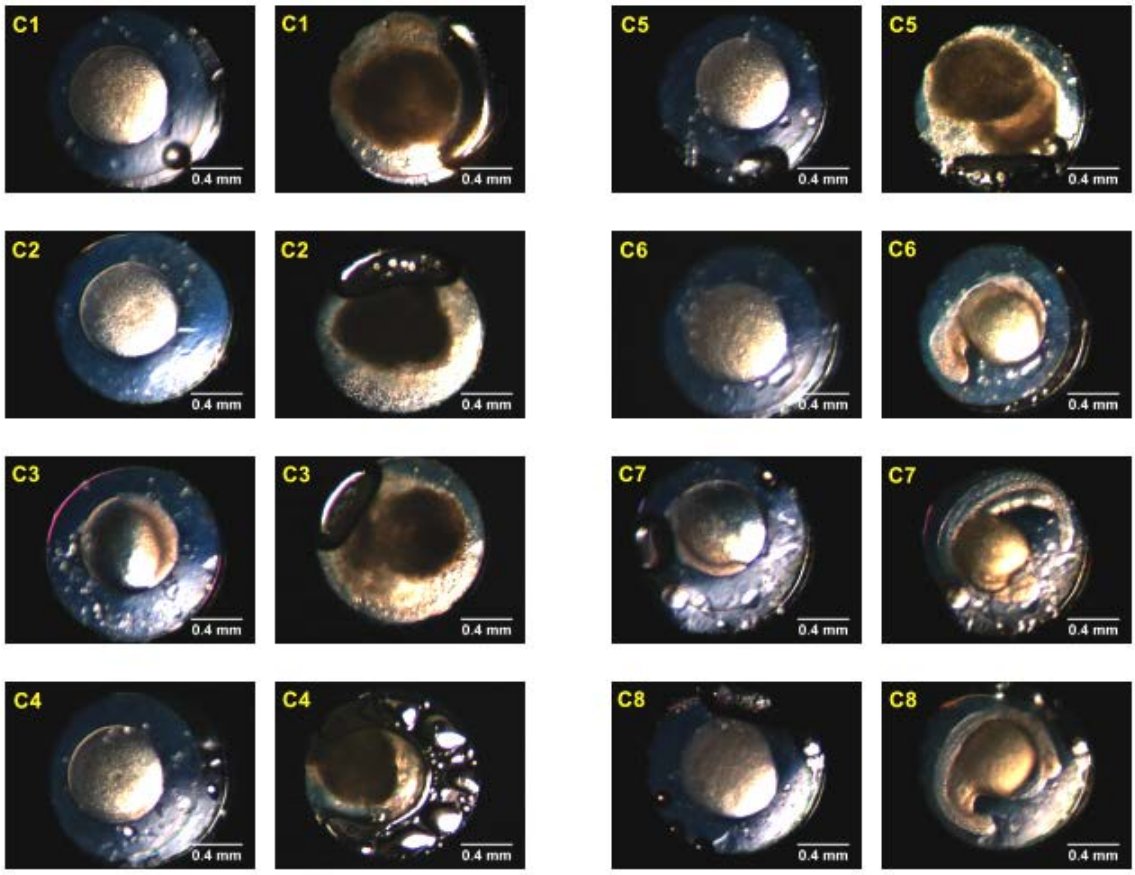

Figure 27: VPA effects on embryos with 1 mM of drug perfusion. The panel on the left are the fish embryos at 8 hpf and placed on chip (zero hrs of drug perfusion). The panel on the right shows the embryos in the fish tanks after 24 hrs of drug perfusion. For the highest 4 concentrations in C1-C4 the embryos died; for the next three concentrations 0.34, 0.1, 0.01mM there was partial development and for the least concentration of 0 mM, there was normal development.

6.3.2 VPA effect on tail length of the embryos in Fish and Chips

Tail growth and straightening are important developmental parameters. The growth rate of tail is a reflection of normal development.[163] Disturbance of this process by VPA[66] and other chemical[183] has already been reported in which the tails become short and crooked on exposure. We checked the effects of VPA on the development of the tail in our Fish and Chips (Fig. 28).

For the lower drug concentration of 0.01 mM, embryos developed crooked and shorter tails while the higher concentration of VPA (0.05 mM) showed the least developed tail morphology (i.e. only the emergence of tail bud and no further development). In comparison, the control embryos showed normal tail development. For control embryos, the length of the tail increased from ~100 µm (15 hpf) to ~900 µm (55 hpf). For 0.01 mM the average tail length increased from ~130 µm (140 hpf) to peak at 240 µm (22 hpf) and later shrunk. In case of 0.05 mM of VPA the tail bud increased slightly from 67 to 72 µm and then shrunk. So in both cases of drug treatment, the tails develop for a while to be shortened later and finally stop as the embryos die.

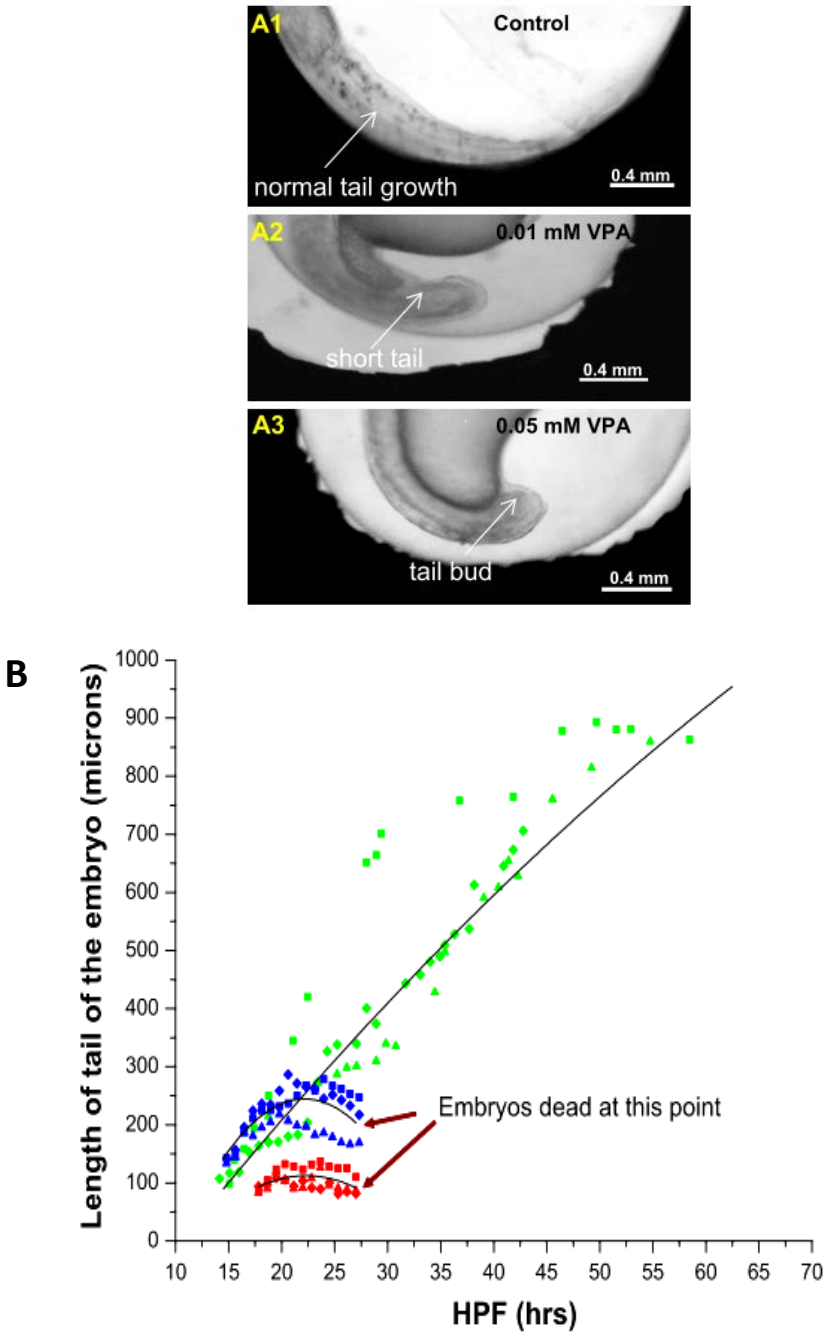

Figure 28: Effects of VPA on tail development in embryos. Representative Images of tails of the embryos for various treatments of VPA. (A1) Control embryos showing normal tail development; (A2) Embryos treated with 0.01 mM show a shorter tail than the controls; (A3) Embryos treated with 0.05 mM show only a tail bud. (B) Plot of length of the tail as a function of time (hpf) hours post fertilization for various drug concentrations. Each colour represents three embryos for each drug concentration (Green 0 mM, blue 0.01 mM, red 0.05 mM). The fitted curves represent the average of the tail length of three embryos. For both drug treatments, the tails develop for a while to be shortened later and finally stop as the embryos die.

6.3.3 VPA effect on eyes of the embryos in Fish and Chips

The development of eyes in zebrafish is another important and complex process and their retina and lens show similar morphology to other vertebrates including humans.[170, 171] Effects of VPA on eyes were more dramatic. As shown (Fig. 29), for 0.01 mM treatment the optic cup developed partially while for 0.05 mM there was no defined optic cup developed at all. In fact, treatment with 0.05 mM VPA caused fast degeneration of the retina anlage (RA) and lens anlage (LA), while with 0.01 mM VPA treatment these primordial structures were maintained. Under these conditions, the optic cups even differentiated forming malformed lens and retina. In control embryos, the optic cup developed into normal retina and lens. We also quantified the size of the eye (area of region of interest) for control embryos and found an increasing trend over time indicating normal eye development (Fig. 30).

The pigmentation of the eyes is a good indicator of retina maturation and can be correlated with eye development.[67] Hence, we measured the pigmentation intensity and found that during development of control embryos pigmentation increases (Fig. 31). For embryos treated with VPA, such quantification of eye area and pigmentation were not possible due to malformed or undeveloped eyes.

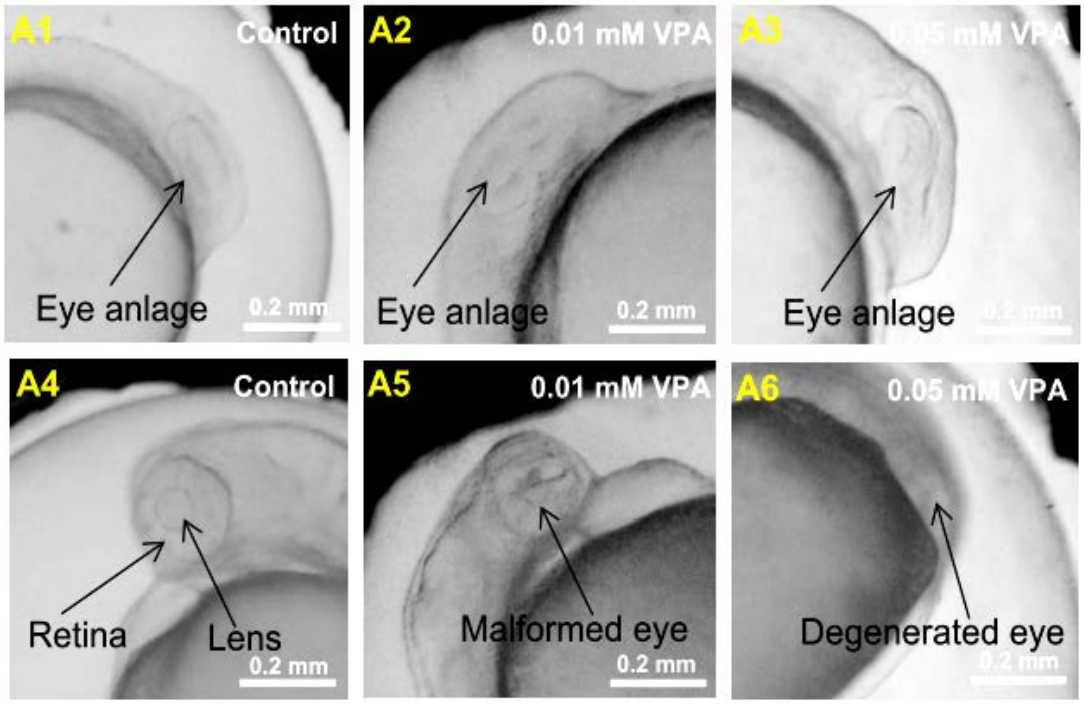

Figure 29: Effects of VPA on eye development in embryos. Representative images of developing eyes of embryos for various treatments of VPA. (A1 and A4) control embryos showing normal eye development with fully developed lens and retina; (A2 and A5) embryos treated with 0.01 mM show a malformed eye with no defined optic cup; (A3 and A6) Embryos treated with 0.05 mM, the eye never develops from the eye anlage (primordium). The top panel of images show eye development at ~15 hpf and the bottom panel show eye development at ~28 hpf.

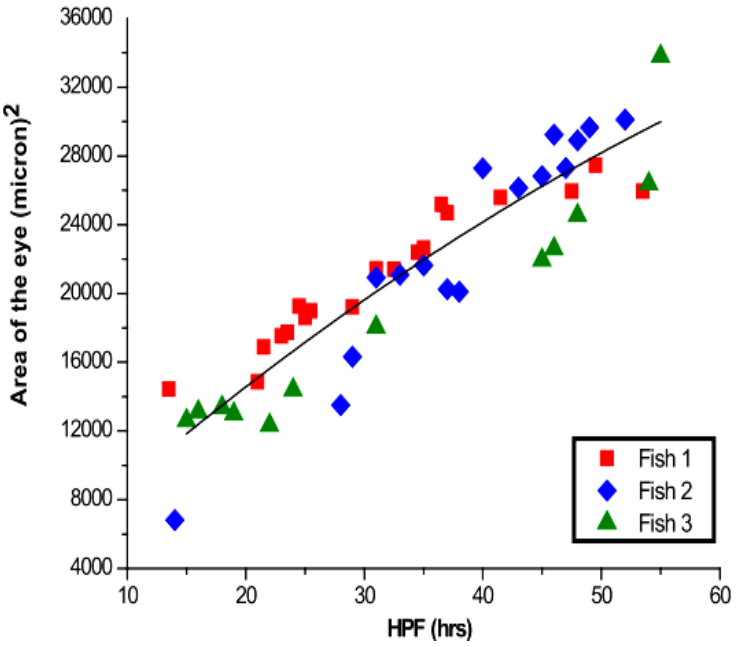

Figure 30: Plot of the area of the eyes of control embryos as a function of time (hpf). Each colour represents the area profile for a single embryo. The fitted curve clearly indicates increase in size of the eye over time. For embryos treated with VPA, such quantification of eye area and pigmentation were not possible due to malformed or undeveloped eyes.

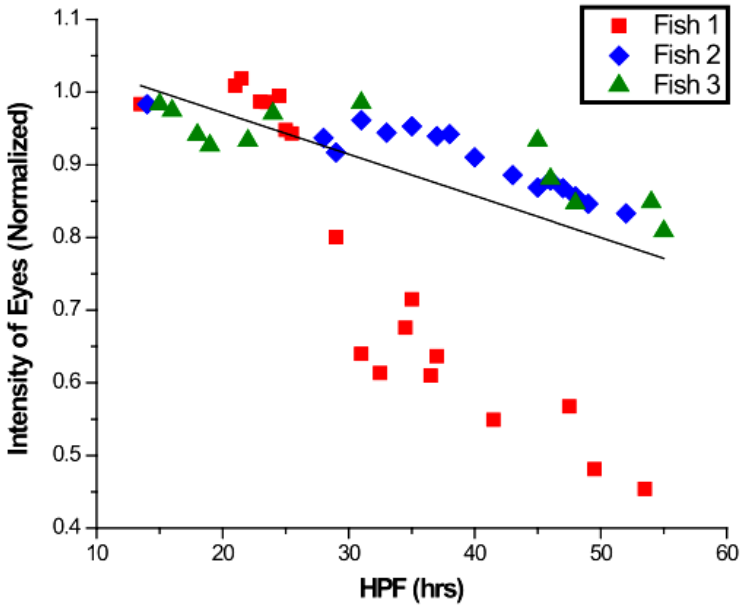

Figure 31: Plot of intensity of eyes of control embryos as a function of time (hpf). Each colour represents the intensity profile for a single embryo. The fitted curve shows decline in intensity of the eyes, which correlates to increase in pigmentation.

6.4 Conclusions

The fish embryos responded to the drug dosage and were more sensitive to higher drug concentrations. The quantification of organ effects was done for the tail and eyes of the embryos. For higher drug concentration, only a tail bud developed and eyes were completely degenerated. For lower concentration of VPA, the tail was shorter than the controls and a partial optic cup developed. These preliminary toxicity studies with VPA, establishes the proof-of-concept evidence for an organ-level drug-screening model.

CHAPTER 7 Cell culture on diffraction gratings (Holographic gratings and optical discs CD-R/DVD-R) for potential drug testing applications

7.1 Introduction

The basic knowledge of cell-substrate interactions is key to many applications like tissue engineering, designing of medical implants and for the development of drugs. [80] Cells inside the vertebrate body are exposed to many topographical cues in form of the basement membrane.[54, 81] The topographical features, mostly at nano-scale, can be broadly classified under biochemical, mechanical, and physical. Biochemical features may consists of the ECM components like the glycosaminoglycans, fibrous proteins like fibronectin and collagen, nanofibers of growth factors and cytokines, hyaluronic acid, laminin etc. Mechanical involves the matrix rigidity. Physical cues could be in the form of pores, fibers and ridges etc.[184, 185]

One of the most common physical cues for cell guidance has been the usage of micro/nanogrooved patterns for aligning cells.[80] There have been numerous chemical [27, 28]and physical methods [29-31] to get the grooves on a substratum. The chemical methods have remained complex and always need rigorous conditions,[29] whereas the physical methods are based on very costly clean room methods and need highly skilled labour to operate.[35] In spite of these limitations, cells have been shown to align on a wide array of materials with different elasticity and mechanical properties. [105]

We realized if there is a cheaper alternative of producing such micro-nanogrooved surface, then more labs can easily adapt that for various practical applications. Our serendipitous experience involved exploring the commercial diffraction gratings for culturing and aligning cells. These gratings, very popular in optics related engineering

applications, had been previously been used to pattern polymers like PDMS,[117] silk films [119]and collagen membranes.[105] We present here the detailed processing and characterization of the diffraction gratings, followed by aligning various cells on them. The proposed device, “Gratings on a dish” is a cheaper method for aligning cells and could be explored for drug-testing applications.

7.2 Materials and Methods

7.2.1 Processing of the diffraction gratings for cell culture

The holographic gratings (6"X12") were first punched to obtain 13 mm round films for 24-well plates. For the CD-Rs, the label, acrylic and the aluminum layers on top were easily peeled off with an adhesive tape to expose the polycarbonate layer. For the DVD-R, we used a tweezer to carefully dislodge the junction exposing two polycarbonate surfaces. The bottom polycarbonate surface of DVD-R was processed further. The exposed polycarbonate surfaces of CD-Rs/DVD-Rs were cut into pieces (1 cm X 1 cm) with help of scissors, so that they also can fit in 24-well plates. Small dots were punched on the grooved surface for easy identification later.

Thereafter, the gratings and CD-R/DVD-R pieces were treated with absolute methanol for 2 hrs followed by sonication for 30 mins. Then the pieces were rinsed with DI water to remove any chemicals/dust particles on the surface and especially the organic dyes in case of the optical discs. The pieces were then treated with 70% ethanol for 2 hrs, followed by sonication for 30 mins and rinsing with DI water to make the surface sterile. To ensure absolute sterility, autoclaving of the diffraction gratings was done at 105 ºC for 21 mins to make them ready for cell culture. The gratings pieces were then placed in a well plate to complete "Gratings on a dish" device (Fig. 32 and Fig. 33).

7.2.2 AFM (Atomic Force Microscope) and SEM (Scanning Electron Microscopy) characterization of the surfaces of the diffraction gratings

SEM/AFM samples were prepared by cutting appropriate sizes of the diffraction gratings. For SEM, the samples were viewed with a JSM 5600 scanning electron microscope (Jeol, Japan) at 5 kV. Prior to imaging, the gratings were sputter-coated with

platinum for 60 s. For CD-R samples with 0.1% gelatin, the protein was fixed by glutraldehyde and serially dehydrated with ethanol before SEM was done. Atomic force microscope, DI Nanoscope Dimension 3100 (Digital Instruments, USA) was used in tapping mode to find out the features on the holographic gratings.

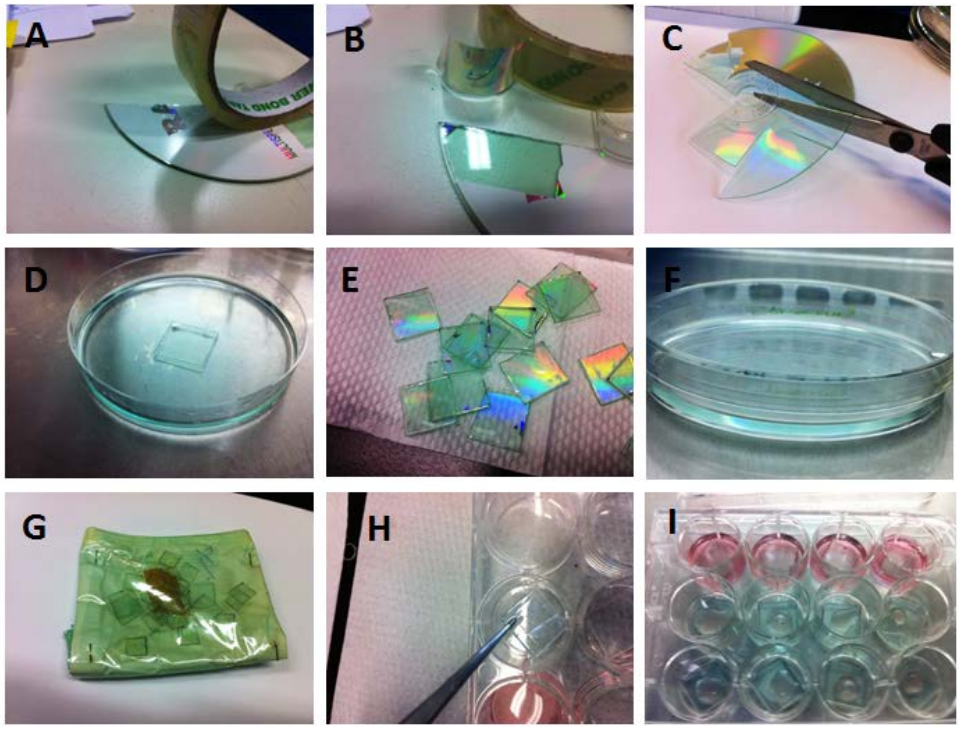

Figure 32: Processing the substrate surface of CD-R and Gratings on a dish. (A) The aluminium foil on the CD-R surface is peeled off (B) after pressing an adhesive tape against it. The CD-R is cut into small pieces (C); for example of dimensions 1 cm x 1 cm for 24-well plates or 1.5 cm x 1.5 cm for 12-well plates. (D) Methanol wash for cleaning dirt, chemical and dyes. (E) Drying (F) Ethanol wash and (G) Autoclaving for making the CD-R pieces sterile. (H) Placing the sterile CD-R pieces in well plates completing the "Gratings on a dish" device (I). Cells were seeded on the top of the gratings with the media.

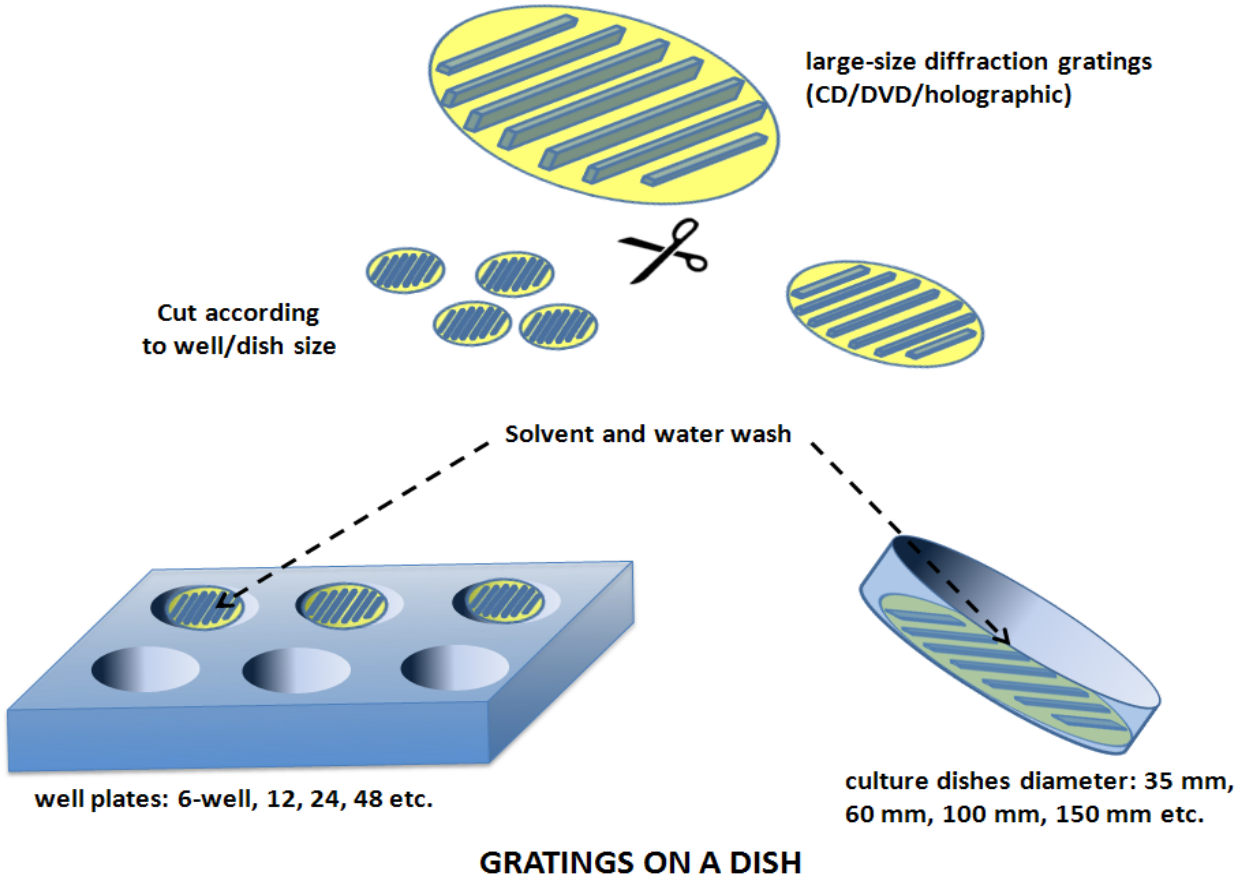

Figure 33: Schematic of Gratings on a dish. Large-sized diffraction gratings are cut into smaller pieces according to the dimensions of the wells and dishes. The diffraction gratings pieces are then processed with organic solvents and placed inside well plates/dishes completing the “Gratings on a dish”.

7.2.3 Zeta potential measurement of the surface

The zeta potentials of the diffraction gratings were measured by using an electro kinetic analyzer (EKA 1.00, Anton-Paar GmbH, Graz, Austria) equipped with a plated sample cell. The membranes were cut into 2 cm X 1 cm pieces. The measurements were conducted at 25ºC in 1 mM of KCl solution at pH 6.8. In each case, measurements were performed with three replicas.

7.2.4 Water contact angle measurement of the surface

Five microliter of DI water was pipetted on the gratings surface at normal velocity of dispension. Water contact angles were measured with a goniometer (Contact Angle System OCA 30, Data Physics Instruments GmbH, Germany) using the SCA20 software.

7.2.5 Coating the surface with extracellular matrix proteins

The gratings and CD-R/DVD-R were coated with gelatin (0.1%) after placing them in the 24-wells. The incubation time was kept at 12 hrs.

7.2.6 Mammalian cell culture in "Gratings on a dish"

Various types of cells; HL-1 (cell line from mouse atrial cardiomyocyte tumor lineage), H9C2 (cell line from embryonic rat ventricle) and 3T3 (cell lines from primary mouse embryonic fibroblast cells) were shown attached and aligned on the diffraction gratings inside the 24-well plates. Firstly, cells were cultured on tissue culture plates with DMEM media and on reaching confluency, were trypsinized and then seeded on the gratings. (Detail cell culture protocol is given in Appendix)

7.2.7 F-actin staining of cells on the optical discs

To stain for F-actin, cells were fixed in 3.7% paraformaldehyde for 20 mins at room temperature. Then the cells were permeabilized for 5 mins with 0.1% Tritin X-100

and then blocked with 2% bovine serum albumin for 15 mins at room temperature. Later, the cells were incubated with 200 mg/ml of TRITC-phalloidin (Molecular Probes, USA) for 20 minutes. Microscopy images were acquired with 20 X lens on a Zeiss Meta 510 upright confocal microscope. The 3D image stack was reconstructed using LSM Browser.

7.2.8 Measurement of cell alignment

Cell outline was determined with the help of an algorithm. The overall cell alignment for an image was found based on the alignment of those outlines (of cells). Then the direction histogram was plotted showing the number of cells aligned in particular angles.

7.2.9 Alamar Blue assay for cell proliferation on the gratings

Alamar blue assay was performed to demonstrate cell proliferation on the gratings. Cells were grown on the Gratings on a dish (CD-R pieces in 24-well microtiter plates). 10 µl of Alamar blue reagent (Life Technologies, USA) was mixed with 90 µl of media and added to each wells of the plates, and incubated for 2 hrs. The processed reagent is then transferred to 96-well plates for measurement of fluorescence by Infinite M1000 plate reader (Tecan, Switzerland) with absorption wavelength at 560 nm and emission wavelength at 590 nm. The control used was the Alamar blue reagent mixed with media (kept in wells inside incubator) without any cells.

7.3 Results and Discussion

7.3.1 Micro/nanogrooves on the gratings surface

The SEM images of the CD-R and DVD-R (Fig. 34A-B) depict the parallel grooves as reported before.[117] The two different holographic gratings were observed under AFM (Fig. 34C-D). For first holographic grating (with 500 lines/mm), the stripe width was found to be 1 μm and stripe height/depth to be 300 nm. For second holographic grating (1000 lines/mm), the stripe width was 500 nm and stripe depth to be 200 nm. Some of the important parameters of the two holographic gratings and the optical discs (CD-R and DVD-R) are summarized in Table.1. Approximate values are cited here.

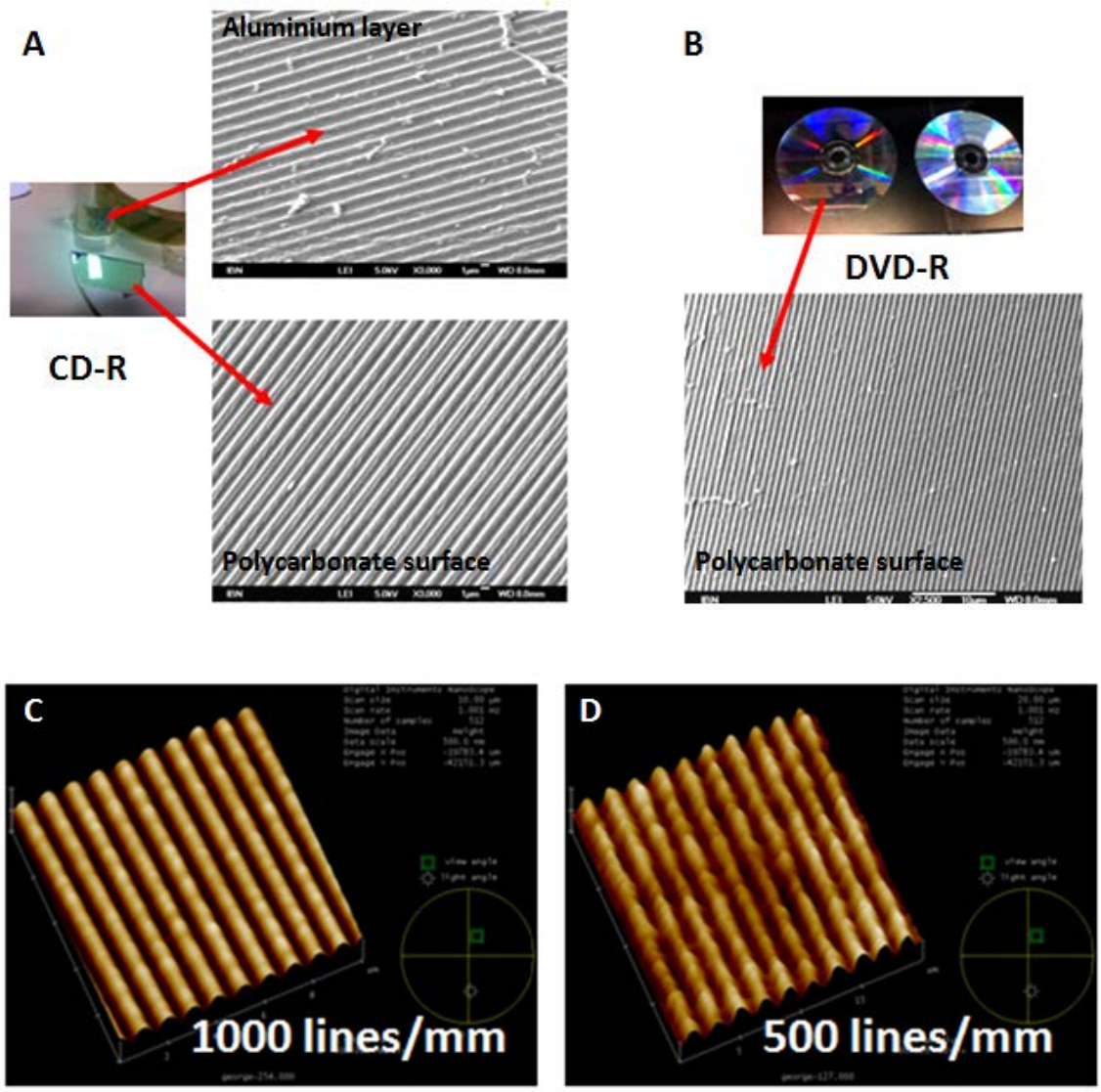

Figure 34: Topography of the diffraction gratings (CD-R/DVD-R/holographic gratings). (A-B) SEM images of the CD-R and DVD-R showing grooves and ridges on the surface. For CD-R, the aluminium foils as well as the polycarbonate were found to have grooves on them. For DVD-R, the inside surface of the bottom part had clear groove pattern. (C-D) AFM images of the holographic gratings showing grooves and ridges on the surface. The stripe width and periodicity of the gratings were similar to the description provided by the manufacturer (Edmund Optics). The stripe depth was found to be ~300 µm (500 lines/mm) and ~200 µm (1000 lines/mm) for the two different gratings.

	Diffraction Gratings	Company	Stripe width	Stripe height	Stripe periodicity	Thickness	Substrate
			OR Ridge and Groove width	OR Depth	OR Pitch		
1	CD-R	e.g. Imation	750 nm	130 nm	1.5 µm	1.2 mm	Polycarbonate
2	DVD-R	e.g. Imation	400 nm	70 nm	800 nm	1.2 mm	Polycarbonate
3	Holographic gratings: 500 lines/mm (12700 lines/inch)	Edmund optics	1 µm	300 nm	2 µm	~ 76 µm	Polyester
4	Holographic gratings 1000 lines/mm (25400 lines/inch)	Edmund optics	500 nm	200 nm	1 µm	~ 76 µm	Polyester

Table 1: Details of the holographic gratings and CD-Rs/DVD-Rs used for the studies.

7.3.2 Characterization of the diffraction gratings surface

The zeta potential of the CD-R/DVD-R surfaces were primarily negative as shown in Fig. 35. The charge interaction between the negatively charged substrate and charged cell may play a role in cell attachment or aggregation.

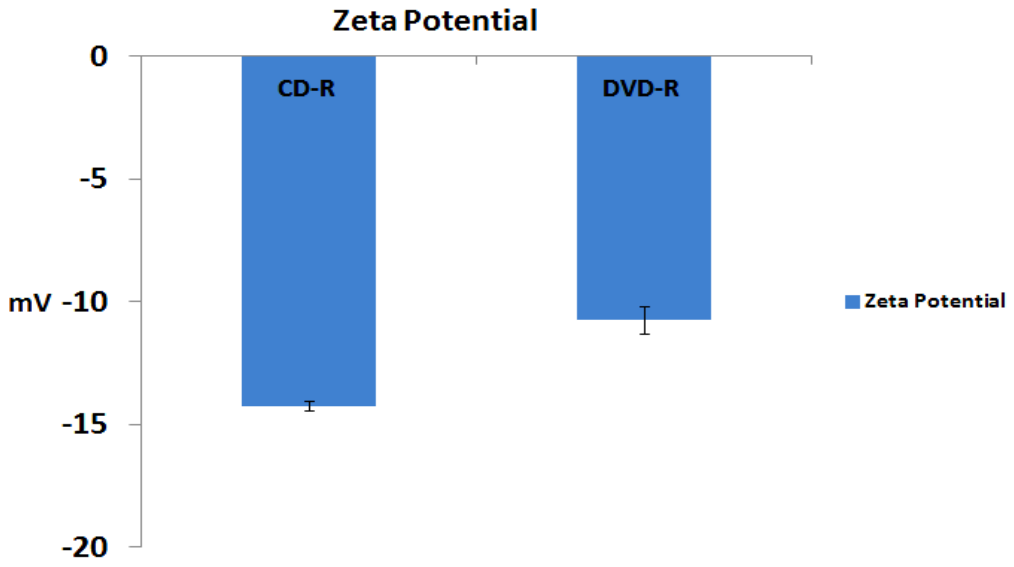

Figure 35: Zeta potential of the top surface of the processed optical discs to demonstrate the charge. Both CD-R and DVD-R had overall negative potential on the surface.

Meanwhile, the water contact angles (WCAs) of the CD-R/DVD-R/gratings are shown in Fig. 36. The water contact angles of untreated CD-R and DVD-R were ~90º and for gratings were ~70º, i.e. hydrophobic. The oxygen-plasma treated samples showed decrease in WCAs. Oxygen plasma treatment leads to a higher density of hydroxyl groups on polymeric surfaces.[186] These groups in turn decrease the water contact angle increasing the hydrophilicity of the surface. It is known that a hydrophilic surface aids in better cell attachment and hence proliferation,[187] so by controlling the plasma treatment we can modulate the hydrophilicity.

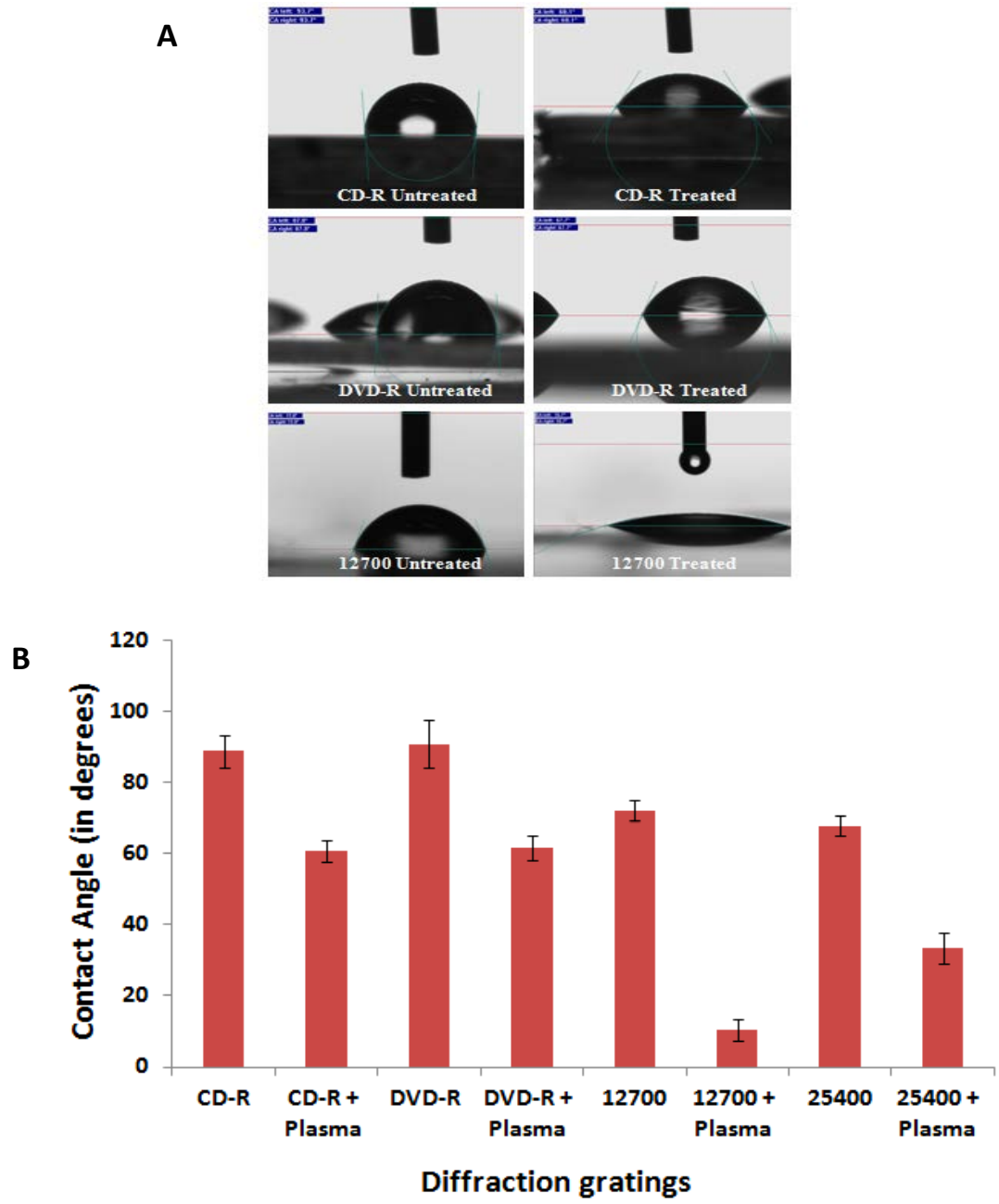

Figure 36: Water contact angles of CD-R/DVD-R/gratings surfaces. (A) Representative images of the water droplets on the surface of CD-R/DVD-R/gratings samples before and after oxygen plasma treatment. The water contact angles for treated CD-R and DVD-R decrease after being plasma-treated. (B) Quantitative analysis of water contact angle of CD-R/DVD-R samples, untreated optical discs and after treatment with oxygen plasma. The water contact angles for CD-R and DVD-R decreased from ~90º to about 60º after being plasma-treated. Whereas for gratings the decrease was more drastic; in case of 12700 gratings WCA decreased to ~ 10º and for 25400 gratings, WCA decreased to ~ 33º.

The surfaces of the gratings can be also modified according to the cell types to be cultured. Ligands like fibronectin, gelatin, laminin etc. can be coated on the surface prior to the cell culture. We demonstrated this by coating the CD-R surface with a 0.1% gelatin solution. The SEM image in Fig. 37 shows that the surface actually has the gelatin nanospheres and the grooves are not blocked or masked with the spheres.

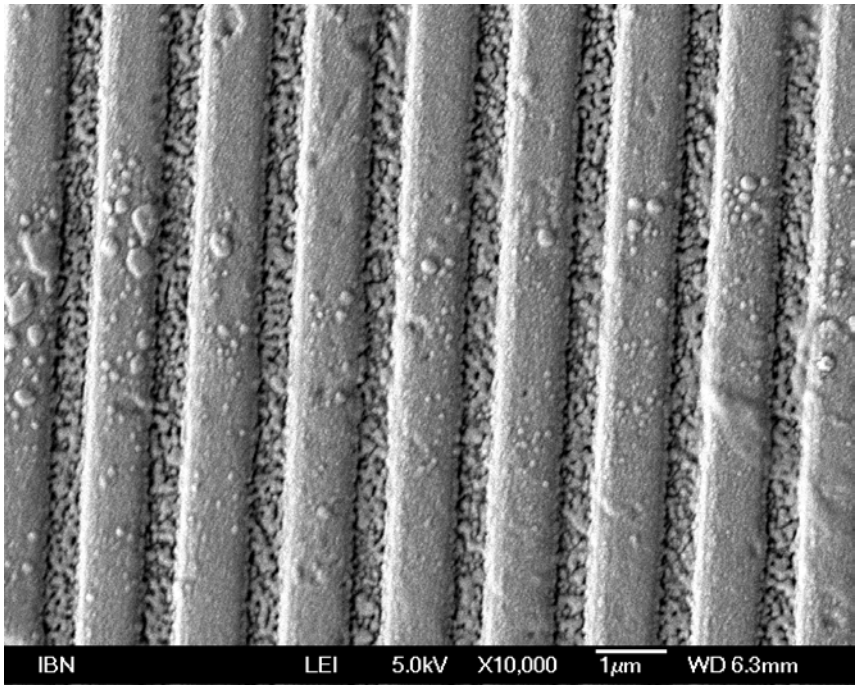

Figure 37: SEM of the CD-R with gelatin coating showing the presence of gelatin nanospheres on the ridges and inside the grooves. This clearly shows that the gratings surfaces can be easily coated with extra-cellular matrix (ECM) proteins and they would not mask the micro-nanogrooves.

7.3.3 Cell attachment and alignment on the surface of the gratings

Cells were cultured on gratings surface (Gratings on a dish) from 1-5 days for various studies. 3T3 cells, for example, attached to the CD-R surface within 4 hours of seeding and aligned along the grooves in 24 hours (Fig. 38). As seen in the bright-field images, the cells on the polycarbonate control (reverse side of the CD-R with no grooves) spread freely and had no particular alignment, whereas the cells cultured on the grooved surface of the CD-R were aligned along the groove directions (highlighted in the magnified inset figures). The aligned cells demonstrated a stretched morphology (clearer in higher magnification images) and enhanced attachment properties.

We also did some preliminary alignment measurements with HL-1 mouse cardiomyocytes growing on CD-R surface (Gratings on a dish) (Fig. 39A). To find the trend of directionality we first found out the edge of all cells (edge map) with an algorithm (Fig. 39B). However, for some cases, the edges get disconnected and hence two or more cells could merge to appear as one cell (with edge). Therefore, to discard those 'merged cells' we superimposed the edge map over the actual image of the cells (Fig. 39C). We selected only those cells for which the edge map co-localized with their actual image (Fig. 39D). As evident (Fig. 39E-F), the majority of the cells aligned at - 50º.

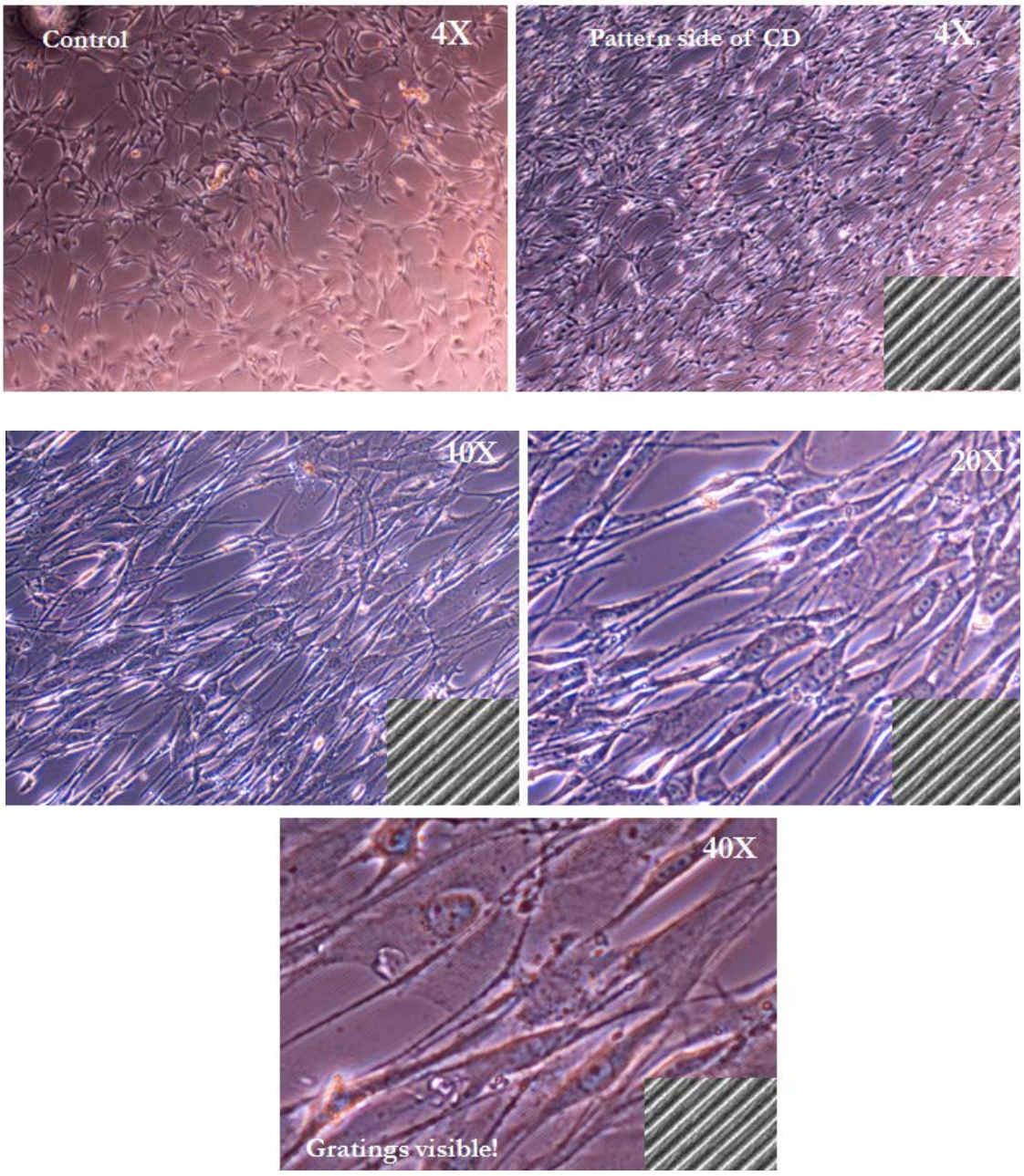

Figure 38: Brighfield images showing 3T3 Cells cultured for 24 hrs on CD-R-Gratings on a dish. The cells on the control (ungrooved side of the CD-R) did not align and in fact are randomly distributed on the surface. On the other hand, the cells on the grooved side, aligned along the grating direction (for convenience, insets indicate the grating direction). Images were taken at various magnifications to demonstrate the aligned and stretched morphology of the fibroblasts. In fact at 40X, the grooves were directly visible.

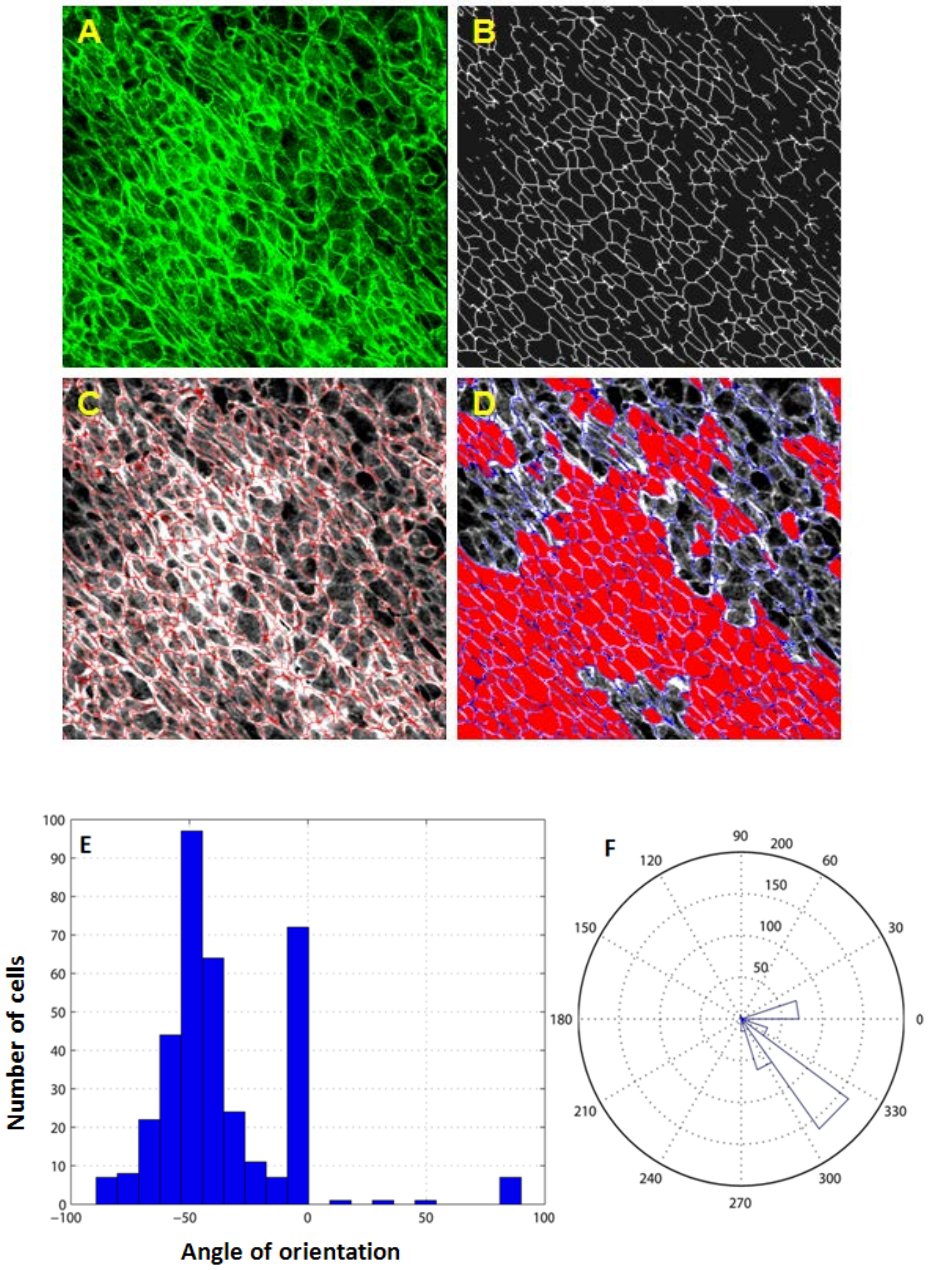

Figure 39: Quantification of alignment of HL-1 cells growing on CD-R-Gratings on a dish. (A) F-actin staining showing clearly the cellular cytoskeleton of HL-1 cells cultured on CD-R surface for 24 hrs. (B) The first step of the measurement algorithm involved identifying the edge (map) of the cells. (C) Actual image of the cells overlayed with the edge map obtained in the previous step. (D) Selected cells (Red) for alignment calculation. Those are the cells for which the edge map co-localized with the actual cell image. (E) Histogram plot of the direction result showing majority of cells preferentially aligning around -50º. (F) Rose-plot of the cell alignment demonstrating the same result in another format.

Cells were also cultured on the holographic gratings (24-wells Gratings on a dish). Fig. 40 shows the F-actin staining of H9C2 cells being seeded on holographic gratings of 1 μm pitch. The cells seeded on the grooved surface had uniformly aligned actin fibers along the groove direction, whereas on control surface (ungrooved surface of the grating) the cells were randomly oriented.

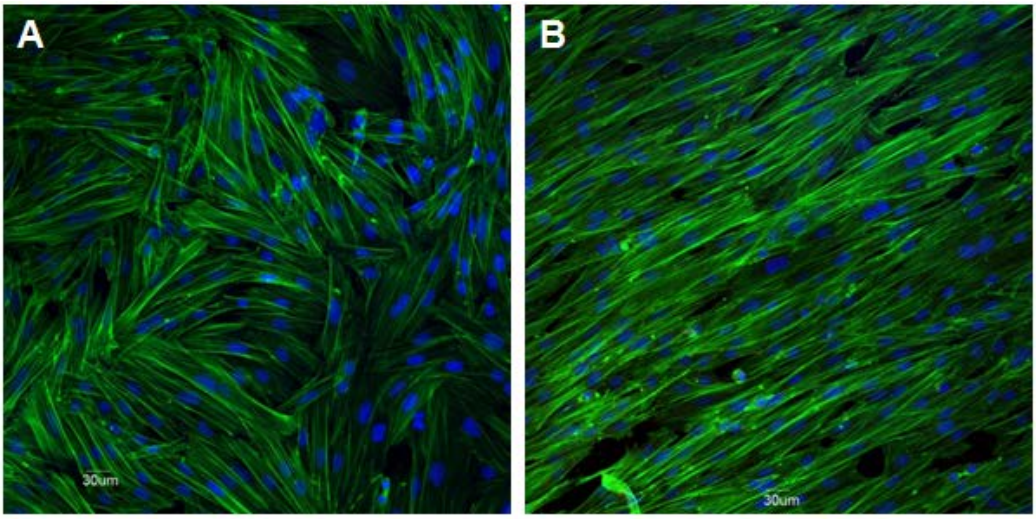

Figure 40: F-actin staining for H9C2 cells after being cultured on holographic gratings (Gratings on a dish) of pitch 1 μm for 2 days. The alignment was prominent in H9C2 cells because of larger size. The blue color was for the DAPI staining for the nuclei of the cells.

7.3.4 Cells showed similar proliferation on the grooves as the control surface

We wanted to check whether cells grow and respond robustly on the Gratings on a dish. Fig. 41 depicts the Alamar blue assay results for 3T3 cells being cultured on CD-R surface. The assay was performed on 1st, 2nd and 3rd day after the cell seeding on the CD-R. The fluorescence readings were normalized to the first day for each configuration of CD-R sample and the ungrooved CD-R control. The cell proliferation on the grooved surface and the unpatterened control appeared to be similar or better with no significant

difference on 2nd or 3rd day. This implies the gratings surface doesn't hinder cell growth in any way.

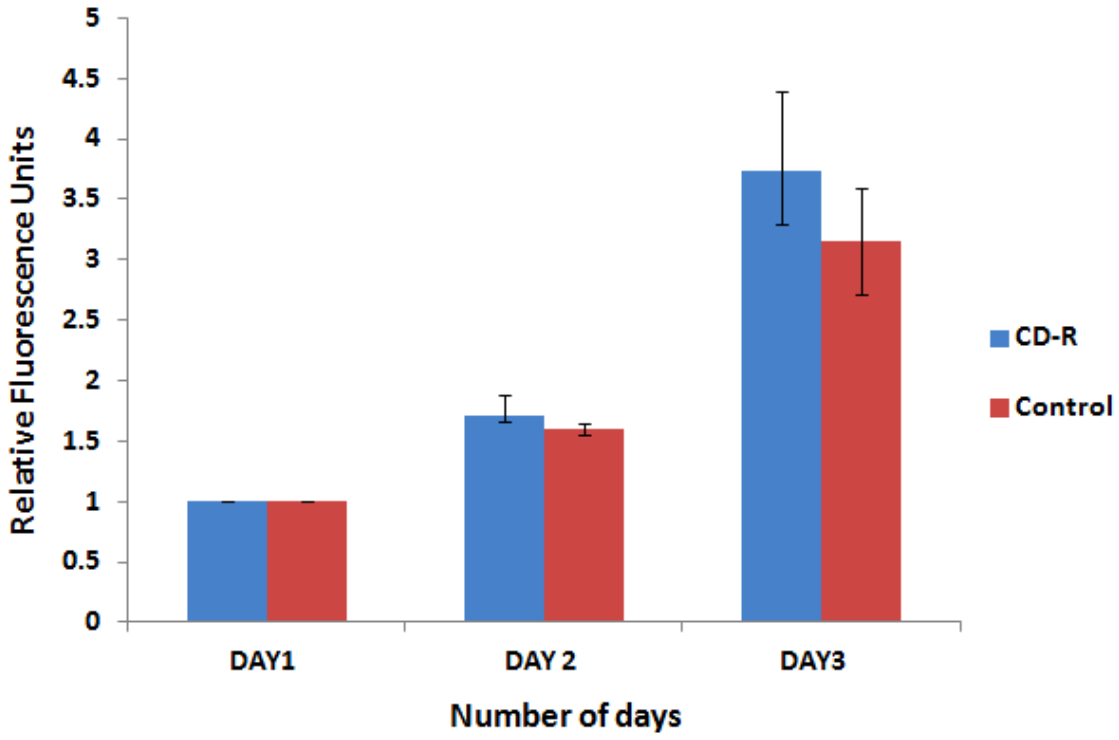

Figure 41: Alamar blue assays for 3T3 fibroblasts proliferation on Gratings on a dish compared to that on the ungrooved opposite side (control). The proliferation was similar for cells growing on grooved side with those growing on the ungrooved surface. Data are represented as average ± standard deviation of 4 samples.

7.4. Conclusions

We have developed a “Gratings on a dish” device for culturing and aligning cells on it. The physical characterization of the gratings revealed parallel grooves in holographic gratings as well as the optical discs. The gratings surface was made more hydrophilic with oxygen plasma for better cell attachment and proliferation. Various cell types (from rat and mouse species) were shown to be aligned on the gratings surface. The quantification of the alignment also indicated the preferential alignment of cells along the groove direction. The growth of the cells on the grooved surface occurred with the same robustness as the ungrooved surface. Gratings on a dish could be potentially used for drug testing applications. Cells that need alignment for maturation, like the cardiomyocytes, can be cultured/grown on this device with an enhanced physiological state (matured phenotype) for pharmacological investigation.

Chapter 8 Conclusions

This thesis documented the development of two different devices for drug testing applications. The first device called Fish and Chips was a multi-channel microfluidics platform for culturing early zebrafish embryos. We selected the silicon-glass prototype over the PDMS due to the many advantages it offered in terms of chip handling, world-to-chip connections and for potential commercialization. The silicon-glass chip was fabricated with standard photolithography, etching and bonding methods. The chip had three parts: inlets leading into microfluidic gradient generator, row of eight fish tanks, in which the fish embryos were individually placed, and eight output channels. The unique diagonal flow across the fish tank ensured the embryo received uniform exposure of drugs and media. Dye studies demonstrated the successful operation of the sigmoidal gradient generator. The dimensions of the fish tank were optimized so that the embryos remained constrained and long-term high-resolution imaging was possible. Fluorescence imaging of transgenic embryos at single-cell resolution was achieved. The embryos remained viable and developed normally when cultured in the chip for 4 days. Various tissues and organs were imaged at higher resolution. The drug valproic acid was used for proof-of-concept studies. Dosage-dependent drug effects were shown on the tail and eye development of fish embryos. Therefore, we conclude that our Fish and Chips could be used as organ-level drug screening model. This can complement the existing *in vivo* mammalian models.

The second device assembled was Gratings on a dish, which was adapting the commercially available diffraction gratings for cell alignment. Gratings on a dish was a simple platform in which the diffraction gratings were cut in to appropriate sizes and

placed in cell culture dishes and well plates. Prior to that the gratings pieces were processed with a sequence of organic solvents and rinsed with DI water. Oxygen plasma treatment made the gratings more hydrophilic and hence better for cell attachment and proliferation. The gratings could incorporate ECM components to make the surface more physiologically relevant for various cell types. Cells from various species were culture and aligned on the grooved surface of the gratings. Quantification of the alignment validated the preferential choice of the cells for the direction of the grooves. This method of exploiting commercially available diffraction gratings for direct cell culture is faster, cost effective and can be easily adapted by labs and start-ups for drug testing and other biomedical applications.

Chapter 9 Recommendations for future research

9.1 Scaling up the Fish and Chips

The Fish and chips can be modified to increase the number of fish tanks from current eight. We have designed a new Fish and Chips, which would have 64 fish tanks in total and can be fabricated in a bigger wafer size. This chip has a unique series of eight tanks that feed into next series of eight tanks and so on (Figure 42). This would enable more embryos for studies and would add to the throughput of the studies and hence the statistics of it.

In addition, the current Fish and Chips design can be easily modified to accommodate embryos of other animal model animals. The gradient generator can also be changed to linear or logarithmic form to get different variations for the drug concentrations.

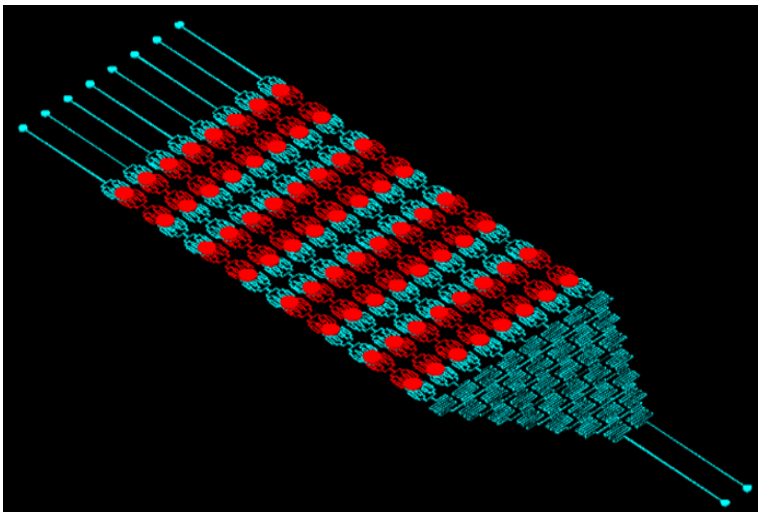

Figure 42: New design for Fish and Chips. This chip would have 64 fish tanks in total, with series of 8 tanks feeding into next 8 and so on.

9.2 More organ-specific toxicity using Fish and Chips

We have already demonstrated the development of various important tissues and organs on the chip. Our initial drug studies involved the effect of VPA on the development of the eyes and tail of the fish embryos. More targeted drug studies could be done for each of the organs. The beating heart of the zebrafish has both a complex cocktail of ion channels and functioning metabolism, which develops within 26 hours of fertilization.[188] Also any drastic effects on cardiac function can be tolerated by the larval fish which survive for 4-5 days without a circulation.[189] So apart from checking a single drug effect on the cardiac functions, we could replicate classical drug-drug interactions like erythromycin and cisapride as well as cimetidine and terfenadine[57] by perfusing one drug after other in Fish and Chips.

In another note, nanoparticles studies performed on microtiter plates can also be replicated on Fish and Chips.[190, 191] With increasing usage of commonly used nanoparticles like silver and gold, it is imperative that we know in more detail about the health and environmental impact of such particles both in terms of their size[192] and in terms of concentration. The usual effects of nanoparticles like hatching rate, mortality, abnormal body axes, pericardial edema and cardiac arrhythmia can be easily studied using our system.

9.3 Drug-testing on Gratings on a dish

We have clearly demonstrated alignment of various cell types on the Gratings on a dish device. Cardiomyocytes were shown to not only survive but also attach and proliferate on those gratings. The alignment of cells followed precisely the direction of

the micro-nanogrooves on the gratings. Freshly isolated cardiomyocytes or neurons from animal models can be aligned on those gratings and remodeled back to the matured phenotype. For primary cardiomyocytes, electrical-field stimulation could be used in tandem with the forced alignment due to the gratings.[92] These phenotypes would be most suitable for practical drug testing applications.

9.4 Other biomedical applications on Gratings on a dish

Apart from the drug testing application, other important usage of the gratings device would be tissue engineering and stem-cell differentiation. Taking cue from previous published work, we could develop small sheets of smooth muscle cells [82] or heal corneal epithelium.[90] The ECM can be easily modulated depending on the desired cells growing on the gratings.

Human mesenchymal stem cells can be differentiated into various lineages like neuronal, osetogenic, chondrogenic or adipogenic when grown on aligned surfaces.[113] In fact, nanogrooves have been shown to directly differentiate human embryonic stem cells to neuronal lineage without using any growth factors.[83] This is advantageous in terms of saving costly growth factors and controlling the exact concentration of these factors for directed differentiation. Our Gratings on a dish gives tremendous flexibility in terms of the depth, pitch of the micro-nanogrooves, and hence can be explored for stem-cell differentiation to all lineages.

Chapter 10 References

1. J. A. DiMasi, R. W. Hansen and H. G. Grabowski, *Journal of Health Economics*, 2003, **22**, 151-185.
2. M. Goodman, *Nature Reviews Drug Discovery*, 2009**8**, 348.
3. B. Hughes, *Nature Reviews | Drug Discovery*, 2009, **8**, 93-96.
4. L. F. Kang, B. G. Chung, R. Langer and A. Khademhosseini, *Drug Discovery Today*, 2008, **13**, 1-13.
5. P. S. Dittrich and A. Manz, *Nature Reviews Drug Discovery*, 2006, **5**, 210-218.
6. B. M. Amore, J. P. Gibbs and M. G. Emery, *Combinatorial Chemistry & High Throughput Screening*, 2010, **13**, 207-218.
7. D. R. Boverhof, M. P. Chamberlain, C. R. Elcombe, F. J. Gonzalez, R. H. Heflich, L. G. Hernandez, A. C. Jacobs, D. Jacobson-Kram, M. Luijten, A. Maggi, M. G. Manjanatha, J. van Benthem and B. B. Gollapudi, *Toxicological Sciences*, 2011, **121**, 207-233.
8. S. C. Gad, *Animal Models in Toxicology*, *Second Edition*, CRC, 2007.
9. H. Olson, G. Betton, D. Robinson, K. Thomas, A. Monro, G. Kolaja, P. Lilly, J. Sanders, G. Sipes, W. Bracken, M. Dorato, K. Van Deun, P. Smith, B. Berger and A. Heller, *Regulatory Toxicology and Pharmacology*, 2000, **32**, 56-67.
10. C. Parng, W. L. Seng, C. Semino and P. McGrath, *Assay and Drug Development Technologies*, 2002, **1**, 41-48.
11. D. H. Freedman, *Technology Review*, 2004.
12. U. Langheinrich, *Bioessays*, 2003, **25**, 904-912.
13. C. Zhang, *Current Protocols in Toxicology*, 2003, 1.7.1–1.7.18.
14. P. Goldsmith, *Current Opinion in Pharmacology*, 2004, **4**, 504-512.
15. P. McGrath and C. Q. Li, *Drug Discovery Today*, 2008, **13**, 394-401.
16. P. M. Eimon and A. L. Rubinstein, *Expert Opinion on Drug Metabolism & Toxicology*, 2009, **5**, 393-401.
17. J. M. Spitsbergen and M. L. Kent, *Toxicologic Pathology*, 2003, **31**, 62-87.
18. G. Kari, U. Rodeck and A. P. Dicker, *Clinical Pharmacology & Therapeutics*, 2007, **82**, 70-80.
19. D. Choudhury, D. van Noort, C. Iliescu, B. Zheng, K.-L. Poon, S. Korzh, V. Korzh and H. Yu, *Lab on a Chip*, 2012, **12**, 892-900.
20. E. M. Wielhouwer, S. Ali, A. Al-Afandi, M. T. Blom, M. B. O. Riekerink, C. Poelma, J. Westerweel, J. Oonk, E. X. Vrouwe, W. Buesink, H. G. J. vanMil, J. Chicken, R. V. Oever and M. K. Richardson, *Lab on a Chip*, 2011, **11**, 1815-1824.
21. M.-H. Wu, S.-B. Huang and G.-B. Lee, *Lab on a Chip*, 2010, **10**.
22. B. Nugraha, X. Hong, X. Mo, L. Tan, W. Zhang, P.-M. Chan, C. H. Kang, Y. Wang, L. T. Beng, W. Sun, D. Choudhury, J. M. Robens, M. McMillian,

J. Silva, S. Dallas, C.-H. Tan, Z. Yue and H. Yu, *Biomaterials*, 2011, **32**, 6982-6994.
23. Y. Du, R. Han, F. Wen, S. N. S. San, L. Xia, T. Wohland, H. L. Leo and H. Yu, *Biomaterials*, 2008, **29**, 290-301.
24. Y. C. Toh, C. Zhang, J. Zhang, Y. M. Khong, S. Chang, V. D. Samper, D. van Noort, D. W. Hutmacher and H. Yu, *Lab Chip*, 2007, **7**, 302-309.
25. G. Kirmizidis and M. A. Birch, *Tissue Engineering Part A*, 2009, **15**, 1427-1436.
26. Y. N. Xia and G. M. Whitesides, *Annual Review of Materials Science*, 1998, **28**, 153-184.
27. E. Detrait, J. B. Lhoest, B. Knoops, P. Bertrand and P. V. D. de Aguilar, *Journal of Neuroscience Methods*, 1998, **84**, 193-204.
28. J. T. Groves, L. K. Mahal and C. R. Bertozzi, *Langmuir*, 2001, **17**, 5129-5133.
29. H. W. Lu, Q. H. Lu, W. T. Chen, H. J. Xu and J. Yin, *Materials Letters*, 2004, **58**, 29-32.
30. D. M. Brunette, *Experimental Cell Research*, 1986, **164**, 11-26.
31. A. M. Rajnicek, S. Britland and C. D. McCaig, *Journal of Cell Science*, 1997, **110**, 2905-2913.
32. T. Peterbauer, S. Yakunin, J. Siegel and J. Heitz, *Modern Trends in Polymer Science-Epf 09*, 2010, **296**, 272-277.
33. S. Y. Chou, P. R. Krauss and P. J. Renstrom, *Science*, 1996, **272**, 85-87.
34. P. Weiss, *International Review of Cytology-a Survey of Cell Biology*, 1958, **7**, 391-423.
35. B. S. Zhu, Q. H. Lu, J. Yin, J. Hu and Z. G. Wang, *Journal of Biomedical Materials Research Part B-Applied Biomaterials*, 2004, **70B**, 43-48.
36. J. L. Charest, M. T. Eliason, A. J. Garcia and W. P. King, *Biomaterials*, 2006, **27**, 2487-2494.
37. G. M. Whitesides, *Nature*, 2006, **442**, 368-373.
38. D. M. Brunette, *Experimental Cell Research*, 1986, **164**, 11-26.
39. B. Hirschler, *Reuters*, 2007.
40. *Medical News Today.com*, 2005.
41. A. Sin, G. T. Baxter and M. L. Shuler, in *Microfluidics and Biomems*, eds. C. H. Mastrangelo and H. Becker, 2001, vol. 4560, pp. 98-101.
42. N. Kaplowitz, *Nature Reviews Drug Discovery*, 2005, **4**, 489-499.
43. J. P. Piccini, D. J. Whellan, B. R. Berridge, J. K. Finkle, S. D. Pettit, N. Stockbridge, J.-P. Valentin, H. M. Vargas, M. W. Krucoff and C. H. W. Grp, *American Heart Journal*, 2009, **158**, 317-326.
44. I. Kola, *Nature Reviews Drug Discovery* 2004.
45. Y. C. Toh, S. Ng, Y. M. Khong, V. Samper and H. Yu, *Assay and Drug Development Technologies*, 2005, **3**, 169-176.

46. C. Zhang, Z. Q. Zhao, N. A. A. Rahim, D. van Noort and H. Yu, *Lab on a Chip*, 2009, **9**, 3185-3192.
47. K. J. Jang and K. Y. Suh, *Lab on a Chip*, 2010, **10**, 36-42.
48. K. Viravaidya, A. Sin and M. L. Shuler, *Biotechnology Progress*, 2004, **20**, 316-323.
49. J. H. Sung and M. L. Shuler, *Lab on a Chip*, 2009, **9**, 1385-1394.
50. M.-H. Wu, S.-B. Huang, Z. Cui, Z. Cui and G.-B. Lee, *Sensors and Actuators B-Chemical*, 2008, **129**, 231-240.
51. J. Lee, M. J. Cuddihy, G. M. Cater and N. A. Kotov, *Biomaterials*, 2009, **30**, 4687-4694.
52. S. Zhang, L. Xia, C. H. Kang, G. Xiao, S. M. Ong, Y. C. Toh, H. L. Leo, D. van Noort, S. H. Kan, H. H. Tang and H. Yu, *Biomaterials*, 2008, **29**, 3993-4002.
53. H. W. Laale, *Journal of Fish Biology*, 1977, **10**, 121-&.
54. J. S. Nelson, *Fishes of the world.*, John Wiley and Sons, Inc. , New York., 1994.
55. G. J. Lieschke and P. D. Currie, *Nature Reviews Genetics*, 2007, **8**, 353-367.
56. Pharmaceutical Industry Faces Multiple Challenges - Future lies in Drug Pipeline Sustainability.
57. D. J. Milan, T. A. Peterson, J. N. Ruskin, R. T. Peterson and C. A. MacRae, *Circulation*, 2003, **107**, 1355-1358.
58. K. Finlayson, H. J. Witchel, J. McCulloch and J. Sharkey, *European Journal of Pharmacology*, 2004, **500**, 129-142.
59. C. Q. Li, W. S. Lin and P. McGrath, *International Journal of Toxicology*, 2009, **28**, P58.
60. T. G. G. Braunbecka, Volker Storcha and Roland Nagelb, *Ecotoxicology and Environmental Safety*, 1990, **19**, 355-374.
61. P. McGrath, *Toxicologist 96 (Suppl.)*, 2007, 244.
62. J. M. Murtha, W. C. Qi and E. T. Keller, *Comparative Medicine*, 2003, **53**, 37-41.
63. A. L. Nielsen and A. L. Jorgensen, *Gene*, 2003, **310**, 123-132.
64. P. Haffter, M. Granato, M. Brand, M. C. Mullins, M. Hammerschmidt, D. A. Kane, J. Odenthal, F. J. M. vanEeden, Y. J. Jiang, C. P. Heisenberg, R. N. Kelsh, M. FurutaniSeiki, E. Vogelsang, D. Beuchle, U. Schach, C. Fabian and C. NussleinVolhard, *Development*, 1996, **123**, 1-36.
65. P. Blader and U. Strahle, *Developmental Biology*, 1998, **201**, 185-201.
66. N. Gurvich, M. G. Berman, B. S. Wittner, R. C. Gentleman, P. S. Klein and J. B. A. Green, *FASEB Journal*, 2005, **19**.
67. K. Herrmann, *Toxicology in Vitro*, 1993, **7**, 41-54.
68. L. G. Beckwith, J. L. Moore, G. S. Tsao-Wu, J. C. Harshbarger and K. C. Cheng, *Laboratory Investigation*, 2000, **80**, 379-385.

69. C. L. Winata, S. Korzh, I. Kondrychyn, W. L. Zheng, V. Korzh and Z. Y. Gong, *Developmental Biology*, 2009, **331**, 222-236.
70. M. Sonawane, Y. Carpio, R. Geisler, H. Schwarz, H. M. Maischein and C. Nuesslein-Volhard, *Development*, 2005, **132**, 3255-3265.
71. D. R. Love, F. B. Pichler, A. Dodd, B. R. Copp and D. R. Greenwood, *Current Opinion in Biotechnology*, 2004, **15**, 564-571.
72. S. U. Son and R. L. Garrell, *Lab on a Chip*, 2009, **9**, 2398-2401.
73. A. Funfak, A. Brosing, M. Brand and J. M. Kohler, *Lab on a Chip*, 2007, **7**, 1132-1138.
74. C. J. Huang, C. T. Tu, C. D. Hsiao, F. J. Hsieh and H. J. Tsai, *Developmental Dynamics*, 2003, **228**, 30-40.
75. T. Bansal, J. Lenhart, T. Kim, C. Duan and M. M. Maharbiz, *Biomedical Microdevices*, 2009, **11**, 633-641.
76. Y.-c. Shen, D. Li, A. Al-Shoaibi, T. Bersano-Begey, H. Chen, S. Ali, B. Flak, C. Perrin, M. Winslow, H. Shah, P. Ramamurthy, R. H. Schmedlen, S. Takayama and K. F. Barald, *Zebrafish*, 2009, **6**, 201-213.
77. C. Pardo-Martin, T.Y. Chang, B.K. Koo, C.L. Gileland, S.C. Wasserman and M.F. Yanik, *Nature Methods*, 2010, **7**.
78. A. L. Rubinstein, *Expert Opinion on Drug Metabolism & Toxicology*, 2006, **2**, 231-240.
79. M. Westerfield, *The zebrafish book. A guide for the laboratory use of zebrafish (Danio rerio)*. Univ. of Oregon Press, Eugene, 2000.
80. H. Kenar, G. T. Kose and V. Hasirci, *Biomaterials*, 2006, **27**, 885-895.
81. H. T. H. Au, I. Cheng, M. F. Chowdhury and M. Radisic, *Biomaterials*, 2007, **28**, 4277-4293.
82. B. C. Isenberg, Y. Tsuda, C. Williams, T. Shimizu, M. Yamato, T. Okano and J. Y. Wong, *Biomaterials*, 2008, **29**, 2565-2572.
83. M. R. Lee, K. W. Kwon, H. Jung, H. N. Kim, K. Y. Suh, K. Kim and K.-S. Kim, *Biomaterials*, 2010, **31**, 4360-4366.
84. E. K. F. Yim, E. M. Darling, K. Kulangara, F. Guilak and K. W. Leong, *Biomaterials*, 2010, **31**, 1299-1306.
85. R. G. Harrison, *Anatomical Record*, 1912, **6**, 181-193.
86. B. Wojciakstothard, A. S. G. Curtis, W. Monaghan, M. McGrath, I. Sommer and C. D. W. Wilkinson, *Cell Motility and the Cytoskeleton*, 1995, **31**, 147-158.
87. K. H. Kim, J. S. Cho, D. J. Choi and S. K. Koh, *Nuclear Instruments & Methods in Physics Research Section B-Beam Interactions with Materials and Atoms*, 2001, **175**, 542-547.
88. H. Tsuji, H. Satoh, S. Ikeda, S. Ikemura, Y. Gotoh and J. Ishikawa, *Nuclear Instruments & Methods in Physics Research Section B-Beam Interactions with Materials and Atoms*, 1999, **148**, 1136-1140.
89. B. D. Ratner, *Surface Modification of Polymeric Biomaterials*, 1997, 1-9.

90. N. Gomez, S. Chen and C. E. Schmidt, *Journal of the Royal Society Interface*, 2007, **4**, 223-233.
91. E. Rebollar, I. Frischauf, M. Olbrich, T. Peterbauer, S. Hering, J. Preiner, P. Hinterdorfer, C. Romanin and J. Heitz, *Biomaterials*, 2008, **29**, 1796-1806.
92. D. M. Brunette, G. S. Kenner and T. R. L. Gould, *Journal of Dental Research*, 1983, **62**, 1045-1048.
93. F. Sun, D. Casse, J. A. van Kan, R. W. Ge and F. Watt, *Tissue Engineering*, 2004, **10**, 267-272.
94. Y. Yang, K. Kulangara, J. Sia, L. Wang and K. W. Leong, *Lab on a Chip*, 2011, **11**, 1638-1646.
95. S. Britland, H. Morgan, B. WojiakStodart, M. Riehle, A. Curtis and C. Wilkinson, *Experimental Cell Research*, 1996, **228**, 313-325.
96. P. T. Ohara and R. C. Buck, *Experimental Cell Research*, 1979, **121**, 235-249.
97. P. Clark, P. Connolly, A. S. G. Curtis, J. A. T. Dow and C. D. W. Wilkinson, *Development*, 1990, **108**, 635-644.
98. E. T. den Braber, H. V. Jansen, M. J. de Boer, H. J. E. Croes, M. Elwenspoek, L. A. Ginsel and J. A. Jansen, *Journal of Biomedical Materials Research*, 1998, **40**, 425-433.
99. J. C. Palmaz, A. Benson and E. A. Sprague, *Journal of Vascular and Interventional Radiology*, 1999, **10**, 439-444.
100. K. Matsuzaka, X. F. Walboomers, J. E. de Ruijter and J. A. Jansen, *Biomaterials*, 1999, **20**, 1293-1301.
101. C. Miller, H. Shanks, A. Witt, G. Rutkowski and S. Mallapragada, *Biomaterials*, 2001, **22**, 1263-1269.
102. C. Miller, S. Jeftinija and S. Mallapragada, *Tissue Engineering*, 2002, **8**, 367-378.
103. E. T. den Braber, J. E. de Ruijter, L. A. Ginsel, A. F. von Recum and J. A. Jansen, *Journal of Biomedical Materials Research*, 1998, **40**, 291-300.
104. B. D. Lawrence, J. K. Marchant, M. A. Pindrus, F. G. Omenetto and D. L. Kaplan, *Biomaterials*, 2009, **30**, 1299-1308.
105. R. B. Vernon, M. D. Gooden, S. L. Lara and T. N. Wight, *Biomaterials*, 2005, **26**, 3131-3140.
106. D.-H. Kim, E. A. Lipke, P. Kim, R. Cheong, S. Thompson, M. Delannoy, K.-Y. Suh, L. Tung and A. Levchenko, *Proceedings of the National Academy of Sciences of the United States of America*, 2010, **107**, 565-570.
107. P.-Y. Wang, J. Yu, J.-H. Lin and W.-B. Tsai, *Acta Biomaterialia*, 2011, **7**, 3285-3293.
108. M. D. M. Evans, G. A. McFarland, S. Taylor and X. F. Walboomers, *Biomaterials*, 2005, **26**, 1703-1711.
109. J.-Y. Yang, Y.-C. Ting, J.-Y. Lai, H.-L. Liu, H.-W. Fang and W.-B. Tsai, *Journal of Biomedical Materials Research Part A*, 2009, **90A**, 629-640.

110. J. L. Charest, A. J. Garcia and W. P. King, *Biomaterials*, 2007, **28**, 2202-2210.
111. R. G. Flemming, C. J. Murphy, G. A. Abrams, S. L. Goodman and P. F. Nealey, *Biomaterials*, 1999, **20**, 573-588.
112. E. K. F. Yim, S. W. Pang and K. W. Leong, *Experimental Cell Research*, 2007, **313**, 1820-1829.
113. B. Lanfer, F. P. Seib, U. Freudenberg, D. Stamov, T. Bley, M. Bornhaeuser and C. Werner, *Biomaterials*, 2009, **30**, 5950-5958.
114. T. Dvir, B. P. Timko, D. S. Kohane and R. Langer, *Nature Nanotechnology*, 2011, **6**, 13-22.
115. Scientific diffraction gratings / cutsom gratings (Product catalog and capabilities) http://www.horiba.com/scientific/.
116. M. Emmelius, G. Pawlowski and H. W. Vollmann, *Angewandte Chemie-International Edition in English*, 1989, **28**, 1445-1471.
117. R. Mukherjee, A. Sharma, G. Patil, D. Faruqui and P. S. G. Pattader, *Bulletin of Materials Science*, 2008, **31**, 249-261.
118. D. Chowdhury, A. Paul and A. Chattopadhyay, *Nano Letters*, 2001, **1**, 409-412.
119. E. S. Gil, S.-H. Park, J. Marchant, F. Omenetto and D. L. Kaplan, *Macromolecular Bioscience*, 2010, **10**, 664-673.
120. M. Radisic, H. Park, H. Shing, T. Consi, F. J. Schoen, R. Langer, L. E. Freed and G. Vunjak-Novakovic, *Proceedings of the National Academy of Sciences of the United States of America*, 2004, **101**, 18129-18134.
121. T. Pong, W. J. Adams, M.-A. Bray, A. W. Feinberg, S. P. Sheehy, A. A. Werdich and K. K. Parker, *Experimental Biology and Medicine*, 2011, **236**, 366-373.
122. M. Valderrabano, *Progress in Biophysics & Molecular Biology*, 2007, **94**, 144-168.
123. http://www.amazon.com/, Imation 17262 52X CD-R-r 700MB/80 Mi.
124. Holographic Diffraction Grating Film, http://www.edmundoptics.com.
125. CD-R Recycling Centre http://www.CD-Rrecyclingcenter.com/.
126. L. Kim, Y. C. Toh, J. Voldman and H. Yu, *Lab on a Chip*, 2007, **7**, 681-694.
127. J. M. Nagarah, P. Wang, Y. Luo, R. Pantoja, N. A. Melosh, D. M. Starace, R. Blunk, F. Bezanilla and J. R. Heath, *Biophysical Journal*, 2005, **88**, 522A-522A.
128. I. Rodriguez, P. Spicar-Mihalic, C. L. Kuyper, G. S. Fiorini and D. T. Chiu, *Analytica Chimica Acta*, 2003, **496**, 205-215.
129. H. Becker and L. E. Locascio, *Talanta*, 2002, **56**, 267-287.
130. S. A. Soper, A. C. Henry, B. Vaidya, M. Galloway, M. Wabuyele and R. L. McCarley, *Analytica Chimica Acta*, 2002, **470**, 87-99.

131. W. Zhang, S. Lin, C. Wang, J. Hu, C. Li, Z. Zhuang, Y. Zhou, R. A. Mathies and C. J. Yang, *Lab on a Chip*, 2009, **9**, 3088-3094.
132. J. C. MCD-Ronald and G. M. Whitesides, *Accounts of Chemical Research*, 2002, **35**, 491-499.
133. M. B. Wabuyele, S. M. Ford, W. Stryjewski, J. Barrow and S. A. Soper, *Electrophoresis*, 2001, **22**, 3939-3948.
134. E. Bormashenko, R. Pogreb, G. Whyman, Y. Bormashenko, R. Jager, T. Stein, A. Schechter and D. Aurbach, *Langmuir*, 2009, **25**, 4828-4828.
135. S. K. Sia and G. M. Whitesides, *Electrophoresis*, 2003, **24**, 3563-3576.
136. T. Fujii, *Microelectronic Engineering*, 2002, **61-2**, 907-914.
137. B. D. Ratner and S. J. Bryant, *Annual Review of Biomedical Engineering*, 2004, **6**, 41-75.
138. T. Thorsen, S. J. Maerkl and S. R. Quake, *Science*, 2002, **298**, 580-584.
139. G. M. Whitesides, E. Ostuni, S. Takayama, X. Y. Jiang and D. E. Ingber, *Annual Review of Biomedical Engineering*, 2001, **3**, 335-373.
140. P. Abgrall and A. M. Gue, *Journal of Micromechanics and Microengineering*, 2007, **17**, R15-R49.
141. M. Ni, W. H. Tong, D. Choudhury, N. A. A. Rahim, C. Iliescu and H. Yu, *International Journal of Molecular Sciences*, 2009, **10**, 5411-5441.
142. G. Kotzar, M. Freas, P. Abel, A. Fleischman, S. Roy, C. Zorman, J. M. Moran and J. Melzak, *Biomaterials*, 2002, **23**, 2737-2750.
143. C. Ronco and A. R. Nissenson, *Blood Purification*, 2001, **19**, 347-352.
144. W. H. Fissell, S. Manley, A. Westover, H. D. Humes, A. J. Fleischman and S. Roy, *Asaio Journal*, 2006, **52**, 221-227.
145. J. Salonen, A. M. Kaukonen, J. Hirvonen and V.-P. Lehto, *Journal of Pharmaceutical Sciences*, 2008, **97**, 632-653.
146. C. Iliescu, H. Taylor, M. Avram, J. Miao and S. Franssila, *Biomicrofluidics*, 2012 **6**, 016505.
147. N. L. Jeon, H. Baskaran, S. K. W. Dertinger, G. M. Whitesides, L. Van de Water and M. Toner, *Nature Biotechnology*, 2002, **20**, 826-830.
148. J. Pihl, M. Karlsson and D. T. Chiu, *Drug Discovery Today*, 2005, **10**, 1377-1383.
149. S. K. W. Dertinger, D. T. Chiu, N. L. Jeon and G. M. Whitesides, *Analytical Chemistry*, 2001, **73**, 1240-1246.
150. S. J. Boyden, *Journal of Experimental Medicine* 1962 **115**, 453-466.
151. H. J. Song and M. M. Poo, *Current Opinion in Neurobiology*, 1999, **9**, 355-363.
152. R. Santos, *A Review of Advances in Multiphase Computational Fluid Dynamics for Microfluidics*, Nova Science Publishers Inc, 2011.
153. M.-C. Kim, Z. Wang, R. H. W. Lam and T. Thorsen, *Journal of Applied Physics*, 2008, **103**.

154. C. Iliescu, J. Jing, F. E. H. Tay, J. M. Miao and T. T. Sun, *Surface & Coatings Technology*, 2005, **198**, 314-318.
155. C. Iliescu, G. L. Xu, V. Samper and F. E. H. Tay, *Journal of Micromechanics and Microengineering*, 2005, **15**, 494-500.
156. C. Iliescu, B. Chen and J. Miao, *Sensors and Actuators a-Physical*, 2008, **143**, 154-161.
157. R. Spence, G. Gerlach, C. Lawrence and C. Smith, *Biological Reviews*, 2008, **83**, 13-34.
158. E. Linney, N. L. Hardison, B. E. Lonze, S. Lyons and L. DiNapoli, *Developmental Biology*, 1999, **213**, 207-216.
159. K. R. Finley, A. E. Davidson and S. C. Ekker, *Biotechniques*, 2001, **31**, 66-+.
160. K.-L. Poon, M. Liebling, I. Kondrychyn, M. Garcia-Lecea and V. Korzh, *Developmental Dynamics*, 2010, **239**, 914-926.
161. N. D. Lawson and B. M. Weinstein, *Developmental Biology*, 2002, **248**, 307-318.
162. S. Parinov, I. Kondrichin, V. Korzh and A. Emelyanov, *Developmental Dynamics*, 2004, **231**, 449-459.
163. C. B. Kimmel, W. W. Ballard, S. R. Kimmel, B. Ullmann and T. F. Schilling, *Developmental Dynamics*, 1995, **203**, 253-310.
164. J. Karlsson, J. von Hofsten and P. E. Olsson, *Marine Biotechnology*, 2001, **3**, 522-527.
165. C. Teh, D. M. Chudakov, K. L. Poon, I. Z. Mamedov, J. Y. Sek, K. Shidlovsky, S. Lukyanov and V. Korzh, *Bmc Developmental Biology*, 2010, **10**.
166. A. Ghysen and C. Dambly-Chaudiere, *Genes & Development*, 2007, **21**, 2118-2130.
167. W. Go, D. Bessarab and V. Korzh, *Cell Calcium*, 2010, **48**, 302-313.
168. L. L. Chiu, L. L. Cunningham, D. W. Raible, E. W. Rubel and H. C. Ou, *Jaro-Journal of the Association for Research in Otolaryngology*, 2008, **9**, 178-190.
169. C. Ton and C. Parng, *Hearing Research*, 2005, **208**, 79-88.
170. A. S. Glass and R. Dahm, *Ophthalmic Research*, 2004, **36**, 4-24.
171. J. Bibliowicz, R. K. Tittle and J. M. Gross, *Progress in Molecular Biology and Translational Science: Animal Models of Human Disease, Vol 100*, 2011, **100**, 287-330.
172. A. Schlegel and D. Y. R. Stainier, *Plos Genetics*, 2007, **3**, 2037-2048.
173. E. J. Flynn, III, C. M. Trent and J. F. Rawls, *Journal of Lipid Research*, 2009, **50**, 1641-1652.
174. D. W. Logan, S. F. Burn and I. J. Jackson, *Pigment Cell Research*, 2006, **19**, 206-213.

175. J. Bilotta, J. A. Barnett, L. Hancock and S. Saszik, *Neurotoxicology and Teratology*, 2004, **26**, 737-743.
176. M. J. Carvan, E. Loucks, D. N. Weber and F. E. Williams, *Neurotoxicology and Teratology*, 2004, **26**, 757-768.
177. J. Bilotta, S. Saszik, C. M. Givin, H. R. Hardesty and S. E. Sutherland, *Neurotoxicology and Teratology*, 2002, **24**, 759-766.
178. T. R. Henry, J. M. Spitsbergen, M. W. Hornung, C. C. Abnet and R. E. Peterson, *Toxicology and Applied Pharmacology*, 1997, **142**, 56-68.
179. D. J. Milan, I. L. Jones, P. T. Ellinor and C. A. MacRae, *American Journal of Physiology-Heart and Circulatory Physiology*, 2006, **291**, H269-H273.
180. E. T. McKinley, T. C. Baranowski, D. O. Blavo, C. Cato, T. N. Doan and A. L. Rubinstein, *Molecular Brain Research*, 2005, **141**, 128-137.
181. S. Bretaud, S. Lee and S. Guo, *Neurotoxicology and Teratology*, 2004, **26**, 857-864.
182. J. A. Tiedeken, J. S. Ramsdell and A. F. Ramsdell, *Neurotoxicology and Teratology*, 2005, **27**, 711-717.
183. B. Fraysse, R. Mons and J. Garric, *Ecotoxicology and Environmental Safety*, 2006, **63**, 253-267.
184. Y. Yamasaki, H. Makino and Z. Ota, *Nephron*, 1994, **66**, 189-199.
185. I. Shirato, Y. Tomino, H. Koide and T. Sakai, *Cell and Tissue Research*, 1991, **266**, 1-10.
186. K. S. Kim, K. H. Lee, K. Cho and C. E. Park, *Journal of Membrane Science*, 2002, **199**, 135-145.
187. J. Wei, T. Igarashi, N. Okumori, T. Igarashi, T. Maetani, B. Liu and M. Yoshinari, *Biomedical Materials*, 2009, **4**.
188. K. Baker, K. S. Warren, G. Yellen and M. C. Fishman, *Proceedings of the National Academy of Sciences of the United States of America*, 1997, **94**, 4554-4559.
189. K. S. Warren and M. C. Fishman, *American Journal of Physiology-Heart and Circulatory Physiology*, 1998, **275**, H1-H7.
190. P. V. Asharani, Y. L. Wu, Z. Gong and S. Valiyaveettil, *Nanotechnology*, 2008, **19**.
191. L. M. Browning, K. J. Lee, T. Huang, P. D. Nallathamby, J. E. Lowman and X.-H. N. Xu, *Nanoscale*, 2009, **1**, 138-152.
192. O. Bar-Ilan, R. M. Albrecht, V. E. Fako and D. Y. Furgeson, *Small*, 2009, **5**, 1897-1910.

APPENDIX I

A. Cell culture of NIH/3T3 and H9C2 cells (Adapted from ATCC)

A1. Handling Procedure for Frozen Cells

To insure the highest level of viability, thaw the vial and initiate the culture as soon as possible upon receipt. If upon arrival, continued storage of the frozen culture is necessary, it should be stored in liquid nitrogen vapor phase and not at –70°C. Storage at –70°C will result in loss of viability.

1. Thaw the vial by gentle agitation in a 37°C water bath. To reduce the possibility of contamination, keep the O-ring and cap out of the water. Thawing should be rapid (approximately 2 minutes).
2. Remove the vial from the water bath as soon as the contents are thawed, and decontaminate by dipping in or spraying with 70% ethanol. All of the operations from this point on should be carried out under strict aseptic conditions.
3. Transfer the vial contents to a centrifuge tube containing 9.0 ml complete growth medium and spin at approximately 125 xg for 5 to 7 minutes.
4. Resuspend cell pellet with the recommended complete growth medium (see the specific batch information for the culture recommended dilution ratio) and dispense into a 25 cm^2 or a 75 cm^2 culture flask. It is important to avoid excessive alkalinity of the medium during recovery of the cells. It is suggested that, prior to the addition of the vial contents, the culture vessel containing the complete growth medium be placed into the incubator for at least 15 minutes to allow the medium to reach its normal pH (7.0 to 7.6).
5. Incubate the culture at 37°C in a suitable incubator. A 5% CO_2 in air atmosphere is recommended if using the medium described on this product.

A2. Subculturing Procedure

Never allow the culture to become completely confluent. Subculture at 80% confluency or less.

Volumes used in this protocol are for 75 cm^2 flask; proportionally reduce or increase amount of dissociation medium for culture vessels of other sizes.

1. Remove and discard culture medium.
2. Briefly rinse the cell layer with 0.25% (w/v) Trypsin-0.53mM EDTA solution to remove all traces of serum, which contains trypsin inhibitor.
3. Add 2.0 to 3.0 ml of Trypsin-EDTA solution to flask and observe cells under an inverted microscope until cell layer is dispersed (usually within 5 to 10 minutes).

Note: To avoid clumping do not agitate the cells by hitting or shaking the flask while waiting for the cells to detach. Cells that are difficult to detach may be placed at 37°C to facilitate dispersal.

4. Add 6.0 to 8.0 ml of complete growth medium and aspirate cells by gently pipetting.
5. Add appropriate aliquots of the cell supension to new culture vessels. Use 3-5 x 10(3) cells/cm^2 and subculture about every 3 days.
6. Incubate cultures at 37°C.

A.3 Medium Renewal

Two times per week.

A.4 Complete Growth Medium

The base medium for this cell line is Dulbecco's Modified Eagle's Medium. To make the complete growth medium, add the following components to the base medium: bovine calf serum to a final concentration of 10%.

This medium is formulated for use with a 5% CO 2 in air atmosphere. (Standard DMEM formulations contain 3.7 g/L sodium bicarbonate and a 10% CO 2 in air atmosphere is then recommend)

A.5 Cryoprotectant Medium

Complete growth medium described above supplemented with 5% (v/v) DMSO.

B. Cell culture of HL-1 Cardiomyocytes (Adapted from Claycomb's lab protocol)

B.1 Making supplemented Claycomb Medium

Supplemented Claycomb Medium	ml	Final Concentration
Claycomb Medium	87	
Fetal bovine serum	10	10%
Penicillin/Streptomycin	1	100 U/ml: 100 µg/ml
Norepinephrine (10 mM stock)	1	0.1 mM
L-Glutamine (200 mM stock)	1	2 mM

1. Wrap the Claycomb Medium bottle in aluminum foil, since the medium is extremely light sensitive.
2. Supplemented Claycomb medium is good for two weeks, at which time L-glutamine is replenished.
3. Norepinephrine [(±)-arterenol], mw 319.3
    a. Norepinephrine is made up in 30 mM ascorbic acid.
    b. Make up 100 ml of 30 mM ascorbic acid by adding 0.59 g ascorbic acid to 100 ml of cell culture grade distilled water.
    c. Add 80 mg norepinephrine to 25 ml of the 30 mM ascorbic acid.
    d. Filter-sterilize using a 0.2 µm Acrodisc syringe filter.
    e. Aliquot in 1 ml volumes into sterile microtubes with screw caps, and store at -20ºC. This is 10 mM (stock) norepinephrine. Use 1 ml of stock per 100 ml medium for a 0.1 mM final concentration.
    f. Norepinephrine needs to be made up fresh monthly.
4. L-Glutamine: L-Glutamine comes as a 100X solution, and is aliquoted into working volumes and frozen.
5. Freezing Medium
    a. Freezing medium is made up of 95% FBS/5% DMSO.
    b. This can be stored up to a week at 4ºC.
6. Soybean Trypsin Inhibitor
    a. Weigh out 25 mg of soybean trypsin inhibitor, and place into a beaker containing 100 ml of Dulbecco's phosphate buffered saline (PBS; Ca^{2+}-free and Mg^{2+}-free) until dissolved.
    b. Filter-sterilize, using a 0.2 µm syringe filter, into a 100 ml bottle.
    c. This is good for a month at 4ºC.

B.2 Pre-coating flasks with Gelatin/Fibronectin

1. Weigh out 0.1 g gelatin and place into a 500 ml glass bottle.
2. Add distilled water to the 500 ml mark, and autoclave. This gelatin will go into solution while being autoclaved. The concentration of gelatin is 0.02%.

3. Fibronectin is received in a tube as a liquid. Dilute 1 ml fibronectin in 199 ml of 0.02% gelatin. Mix gently, and immediately aliquot 6 ml per 15 ml centrifuge tube. Freeze aliquots at -20ºC.
4. Before culturing cells, coat tissue culture flasks with gelatin/fibronectin (1 ml/T25 or 3 ml/T75 flask). Cap the flasks, and incubate at 37ºC for at least an hour.
5. Remove the gelatin/fibronectin by aspiration just before adding cells to the flasks.

B.3 Culturing cells

1. Cultures are fed (5 ml/T25 flask) with supplemented Claycomb Medium every weekday.
2. To avoid feeding the cells on weekends, 10 ml of supplemented Claycomb Medium is added to each T25 flask on Friday afternoons; this medium is not changed until the following Monday morning.

B.4 Passaging: this is the procedure for a 1:2 split.

After the cells first arrive, it is recommended that they be split when they reach confluency.

1. Split one of the T25 flasks 1:2, resulting in two T25 flasks. This set of two T25 flasks will be your "working" set of cells.
2. Split the other T25 flask 1:3, and place the contents into one T75 flask (protocol follows). After the cells in this T75 flask are confluent, they should be split into two T75 flasks. When the cells in these two flasks reach confluency, they can either be frozen (protocol follows under ―Freezing), or further split 1:2, resulting in 4 T75 flasks to be frozen.
3. It is recommended that cultures be split only after full confluence.
4. Rinse each T25 flask briefly with 3 ml of phosphate buffered saline (PBS) warmed to 37 ºC (use 6 ml for T75) by pipetting the PBS onto the bottom of the flask (side opposite the cap), trying not to hit cells directly. Rinse gently and remove by aspiration.
5. Add 1 ml of 0.05% trypsin/EDTA per T25 flask (3 ml per T75). Incubate at 37 ºC for 1 minute.
6. Remove and add fresh 0.05% trypsin/EDTA. Incubate for an additional 2 minutes.
7. Examine microscopically and, if cells are still adhered, rap the flask on the benchtop to dislodge remaining cells.
8. To inactivate the enzyme, add an equal amount (1 ml per T25) of soybean trypsin inhibitor directly onto cells.
9. Transfer cells from the flask into a 15 ml centrifuge tube.
10. Rinse the empty flask with 5 ml wash medium (Claycomb Medium containing only 5% FBS and penicillin/streptomycin), and add to the cells already in the 15 ml centrifuge tube.
11. Centrifuge at 500×g for 5 minutes.

12. Meanwhile, remove the gelatin/fibronectin solution from each T25 flask, and add 4 ml supplemented Claycomb Medium/flask. Set aside.
13. Remove the tube containing the HL-cardiomyocytes from the centrifuge. Remove the supernatant by aspiration, and gently resuspend the pellet in 3 ml of supplemented Claycomb Medium.
14. Transfer 1 ml of the cell suspension into each of three labeled, gelatin/fibronectin-coated T25 flask. Each flask now contains 5 ml.
15. If the cells are passaged on a Friday, use 2x the volume of supplemented Claycomb Medium per flask.

B.4 Freezing HL-1 Cells:

1. It is advised to freeze the contents of one confluent T75 flask into one cryovial. (When cells are needed, this cryovial is thawed into one T75 flask.)
2. Briefly rinse the T75 flask containing the HL-1 culture with 5 ml of PBS warmed to 37 ºC. Remove by aspiration.
3. Transfer 3 ml of 0.05% trypsin/EDTA into the flask.
4. Incubate the flask at 37º C for 1 minute.
5. Remove the trypsin/EDTA from the flask, and replace with 3 ml of fresh 0.05% trypsin/EDTA.
6. Incubate at 37º C for 2 minutes.
7. Check under a microscope that cells are dislodged. If not, rap the flask on the benchtop to dislodge any adherent cells.
8. Add 3 ml of soybean trypsin inhibitor to the flask, and transfer the 6 ml into a 15 ml centrifuge tube.
9. Rinse each empty flask with 8 ml wash medium, and add to the cells already in the 15 ml centrifuge tube. Total volume is now 14 ml.
10. Centrifuge tube for 5 minutes at 500×g.
11. Remove wash medium by aspiration.
12. Gently resuspend each pellet in 1.5 ml of freezing medium (95% FBS/5% DMSO).
13. Pipette resuspended cells into a cryovial. Place the cryovial containing the cells into a Nalgene freezing jar containing room temperature isopropanol.
14. Immediately place the freezing jar into a –80º C freezer, and freeze cells at a rate of -1ºC/minute.
15. Six to twelve hours later, transfer the vial to a liquid nitrogen dewar.

B.5 Thawing HL-1 Cells:

1. Gelatin/fibronectin-coat a tissue culture flask for at least an hour in a 37ºC incubator.
2. Remove the gelatin/fibronectin from the culture flask, and replace with 10 ml of supplemented Claycomb Medium. Place this flask back into incubator.
3. Transfer 10 ml wash medium into an empty 15 ml centrifuge tube. Incubate tube in a 37ºC water bath.
4. Quickly thaw the cells in a 37ºC water bath (about 2 min), and transfer into the 15 ml centrifuge tube containing the wash medium.

5. Centrifuge for 5 minutes at 500×g.
6. Remove the tube from the centrifuge and remove the wash medium by aspiration.
7. Gently resuspend the pellet in 5 ml supplemented Claycomb Medium, and add to the 10 ml of medium already in the T75 flask.
8. Replace the medium with 15 ml of fresh supplemented Claycomb Medium 4 hours later (after cells have attached).

C. Theoretical calculation of the concentrations due to the gradient generator

As described earlier in section 4.3.6 the sigmoidal gradient generator is made up of a branching microfluidic network that creates a concentration gradient by utilising laminar flow and diffusive mixing. When streams of various solutions flow down the microfluidic network, they split at the nodes, then combine with neighbouring streams and are mixed 1:1 by diffusion as they pass through the subsequent channels. In Fig. 43, the operation of the gradient generator is shown at the first few nodes of the meander.

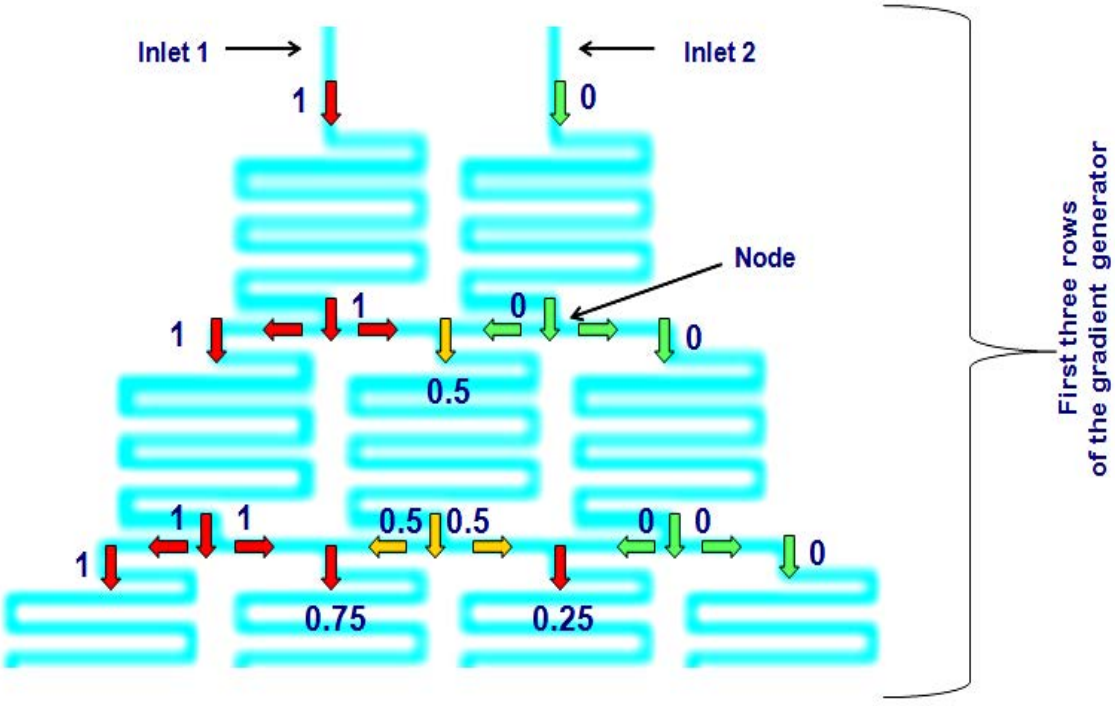

Figure 43: Operation of the gradient generator. Part of the gradient generator depicting the mixing of the solutions perfused via the two inlets.

If the two inlets are perfused with a chemical/dye/drug concentration of 1 and zero respectively, then due to the flow and mixing the concentrations obtained at the nodes and outlets are depicted in Table.2. The first row in the table represents the starting

concentration at the inlets and the last row represents the final concentration obtained at the eight outlets. Rest of the rows in the table shows the concentrations obtained at the nodes after flow passes through subsequent rows of the gradient generator (microfluidic network). Hence, the theoretical values of the concentrations were calculated based on the design of the concentration gradient generator.

C1	C2	C3	C4	C5	C6	C7	C8
1	0						
1	0.5	0					
1	0.75	0.25	0				
1	0.875	0.5	0.125	0			
1	0.9375	0.6875	0.3125	0.0625	0		
1	0.9688	0.8125	0.5	0.1875	0.0313	0	
1	**0.9844**	**0.8906**	**0.6563**	**0.3438**	**0.1094**	**0.0156**	**0**

Table. 2: Concentrations obtained at various nodes along the microfluidic network

. . . . . .